Primary electron identification in NEWS-G's S140 SPC

Francisco Vazquez de Sola

GDR DUPHY, November 2021

Introduction

New Experiments With Spheres - Gas

- Focus on **Dark Matter Direct Detection**
- NEWS-G collaboration:
  - 5 countries
  - 11 institutes
  - ~ 40 collaborators
- Three underground laboratories:
  - Laboratoire Souterrain de Modane
  - SNOLAB
  - Boulby Underground Laboratory

Working principle

Ionization detector

- Incident particle induces recoil, releasing ionisation energy
- Primary electrons drift and diffuse towards central anode
- High field in $1/r^2$ at anode produces $\sim 10^3$-10^4 avalanche multiplication
- Drifting ions induce current on anode

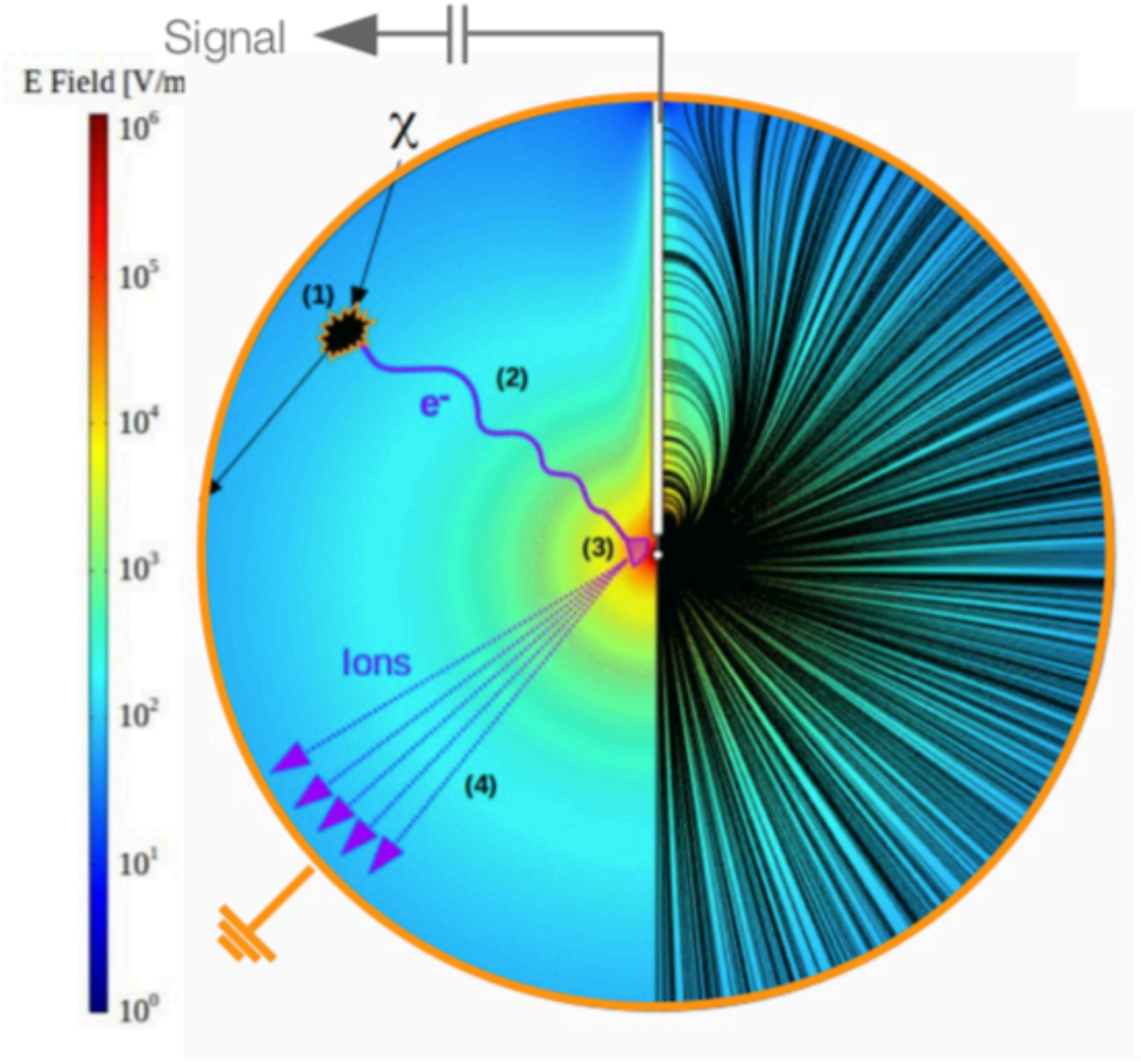

Working principle

Main advantages:

- Low capacitance + high gain -> single electron threshold
- Variable gas (H, He, Ne) / pressure choice for different physics goals
- Radiopurity of materials
- Pulse-Shape Discrimination to reduce backgrounds

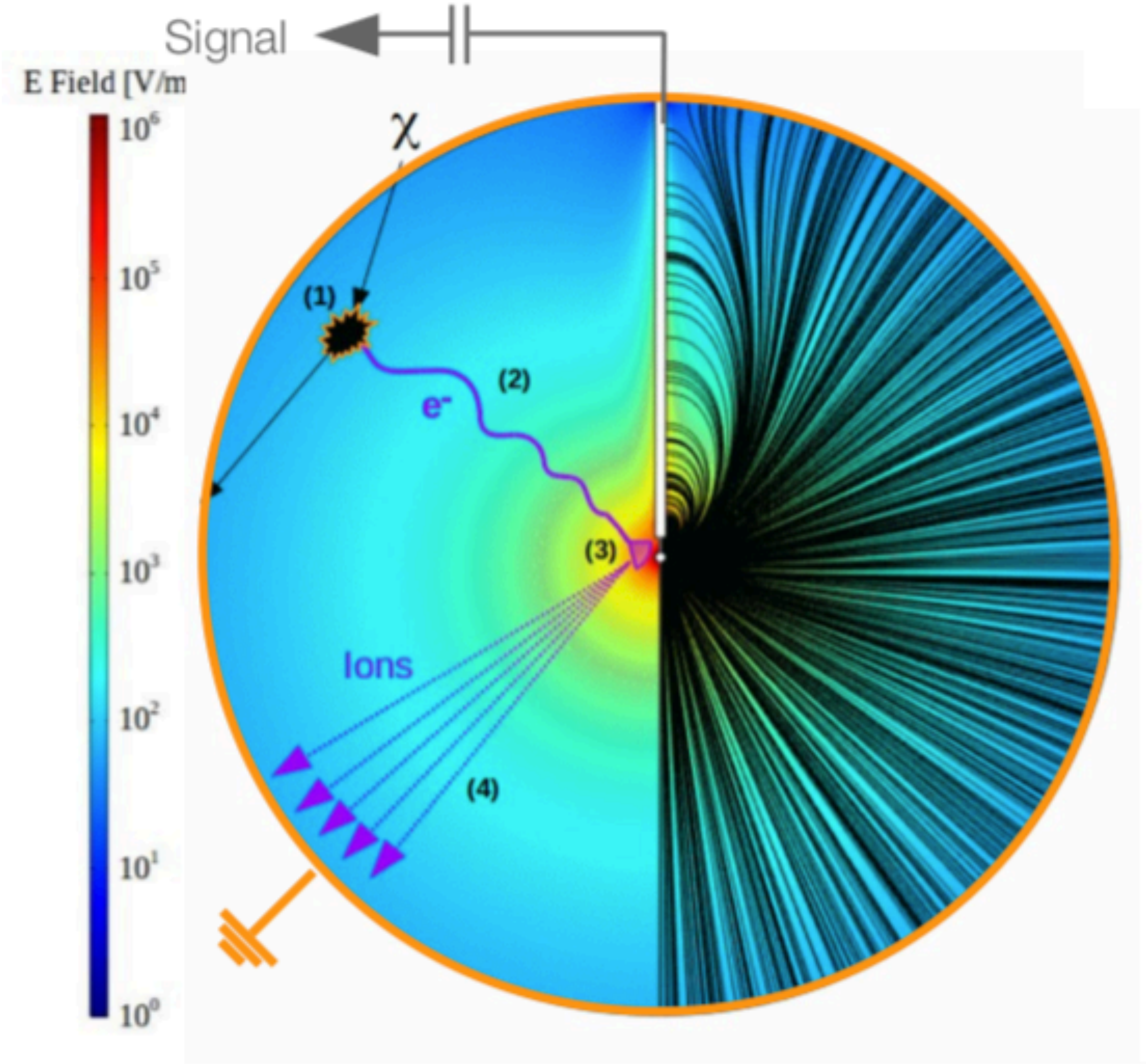

Pulse Shape Discrimination

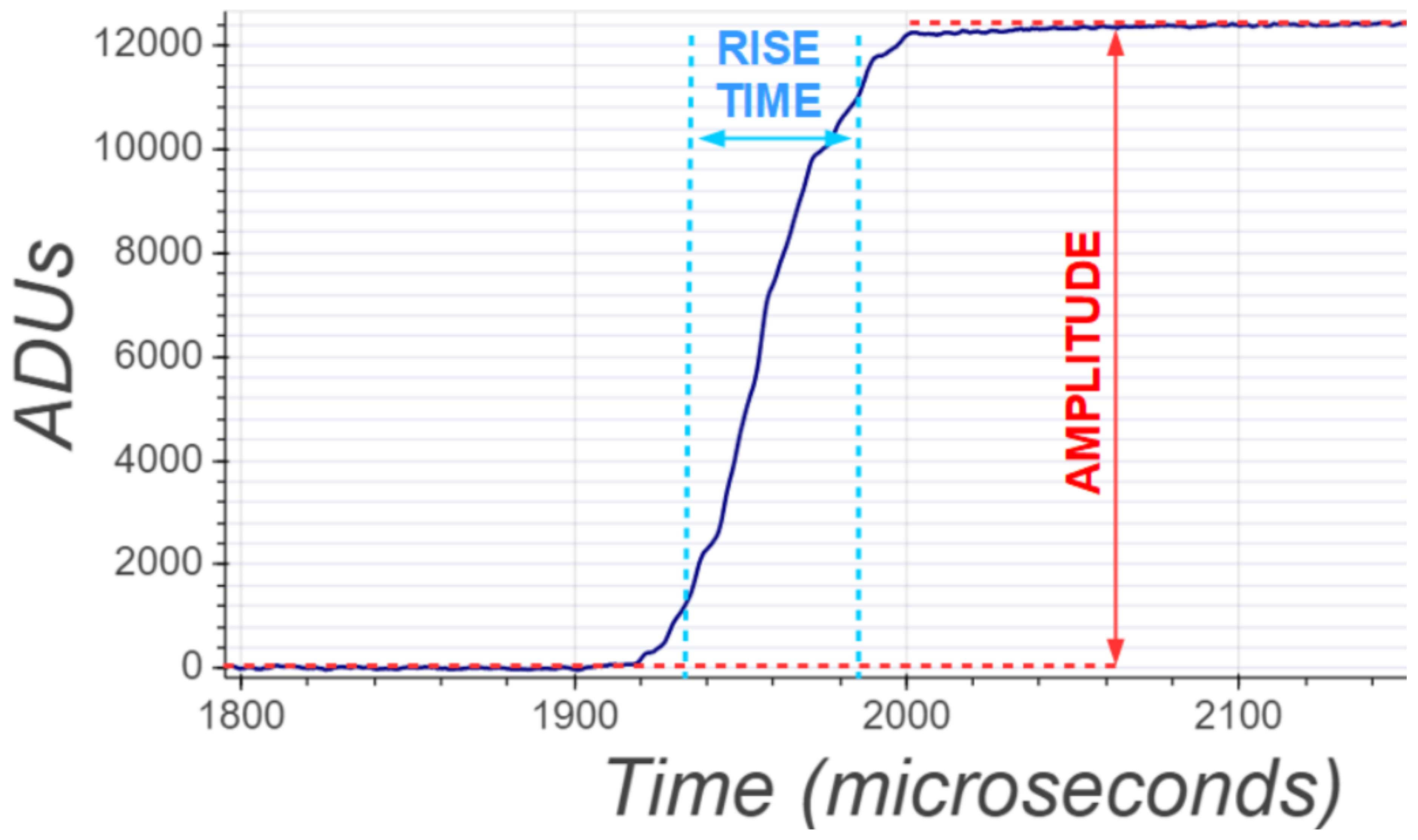

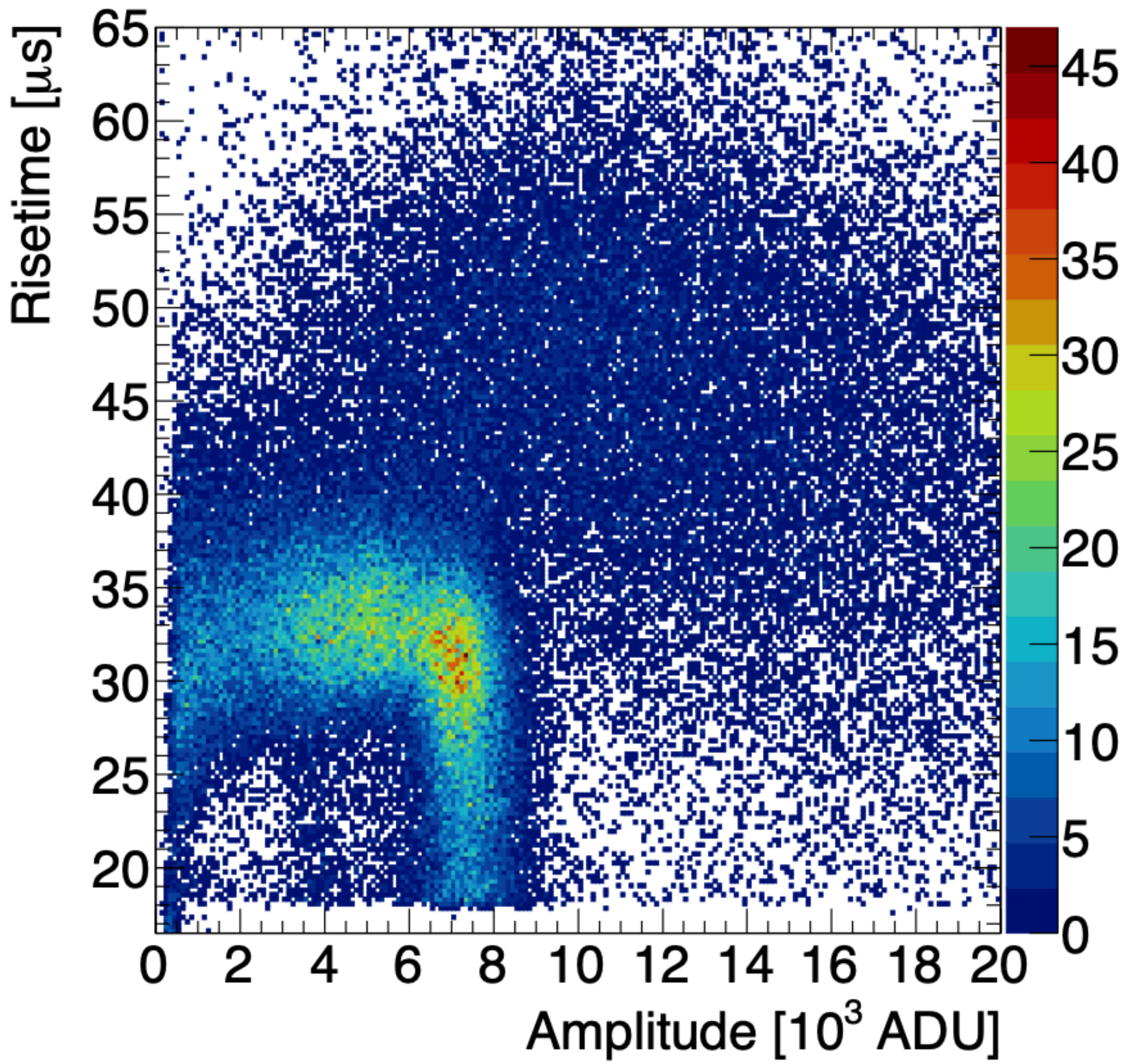

Amplitude: Energy of event
Risetime: Determine type of interaction

Pulse Shape Discrimination

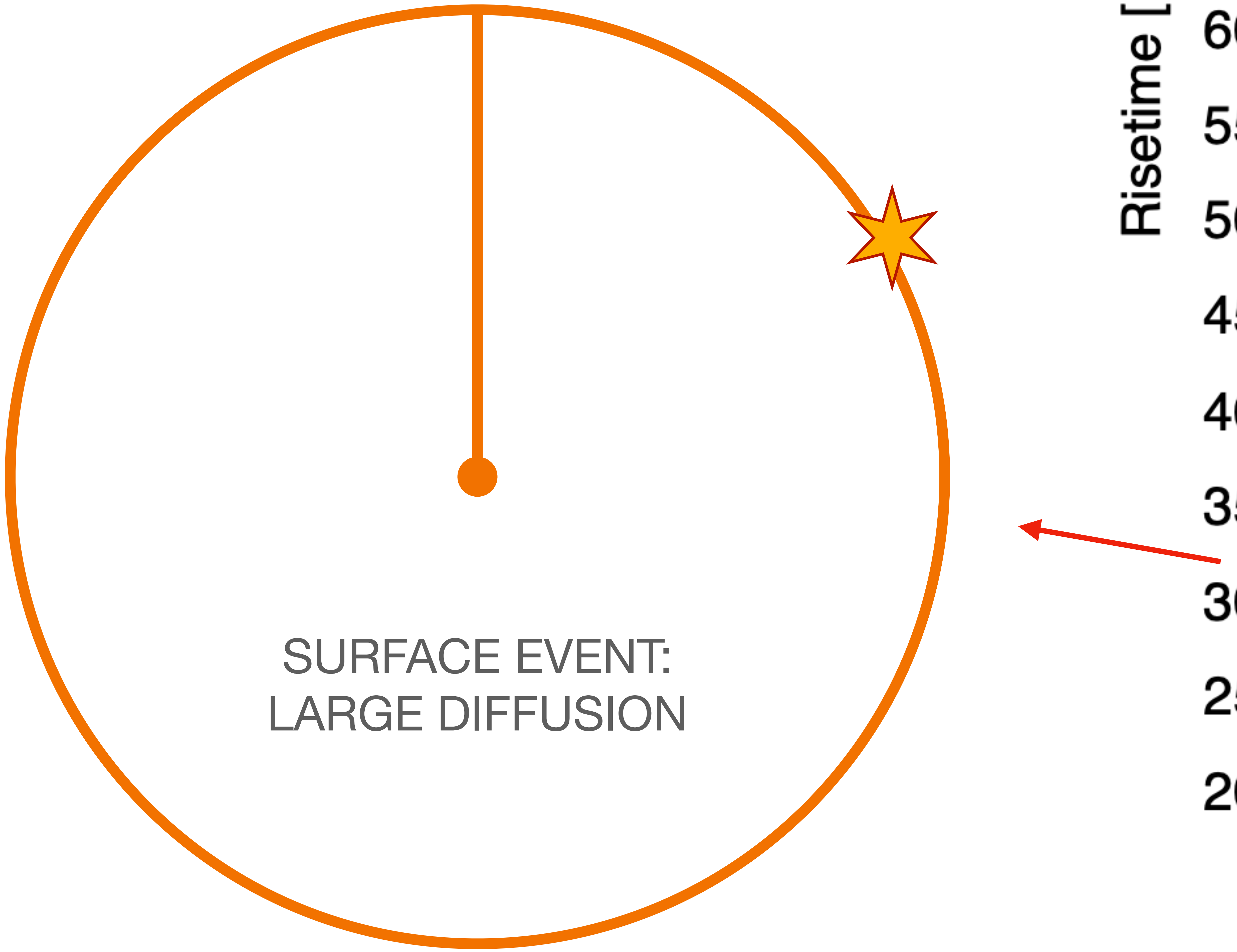

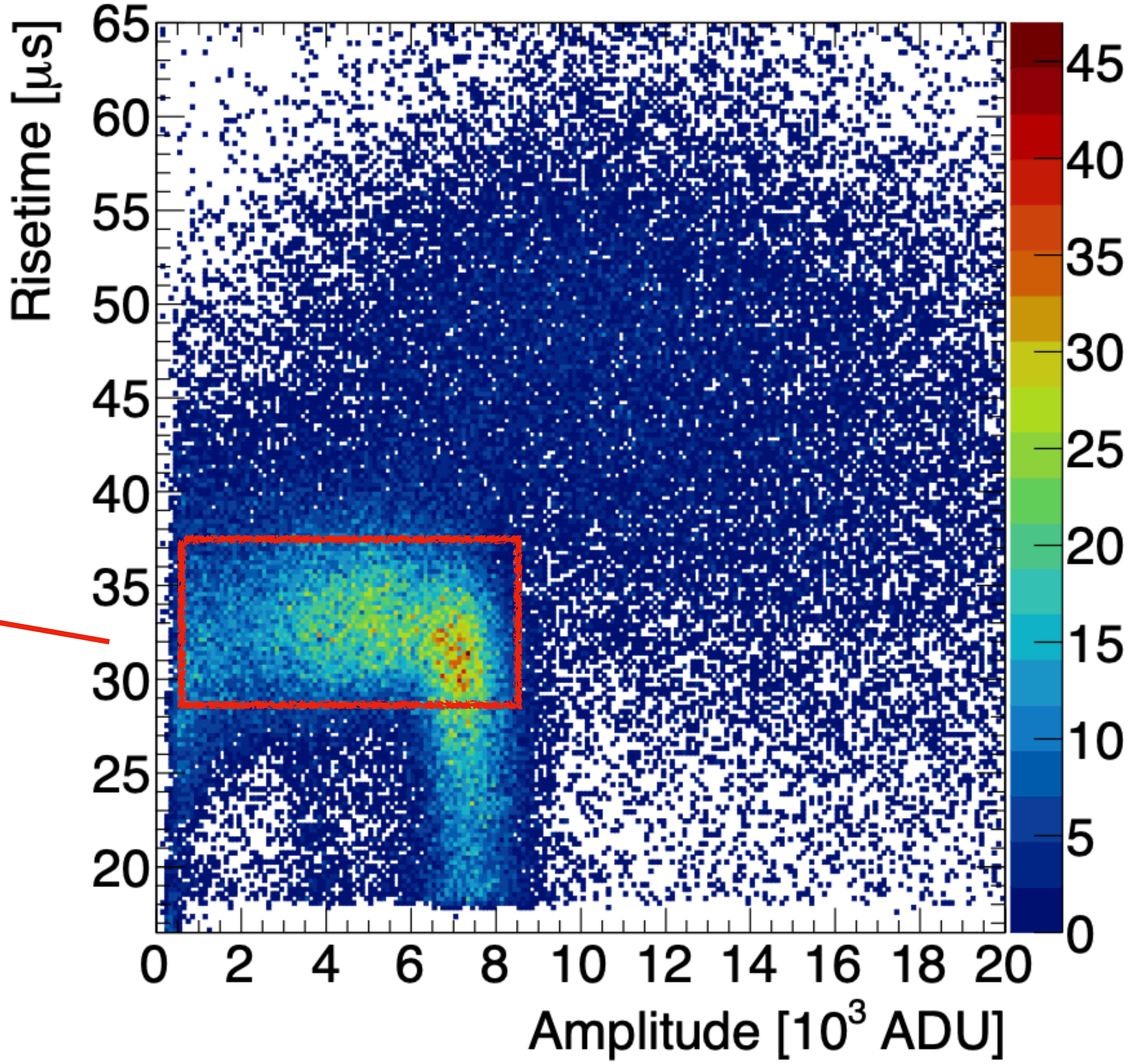

Pulse Shape Discrimination

^{55}Fe calibration:
5.9 keV X-rays

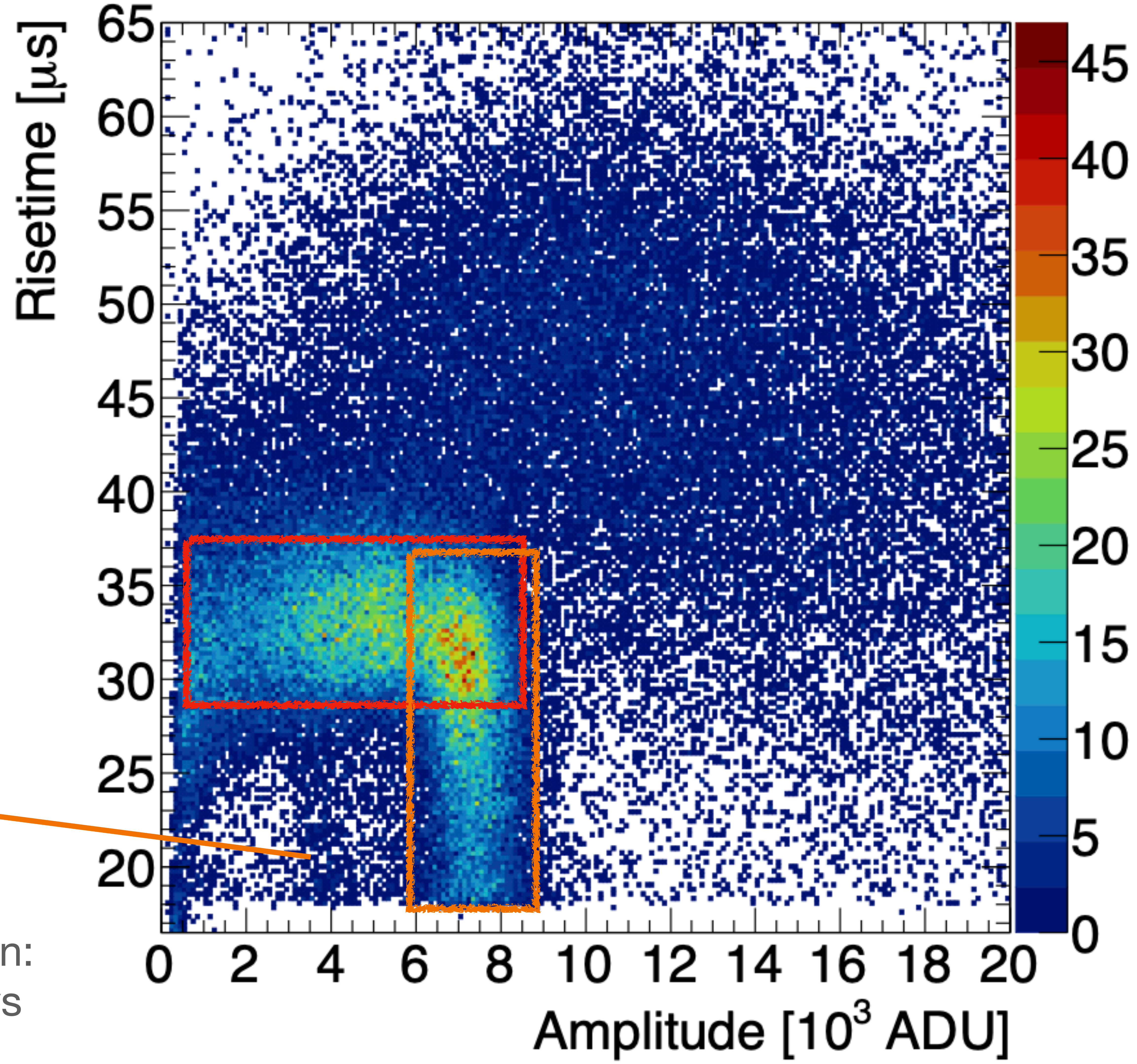

Pulse Shape Discrimination

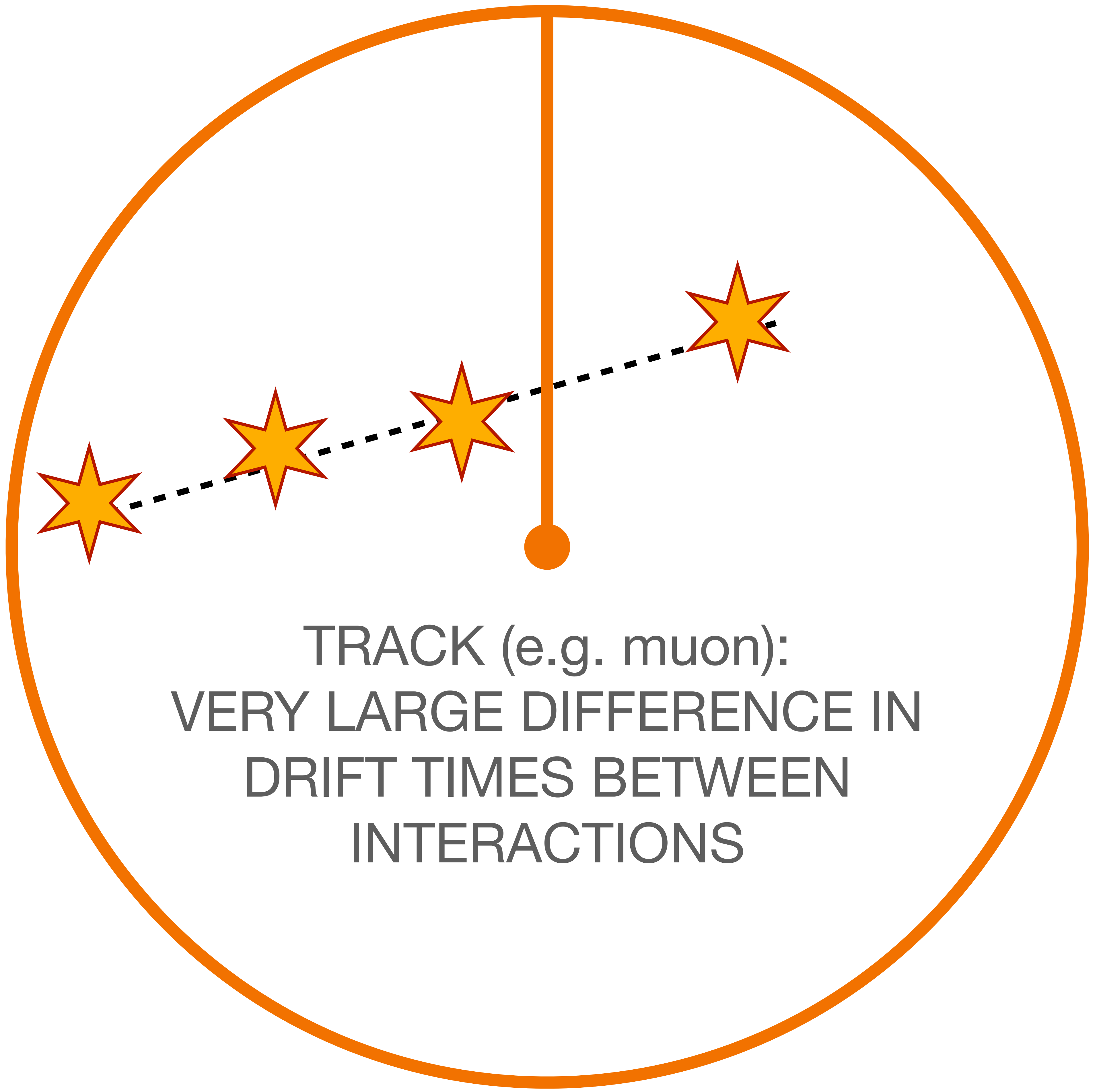

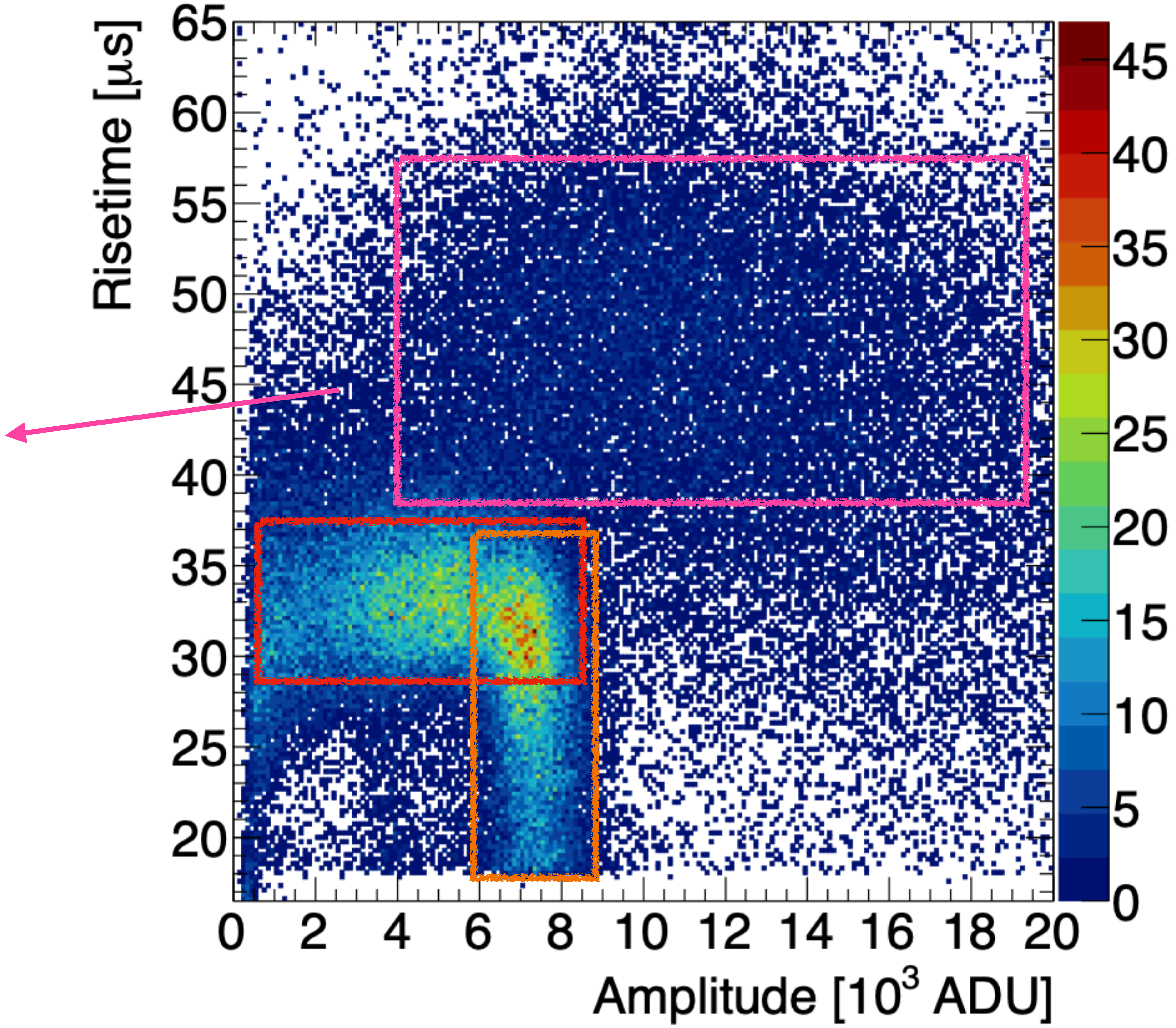

SEDINE

Detector

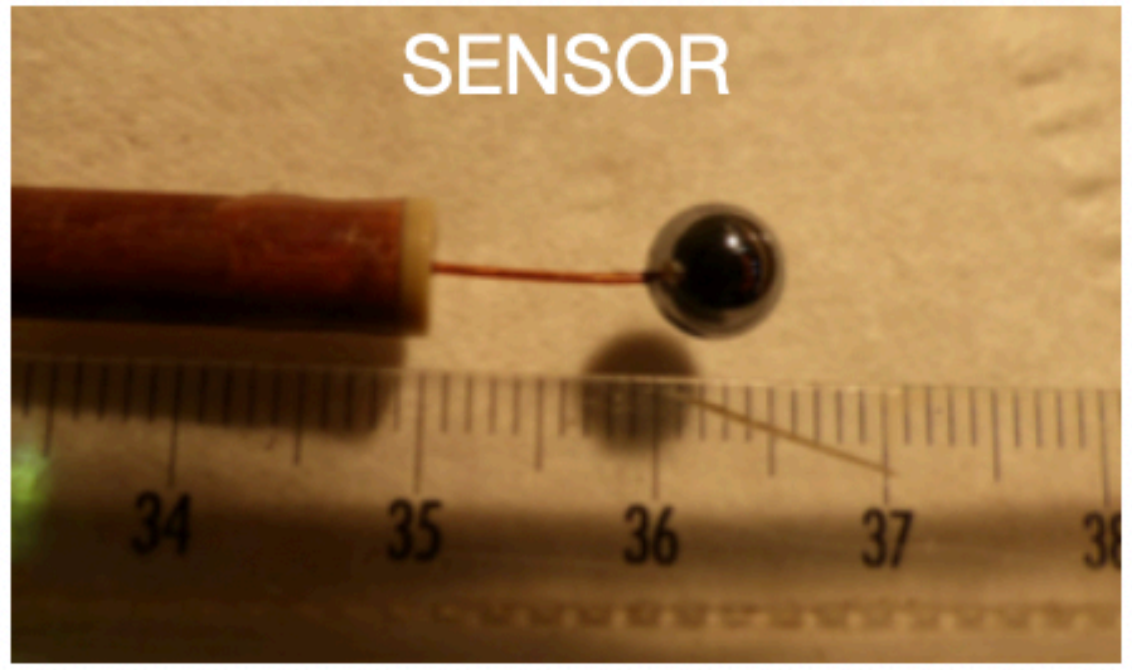

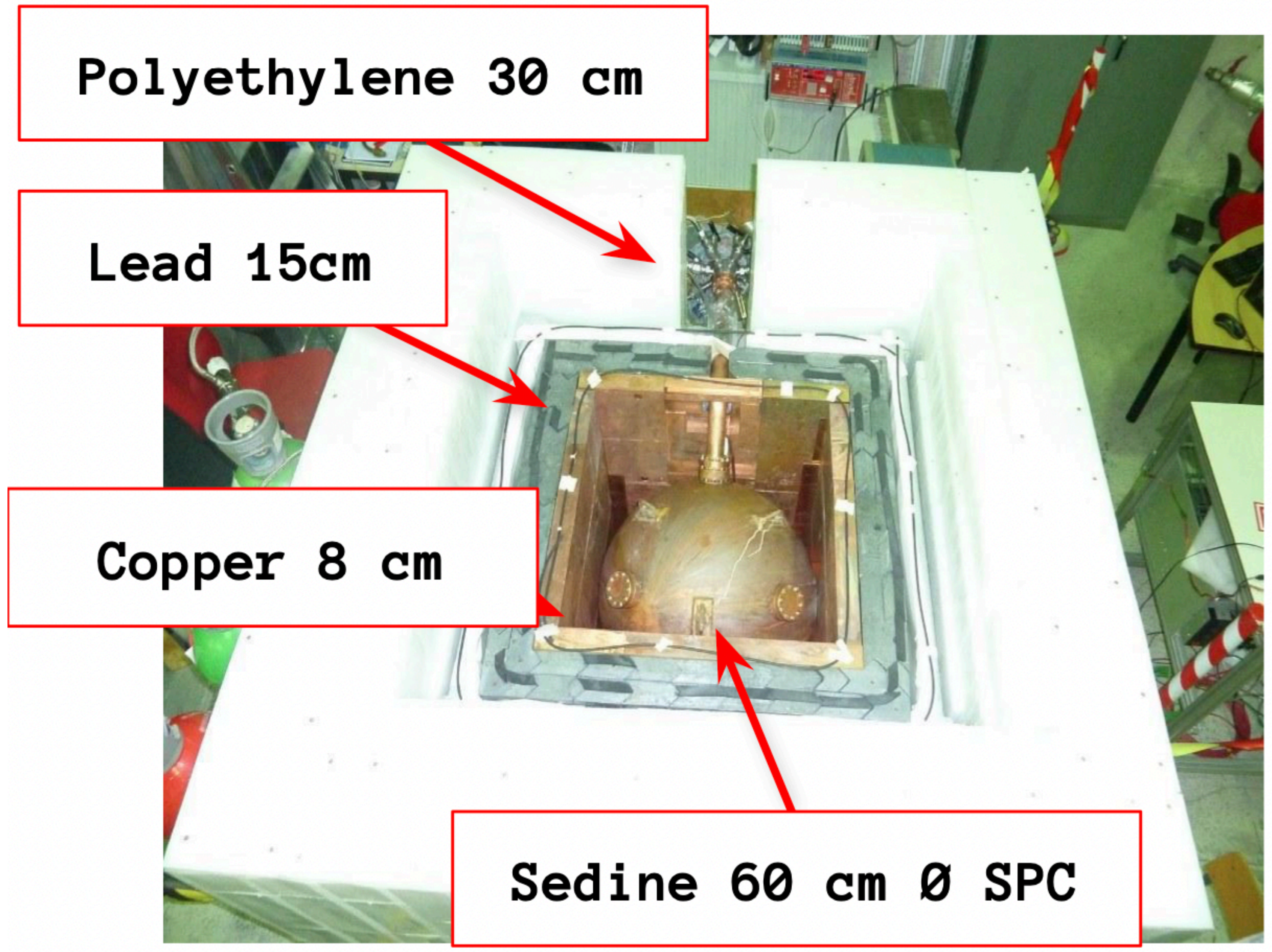

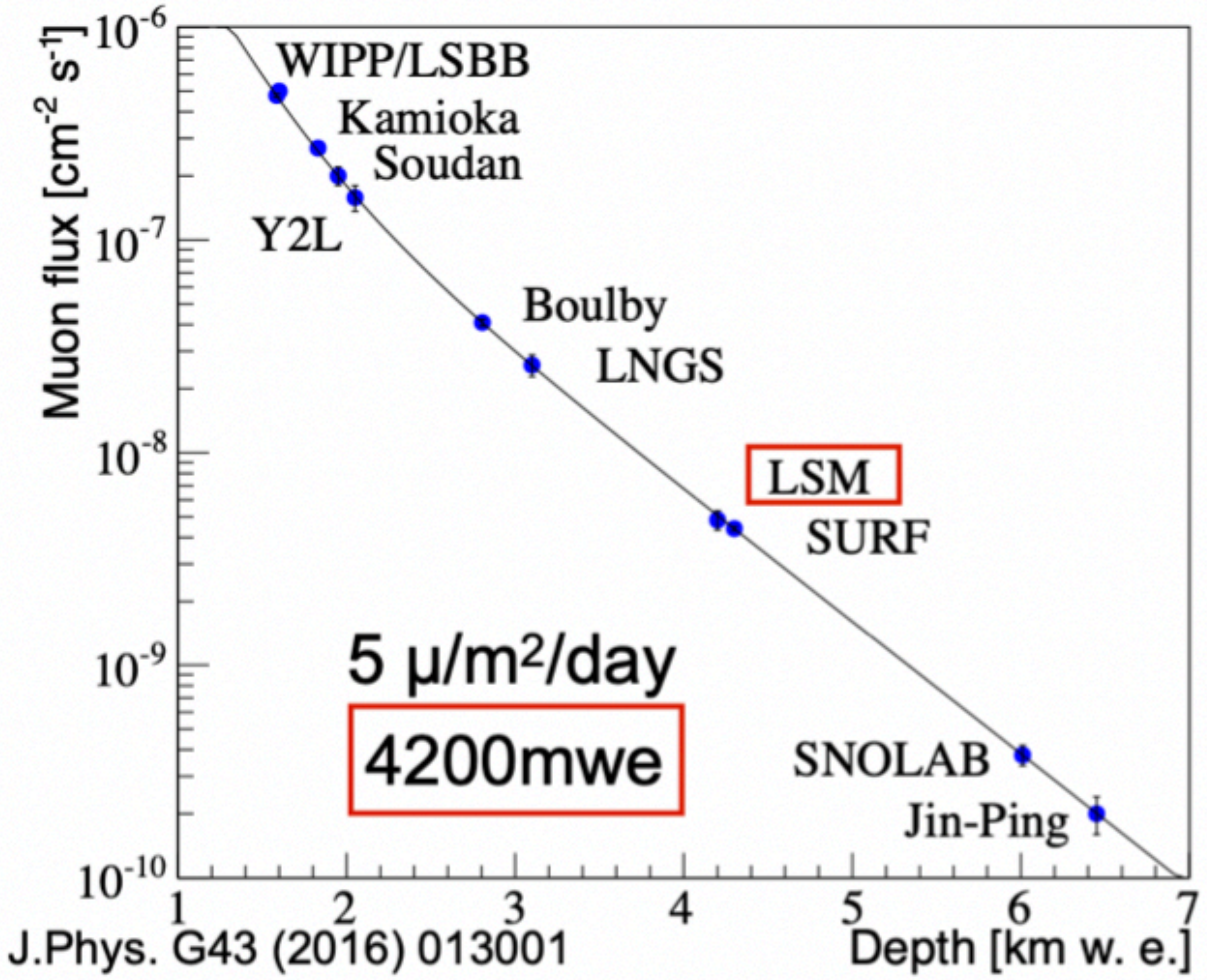

- 60cm NOSV copper vessel, 6.3 mm single-anode sensor
- Physics: 42-day run with 3.1bar of Neon + 0.7% CH_4 (280g)
- Background dominated by Radon daughters deposited on inner surface of vessel

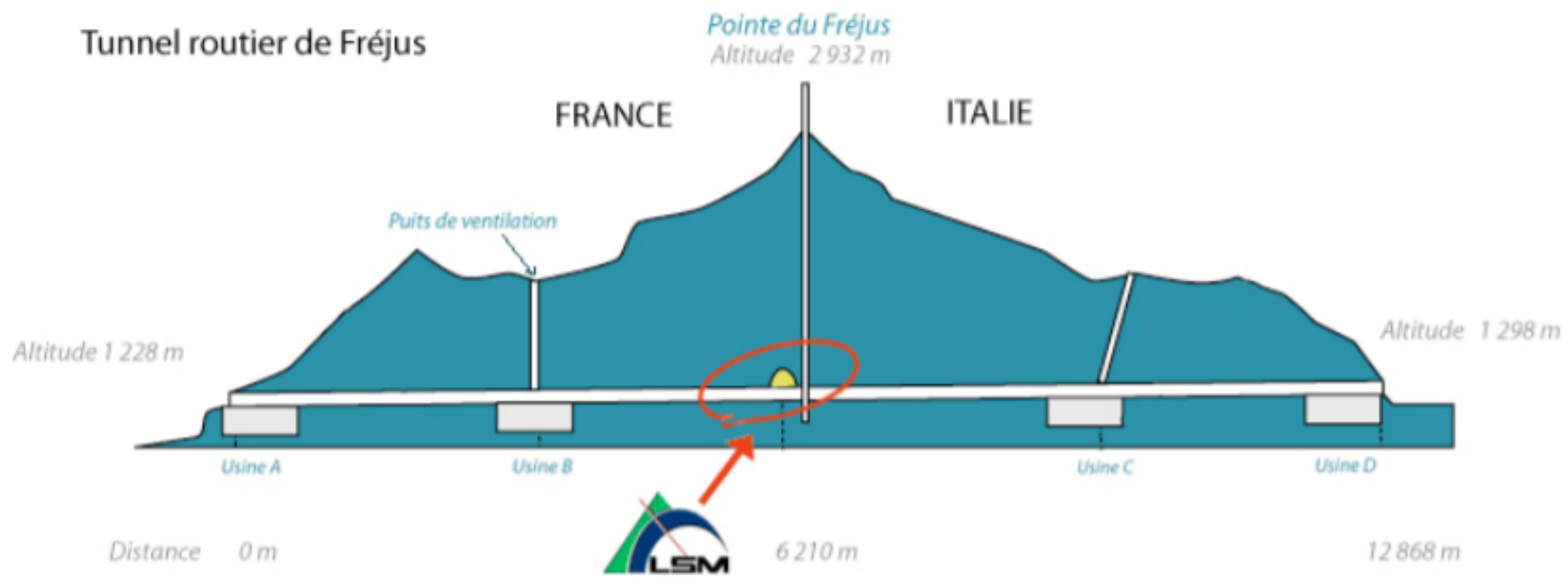

SEDINE

WIMP Results

NEWS-G collaboration, Astropart. Phys. 97, 54 (2018)

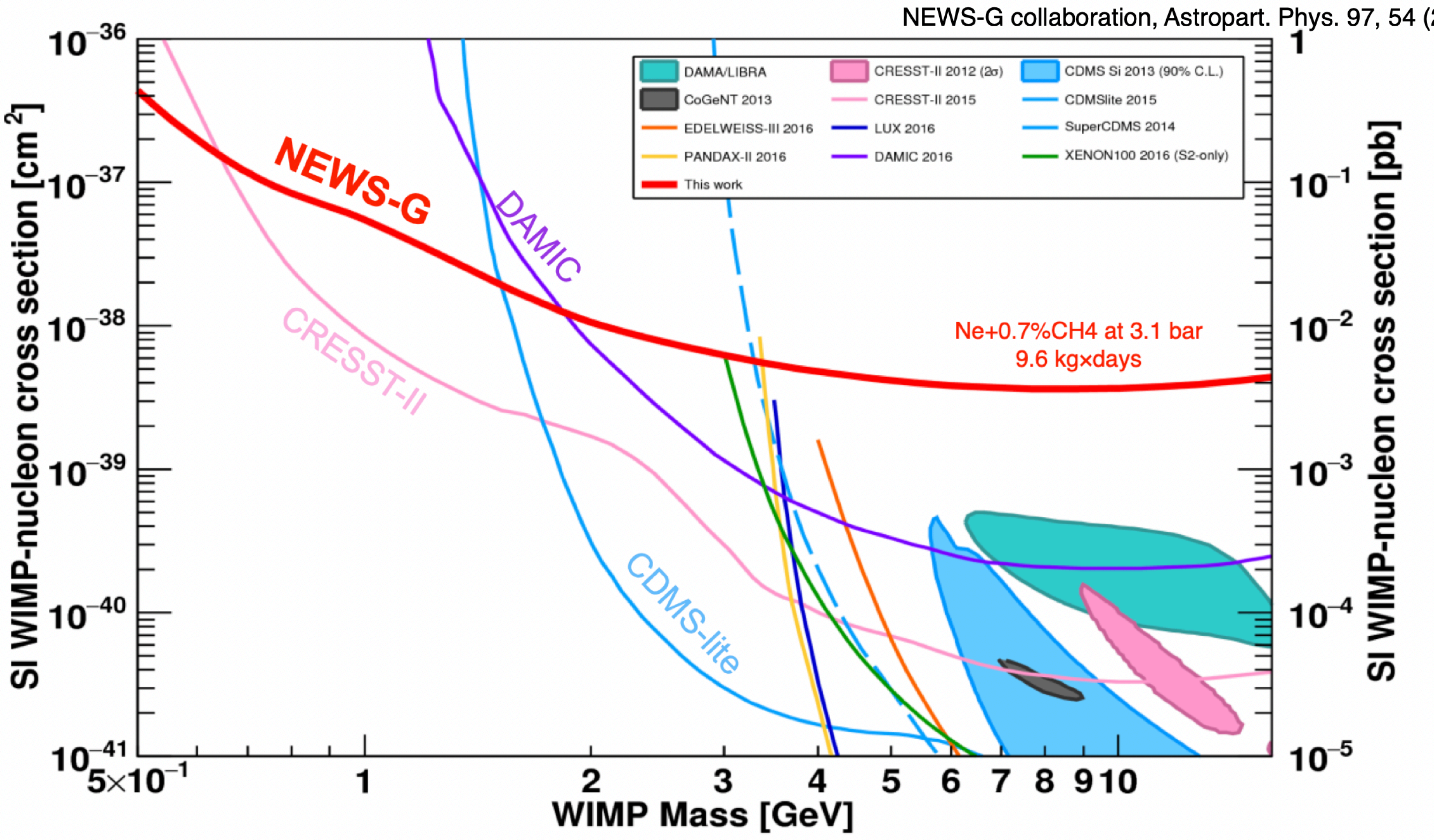

SEDINE

WIMP Results

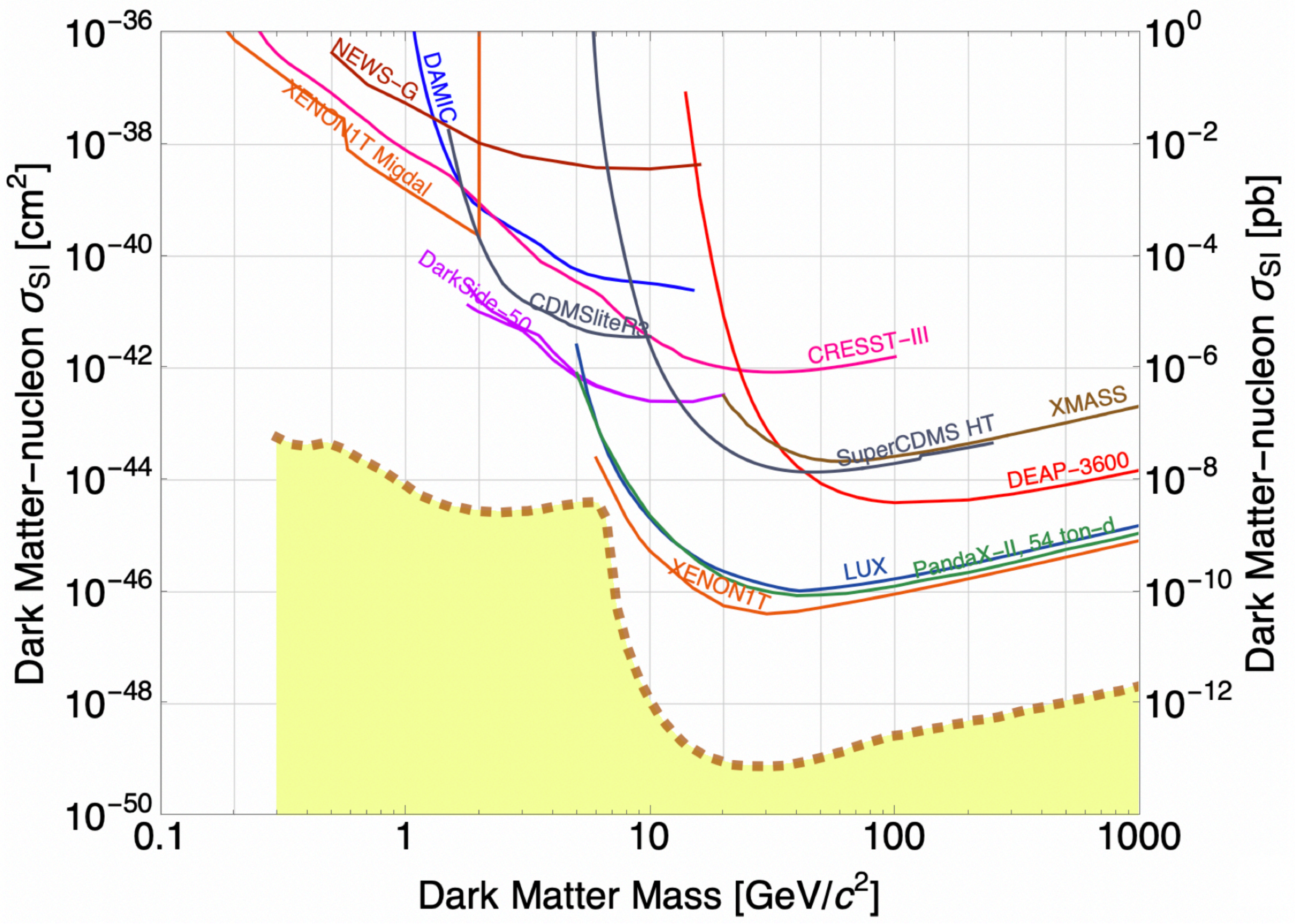

SEDINE

WIMP Results

- Use low mass targets, improve energy threshold

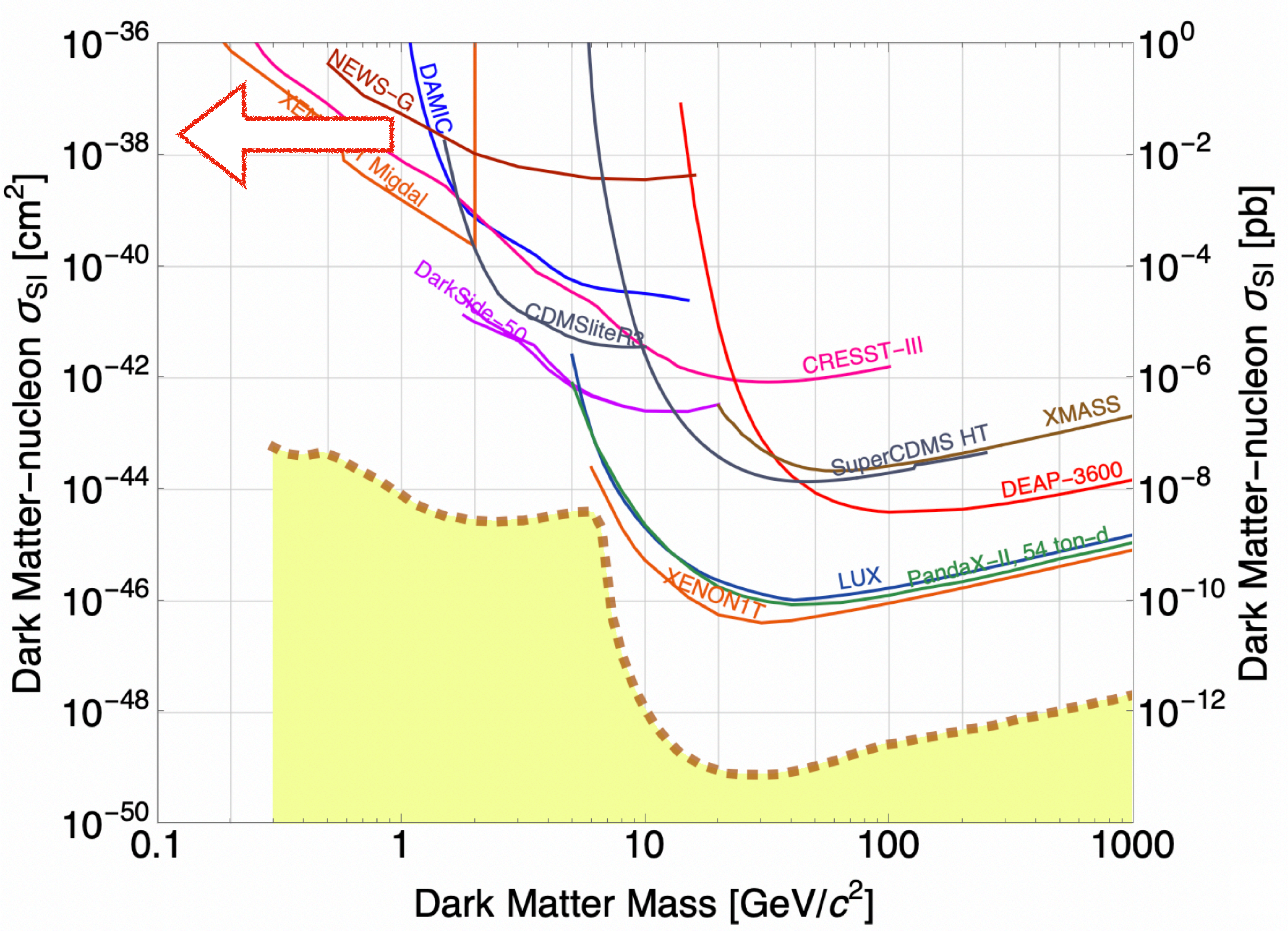

SEDINE

WIMP Results

- Use low mass targets, improve energy threshold

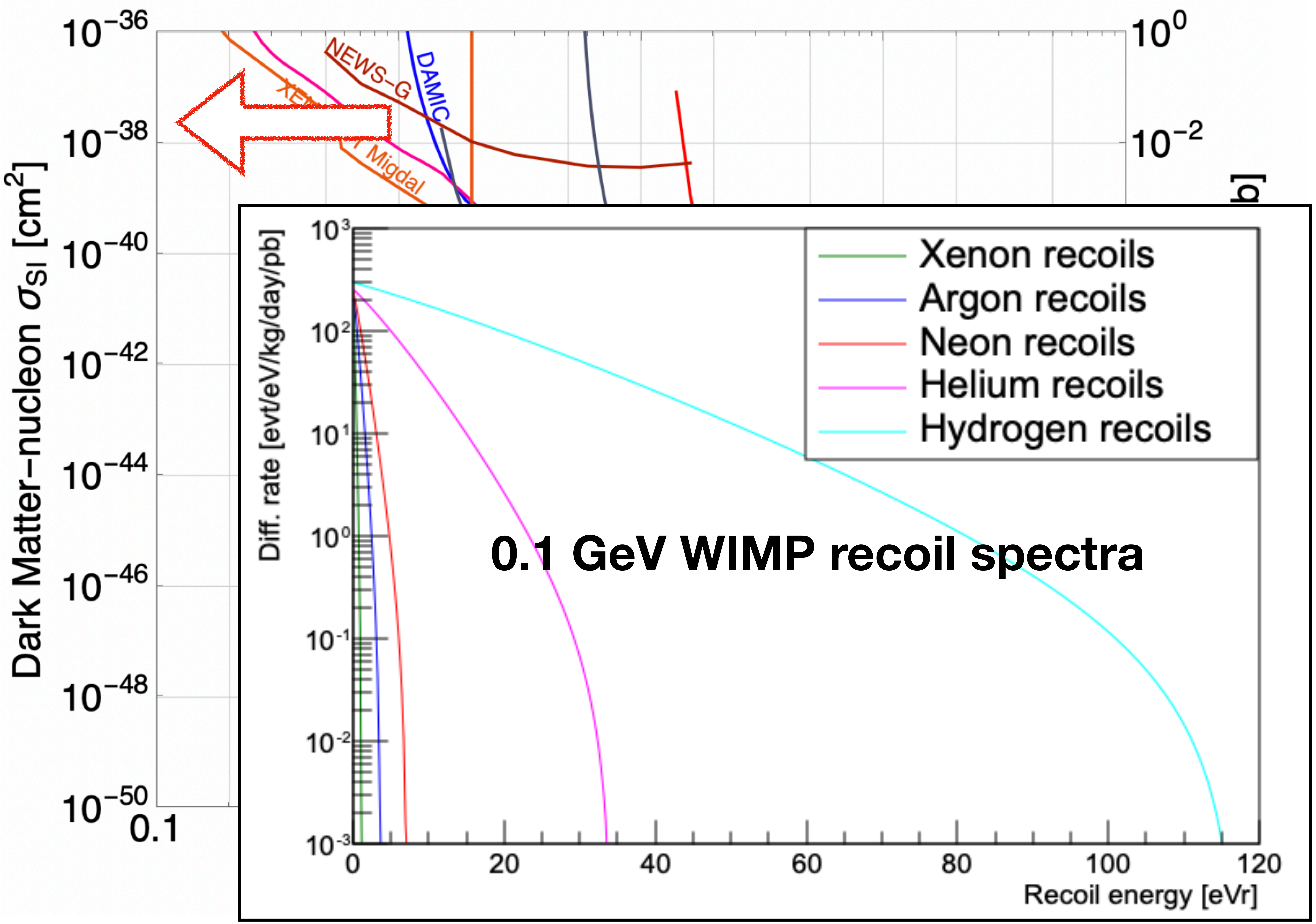

SEDINE

WIMP Results

- Use low mass targets, improve energy threshold
- Increase exposure, reduce backgrounds

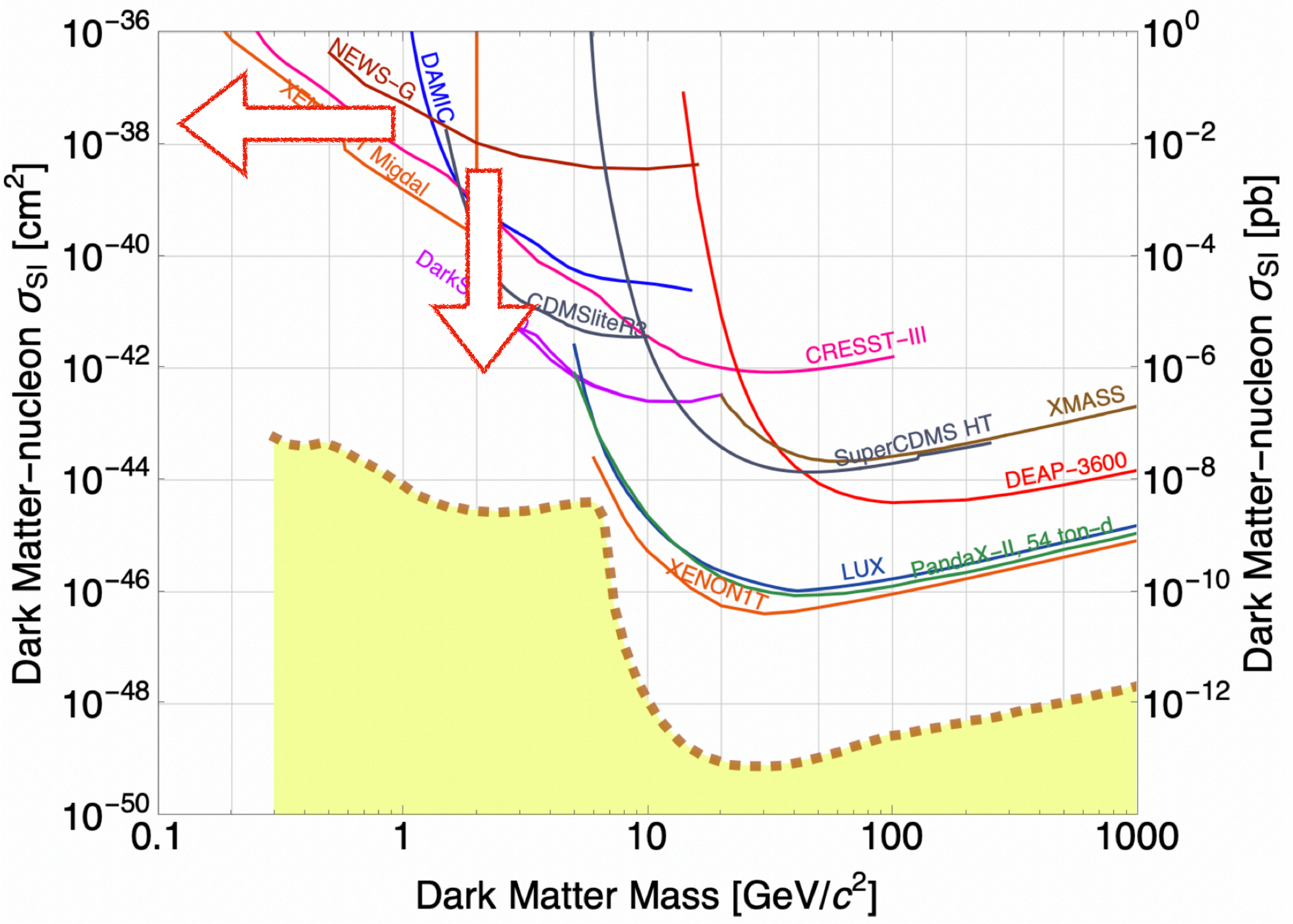

New detector: S140

S140

« SNOGLOBE »

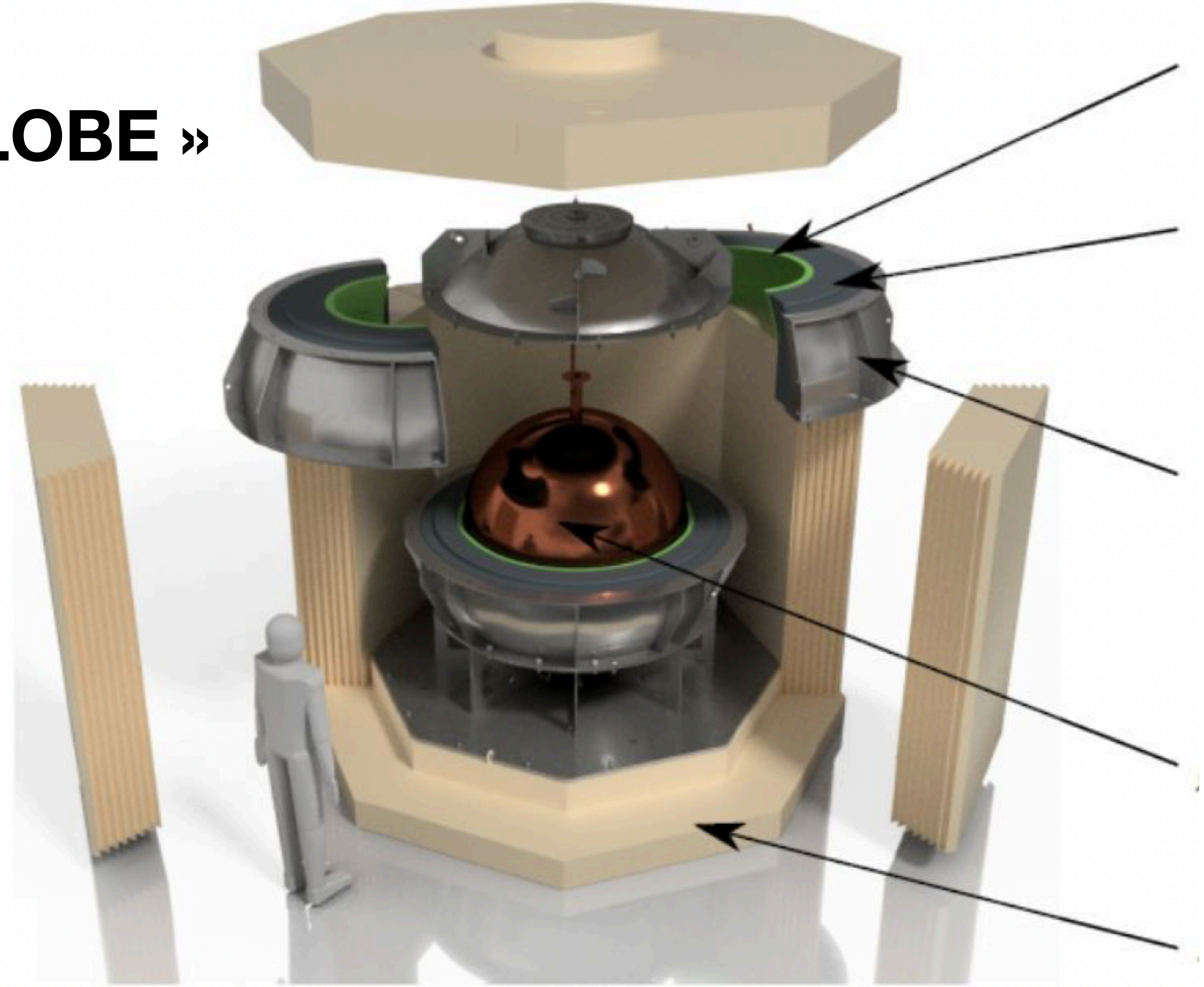

3 cm of archeological Lead

22 cm of low-activity Lead

Stainless steel skin

C10100 copper S140

40 cm borated Polyethylene

Paper on S140 detector coming early next year!

S140

Projections

S140 improvements:

- Larger volume
- Increased radiopurity of materials
- ~0.5 mm of electroplated copper on inner surface of copper shell
- Radon and oxygen filtering
- Laser calibrations (gain, drift…)
- Multi-anode sensor

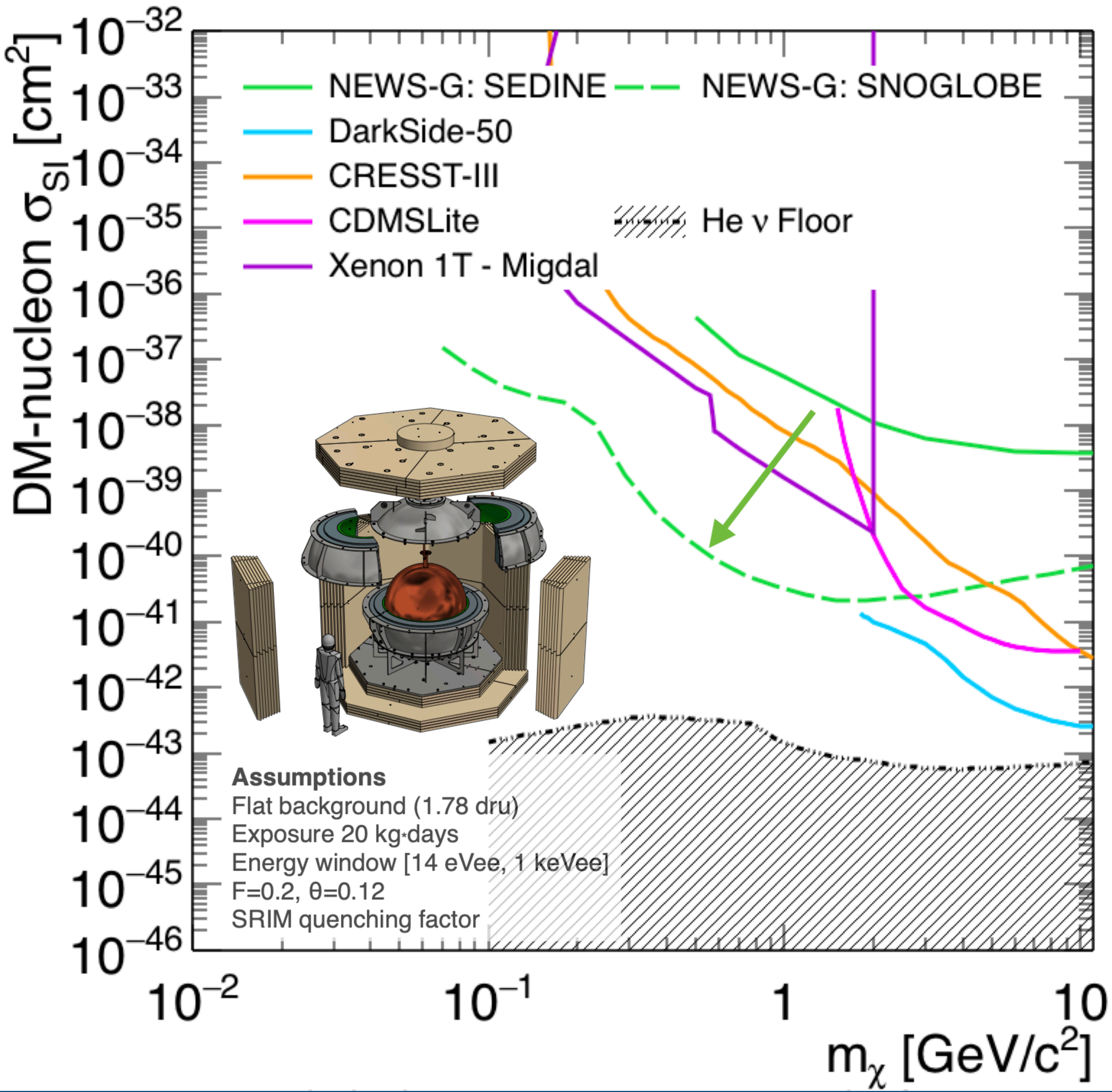

Sensor development

Limits of single anode

- Single anode sensor field: $E \approx r_A \frac{V}{r^2}$
- Contradictory constraints:
  - Avalanche requires small radius anode
  - Field far from anode requires large radius anode

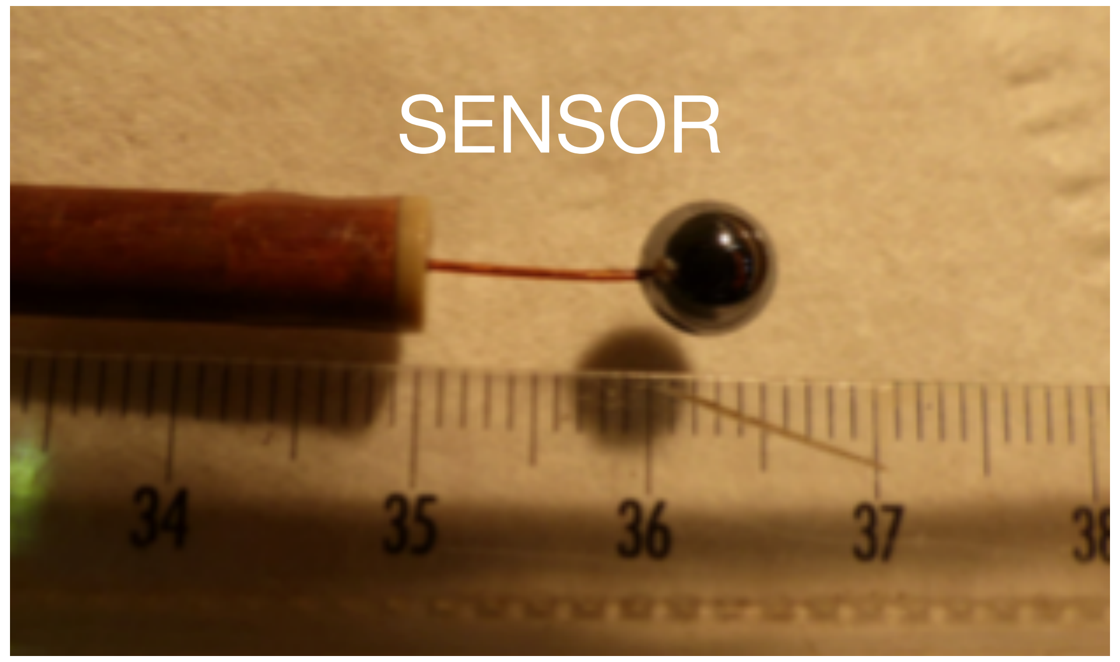

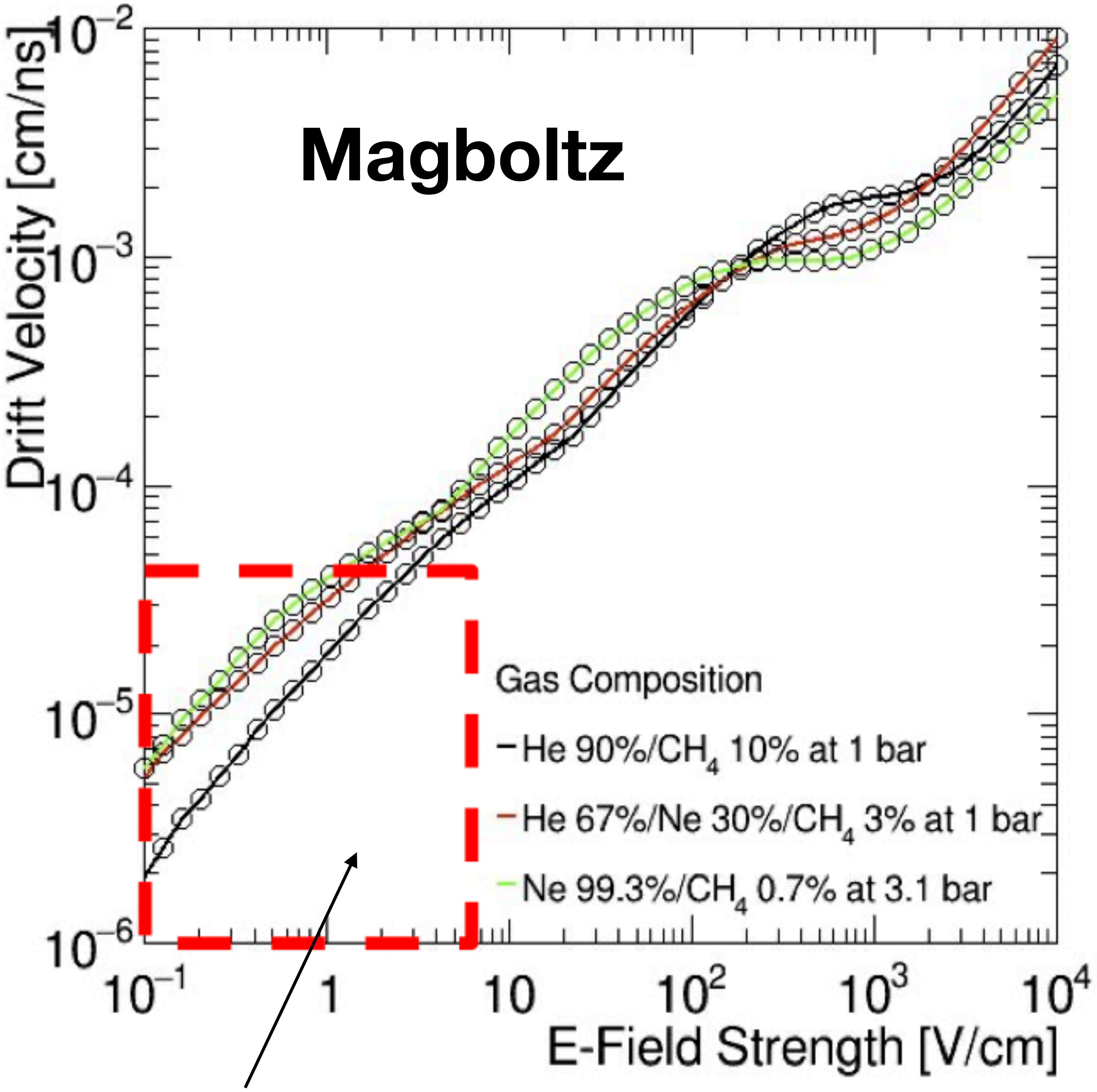

Low electric field far from anode:
Increased trapping for primary electrons

Sensor development

ACHINOS

- Multiple anodes placed at equal radii
- Boosted field far from anodes, without changing avalanche field: can scale detector up!
- Potential for individual readout from each anode, but commissioning taken in 2-channel configuration: identify hemisphere of original interaction from proportion of signal on each channel

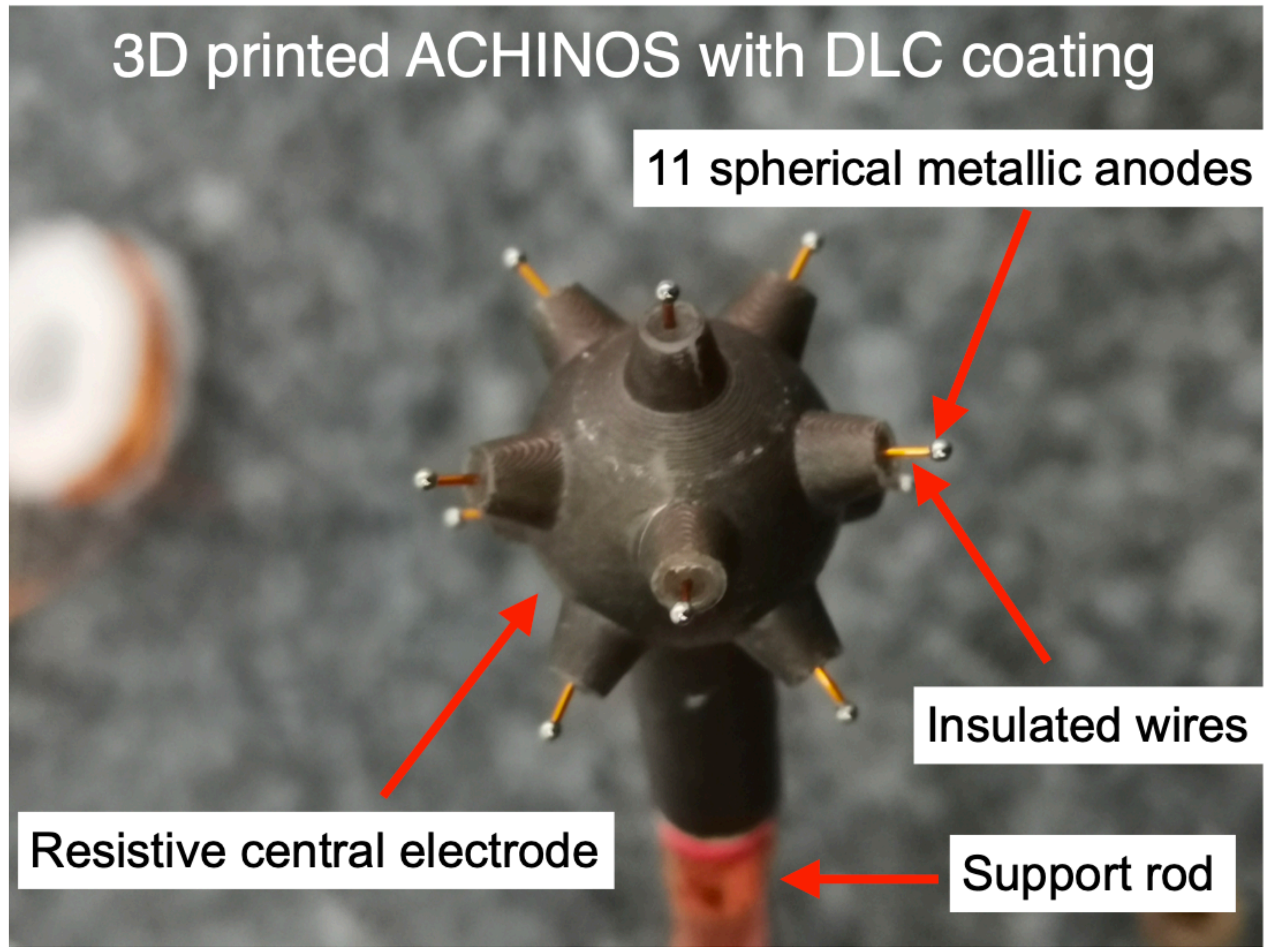

Αχινός (greek. sea urchin)

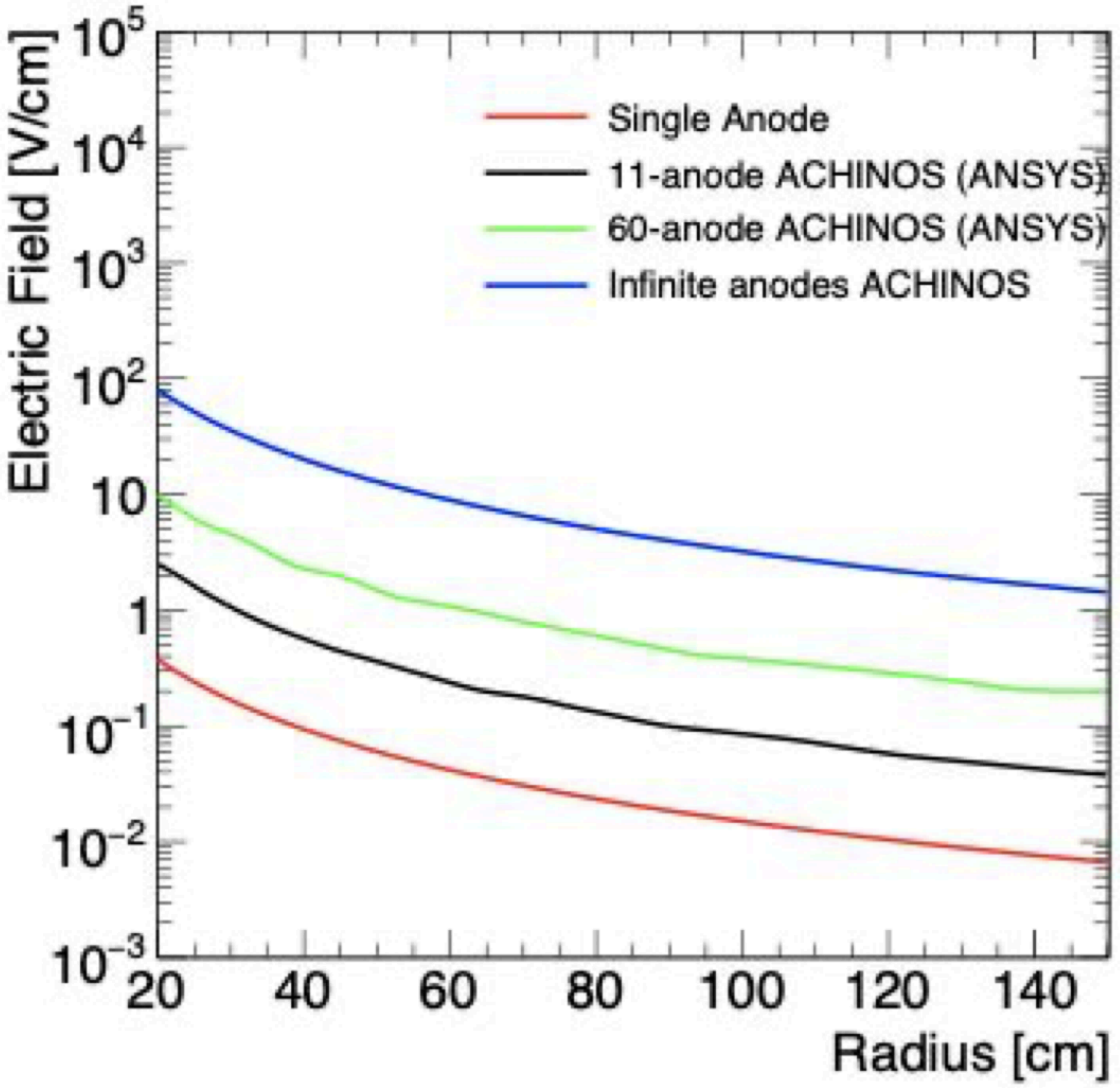

S140: Commissioning at LSM

S140: Commissioning at LSM

S140 arrives at LSM in April 2019, starting first commissioning

S140: Commissioning at LSM

S140 arrives at LSM in April 2019, starting first commissioning

Lead and water shield assembled at LSM in July 2019, starting second commissioning until October 2019 *(including two weeks of physics data with 135 mbar of CH4)*

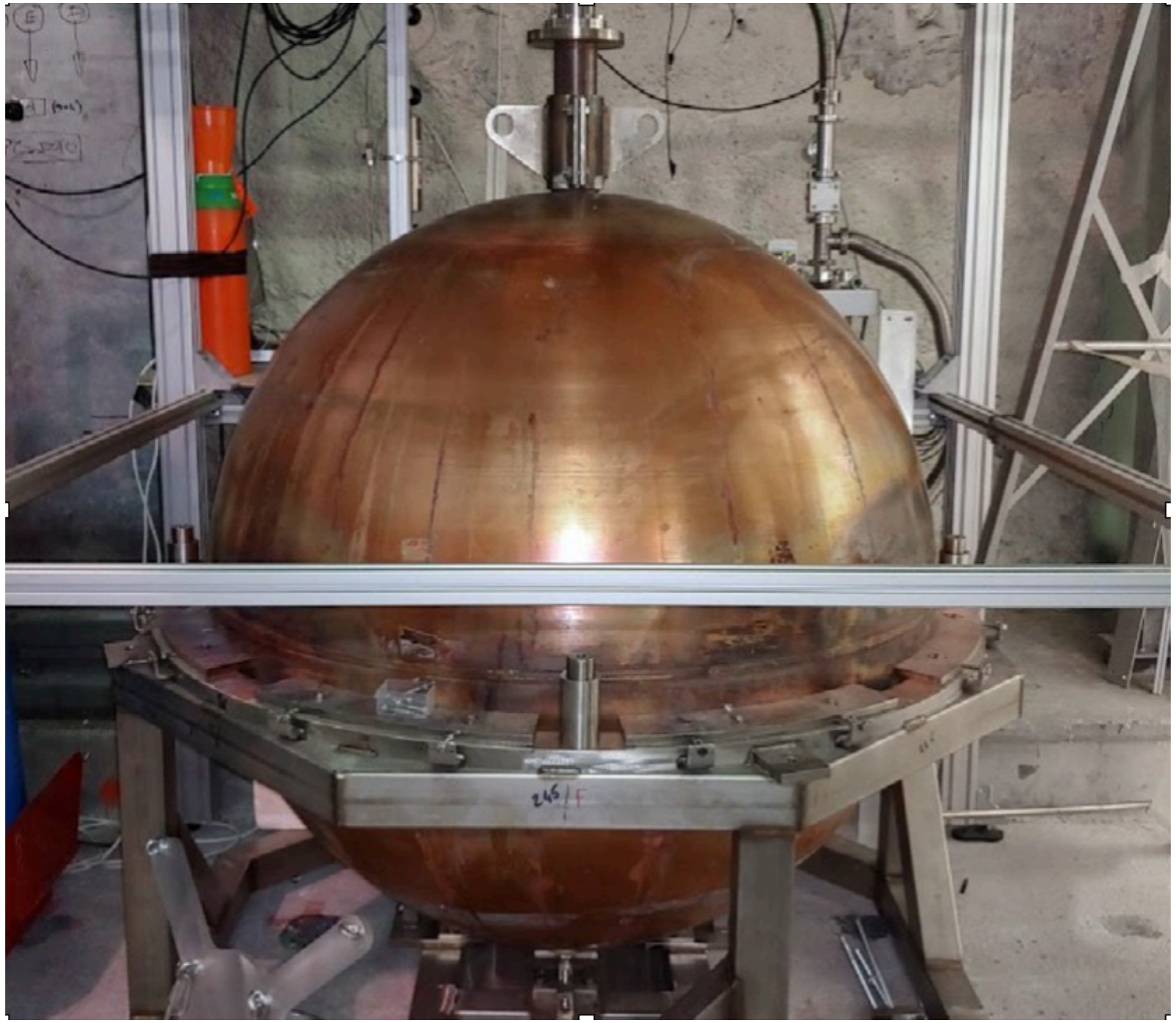

S140: Commissioning at LSM

S140 arrives at LSM in April 2019, starting first commissioning

Lead and water shield assembled at LSM in July 2019, starting second commissioning until October 2019 *(including two weeks of physics data with 135 mbar of CH_4)*

Packed in November 2019 to go to SNOLAB! Currently undergoing new commissioning.

Peak counting algorithms

S140: Improvements

Unexpected boon: electron counting

Commissioning run at LSM with 135 mbar CH_4 revealed >100 μs diffusion, >5 times larger than SEDINE's Neon data

- After deconvolution, can see individual electrons reach the anode. Can « count » electrons, despite avalanche process having standard deviation ~ mean!
- Want to keep only >1 e- events, to reject large Single Electron background
- Need to implement algorithm to count number of peaks in signal

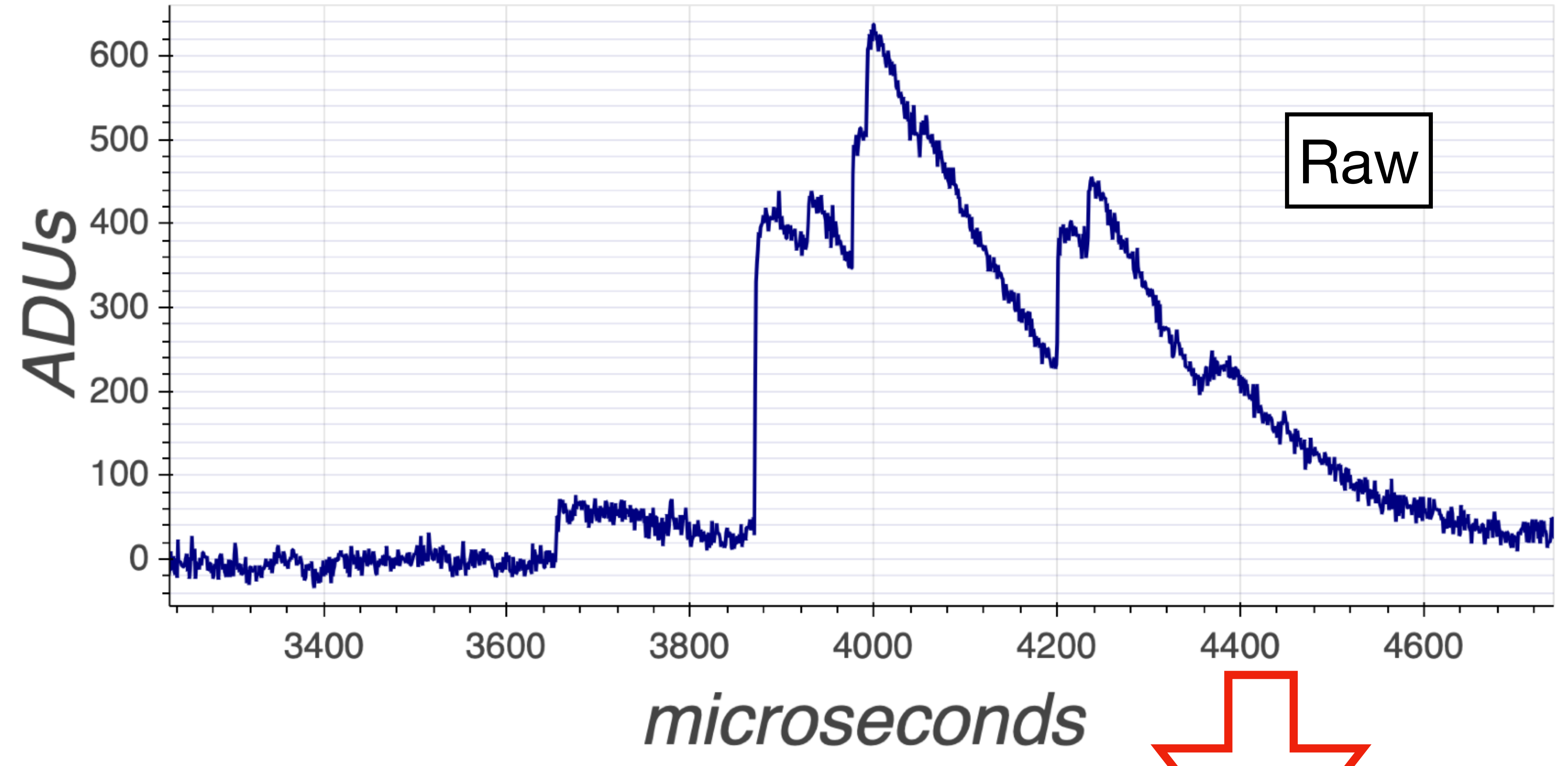

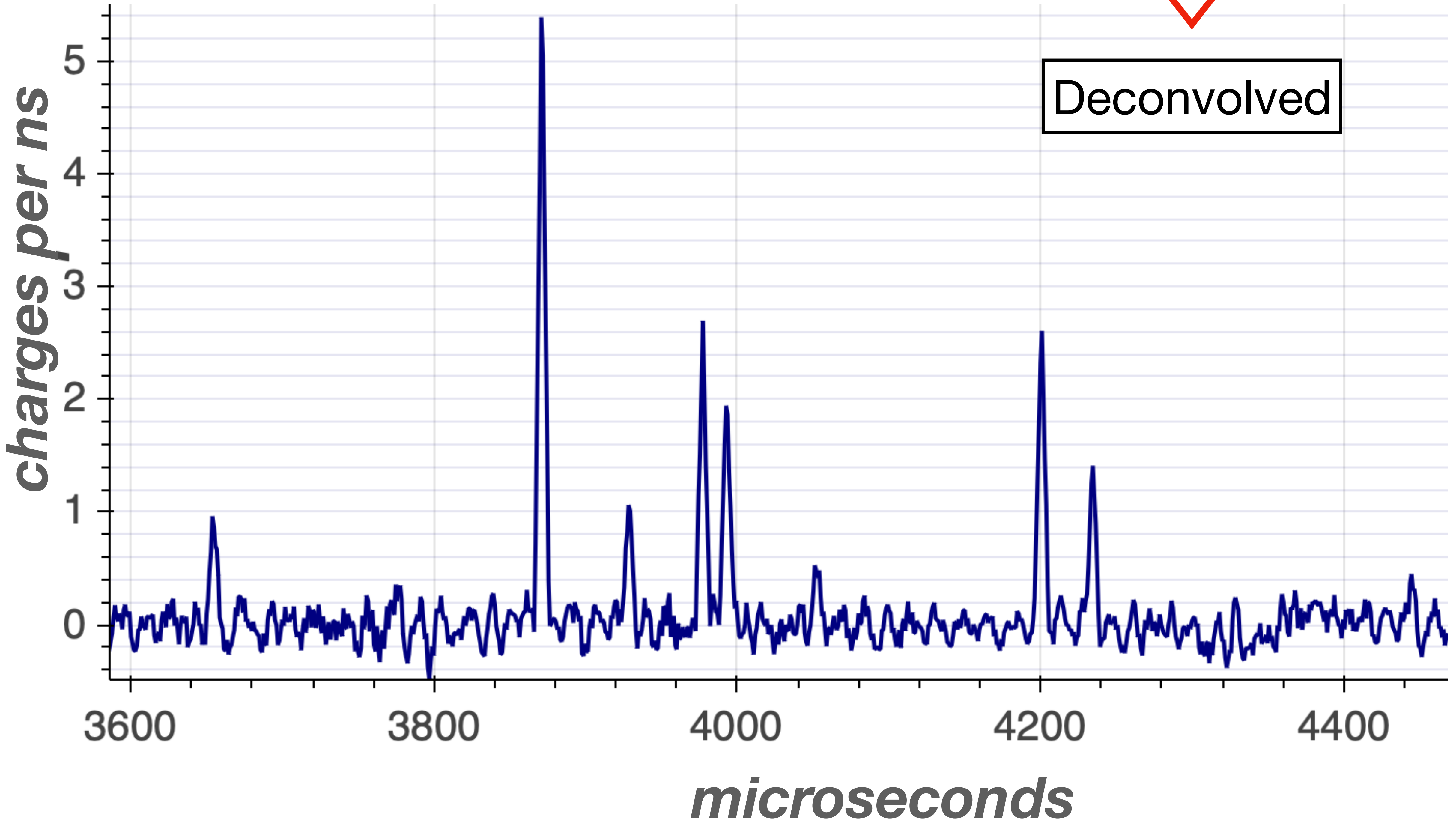

Peak counting algorithms

Looking for an algorithm to separate signal into individual avalanches from primary electrons

- Attempt 1 (GG): Deconvolve « tuned » exponential from signal, do running average over 5 bins twice, then use threshold

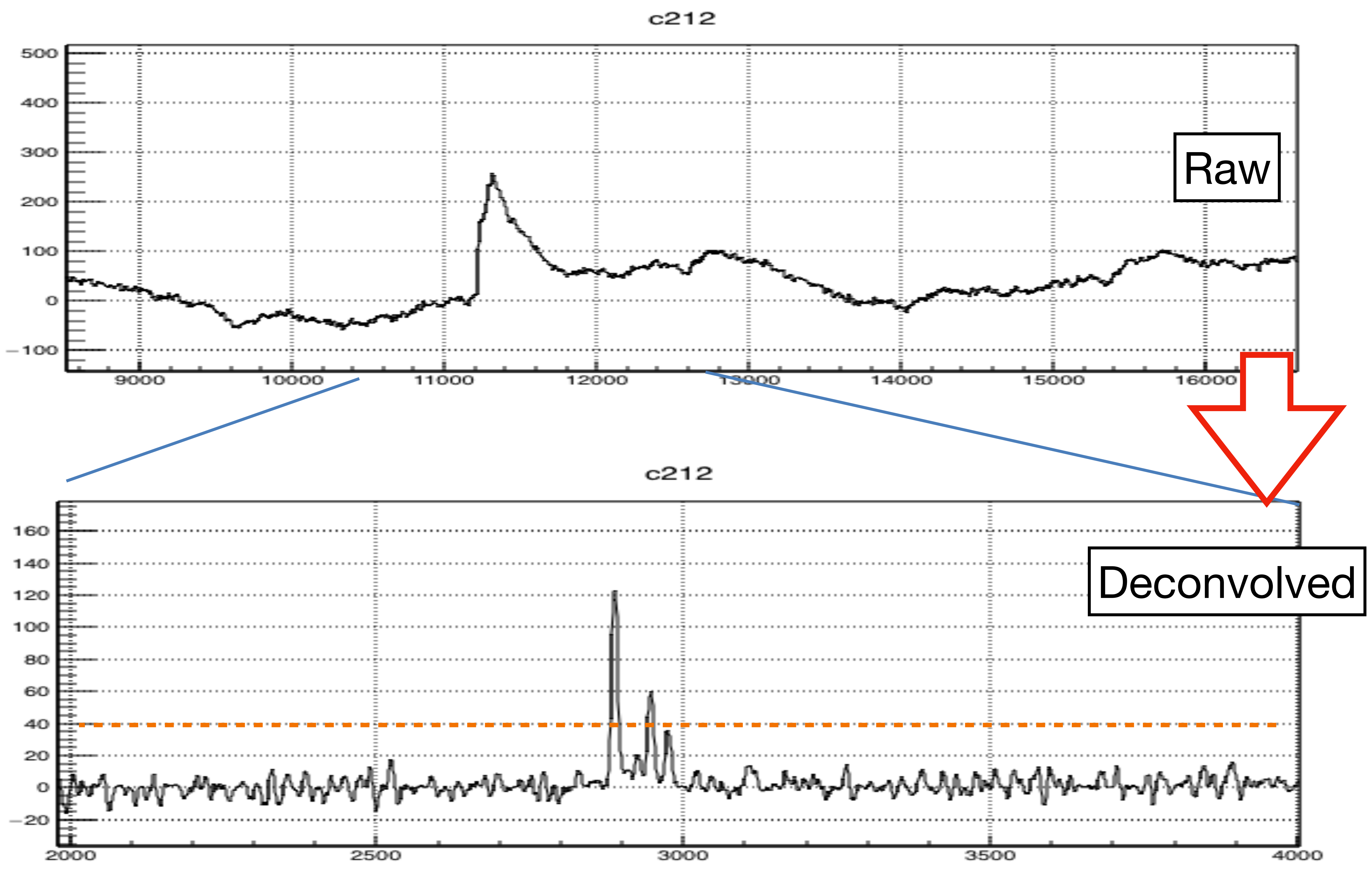

Peak counting algorithms

Looking for an algorithm to separate signal into individual avalanches from primary electrons

- Attempt 1 (GG): Deconvolve « tuned » exponential from signal, do running average over 5 bins twice, then use threshold
- Attempt 2 (PL): Deconvolve preamplifier response from signal, apply filter to remove high frequency noise and specific noise lines, then use threshold or scipy.find_peak()

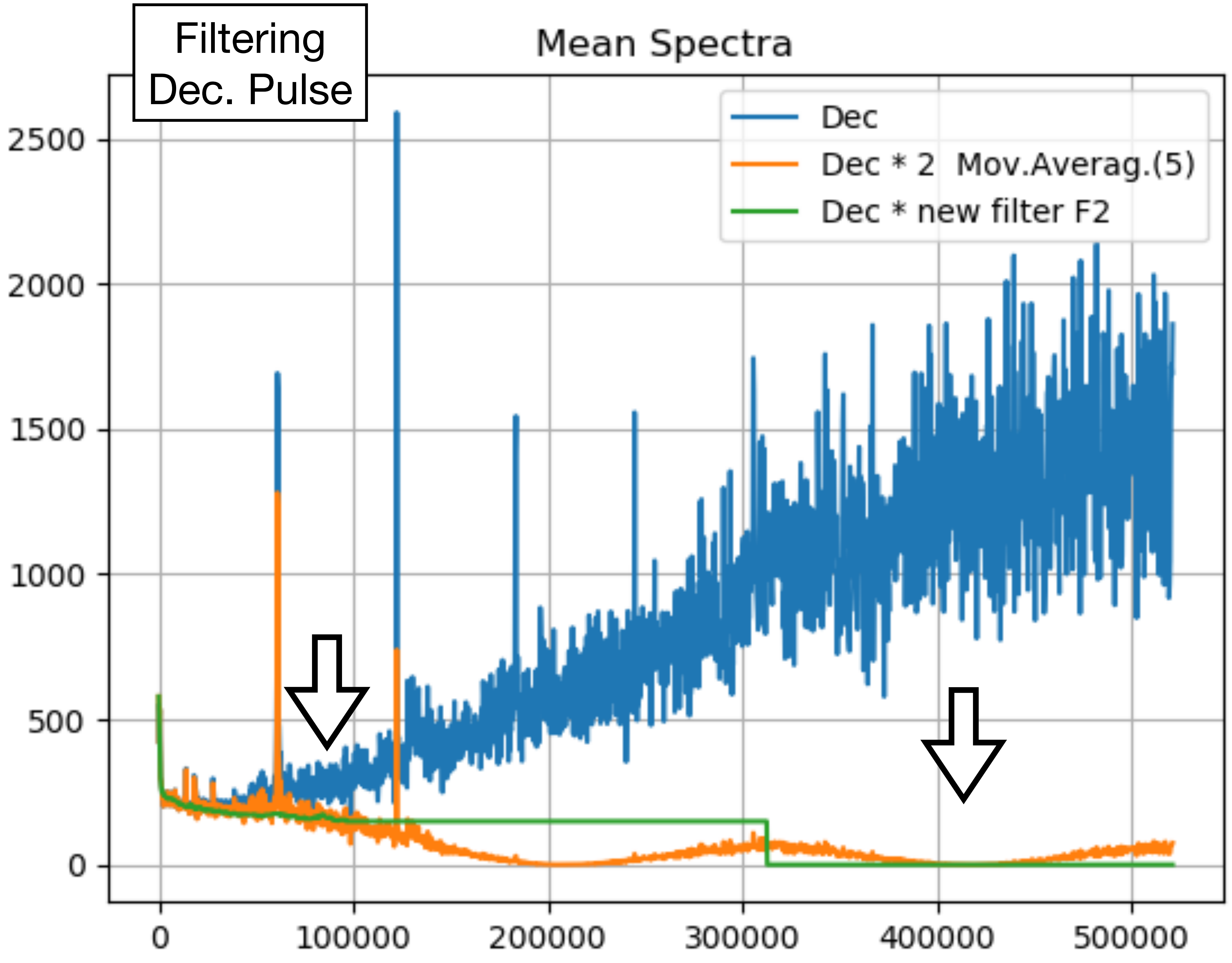

Peak counting algorithms

Looking for an algorithm to separate signal into individual avalanches from primary electrons

- Attempt 1 (GG): Deconvolve « tuned » exponential from signal, do running average over 5 bins twice, then use threshold
- Attempt 2 (PL): Deconvolve preamplifier response from signal, apply filter to remove high frequency noise and specific noise lines, then use threshold or scipy.find_peak()
- Attempt 3 (DD): Deconvolve both preamplifier and ion current response from signal, do running average over 5 bins twice, then use ROOT's TSpectrum::Search() + gaussian fits

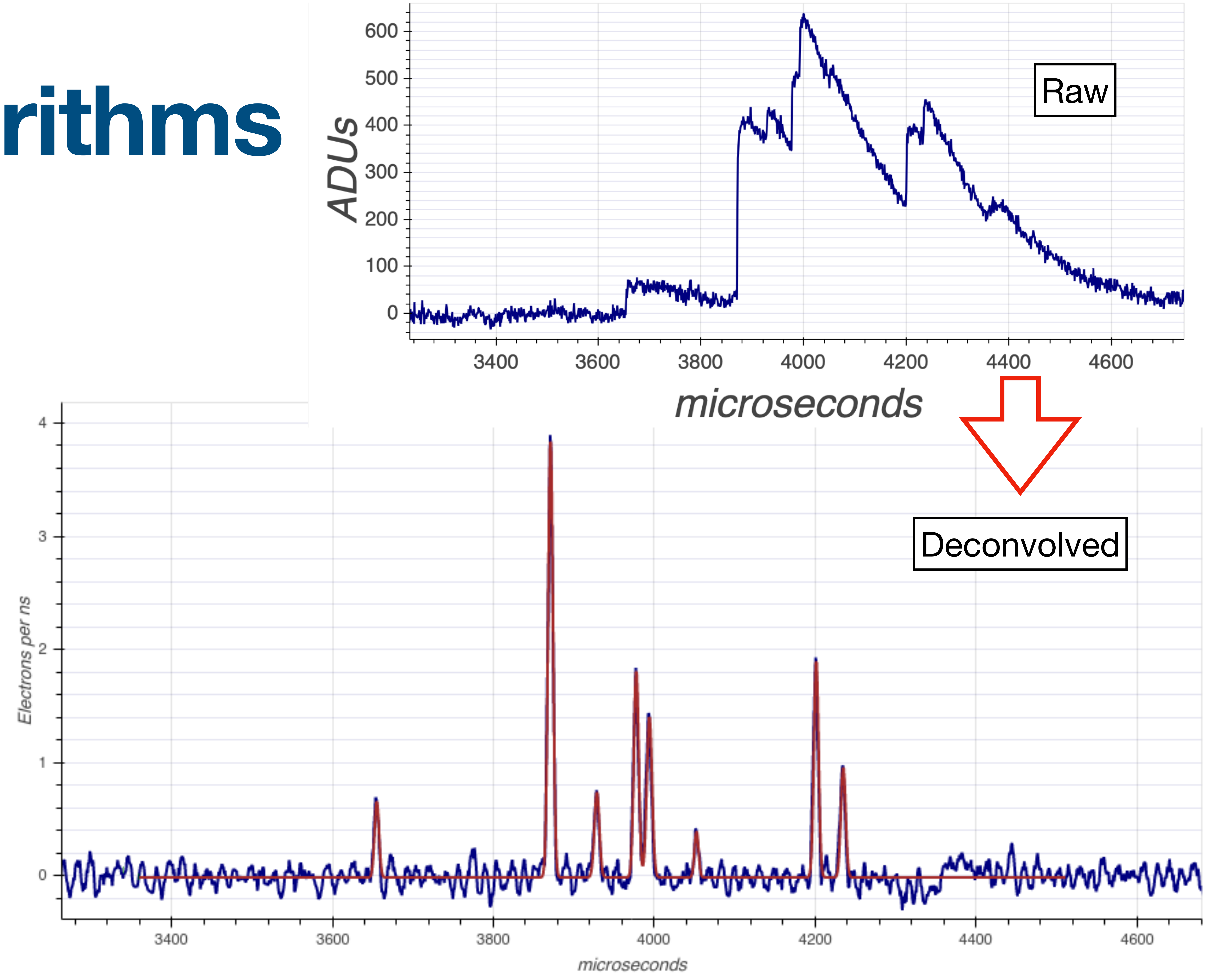

Detector simulation

ACHINOS : 5-6 configuration

- Detector simulation performed with Geant4, Garfield++, ANSYS
- Used to estimate fiducial volume of each channel, effect of the support structure, gas choice, etc.
- Predicted negative « crosstalk » signal on nearby anodes allows spurious pulse rejection

Use these (semi-calibrated) simulations to generate events to test the peak-counting algorithms on

Near/North

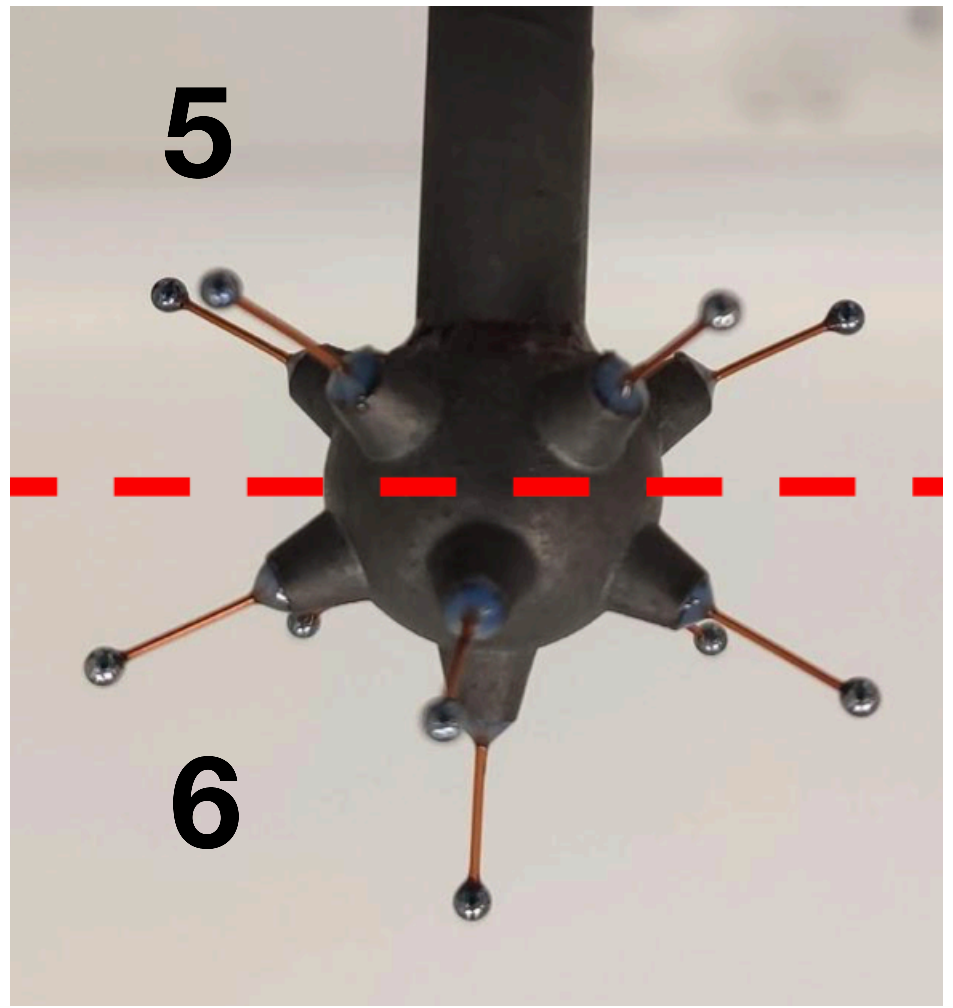

Far/South

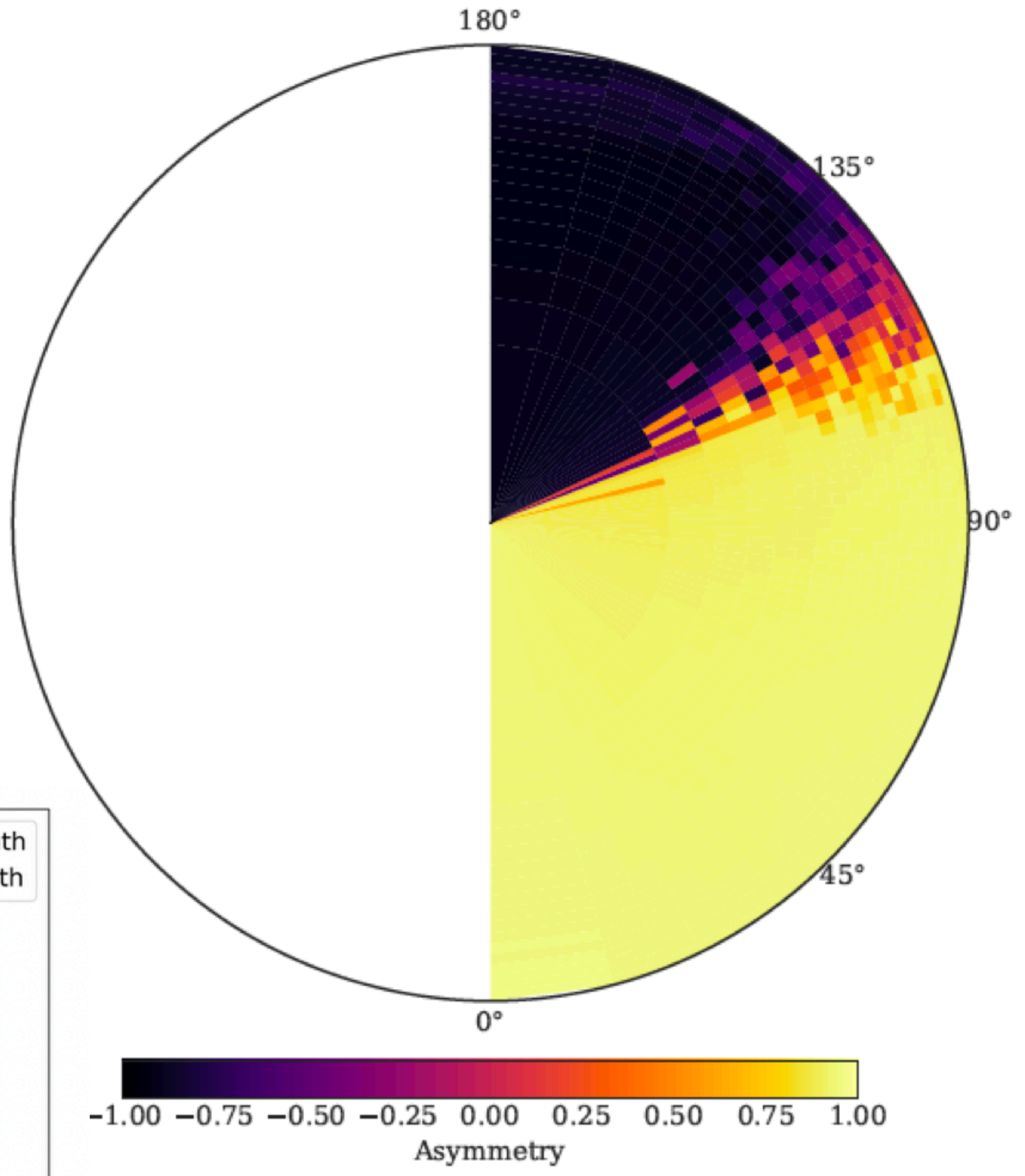

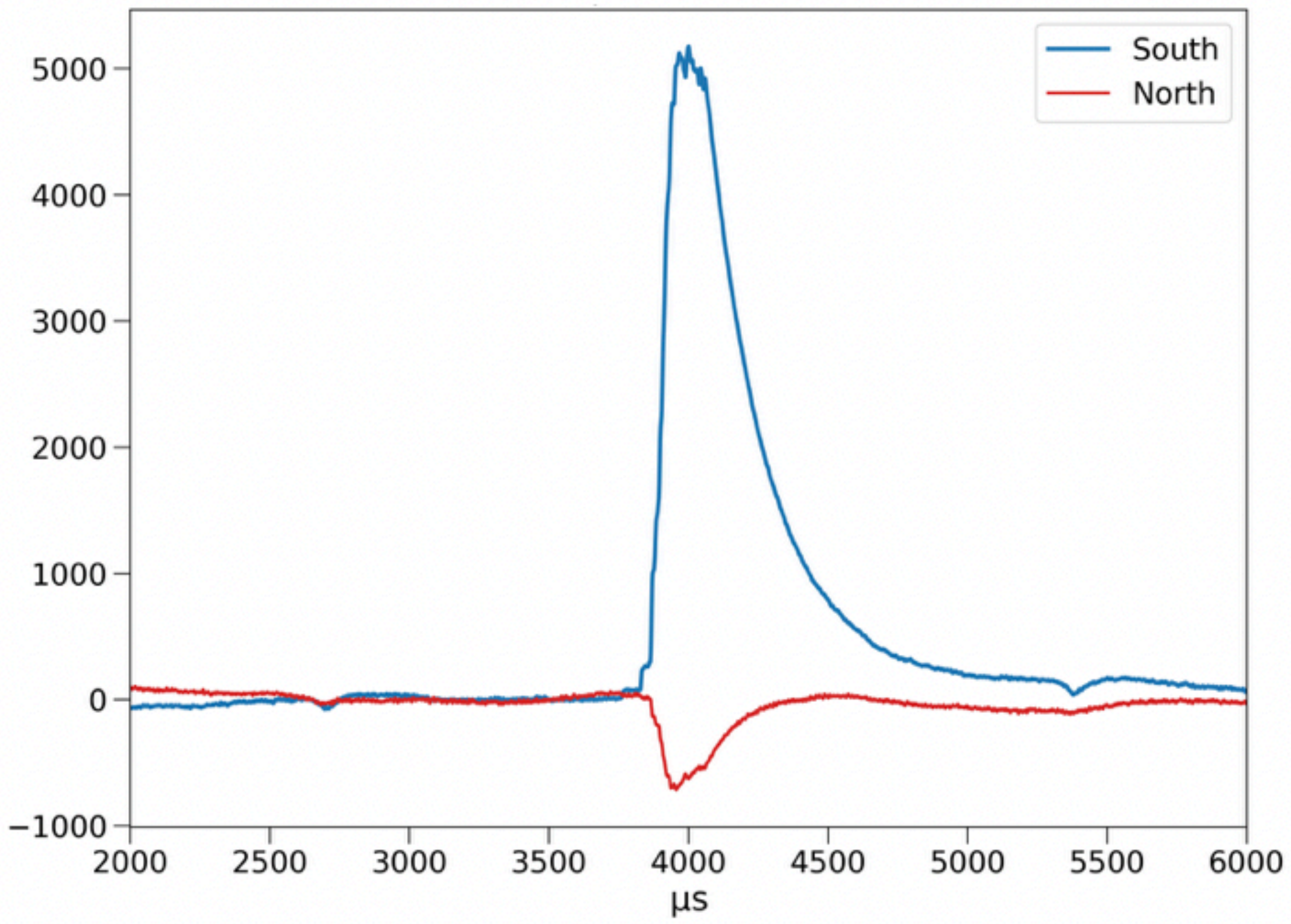

R. Ward et al 2020 JINST 15 C06013

I. Giomataris et al 2020 JINST 15 P11023

Peak counting: Performance

- 1st measure of quality: identification of electrons vs rate of false positives due to baseline noise
  - NOTE: This is not used as triggering algorithm, the « FP rate » is only applied for ~1ms around each trigger.
  - Maximum allowed FP rate set such that « natural » 2-peak event rate much larger than the one induced by baseline noise in 21h test physics data

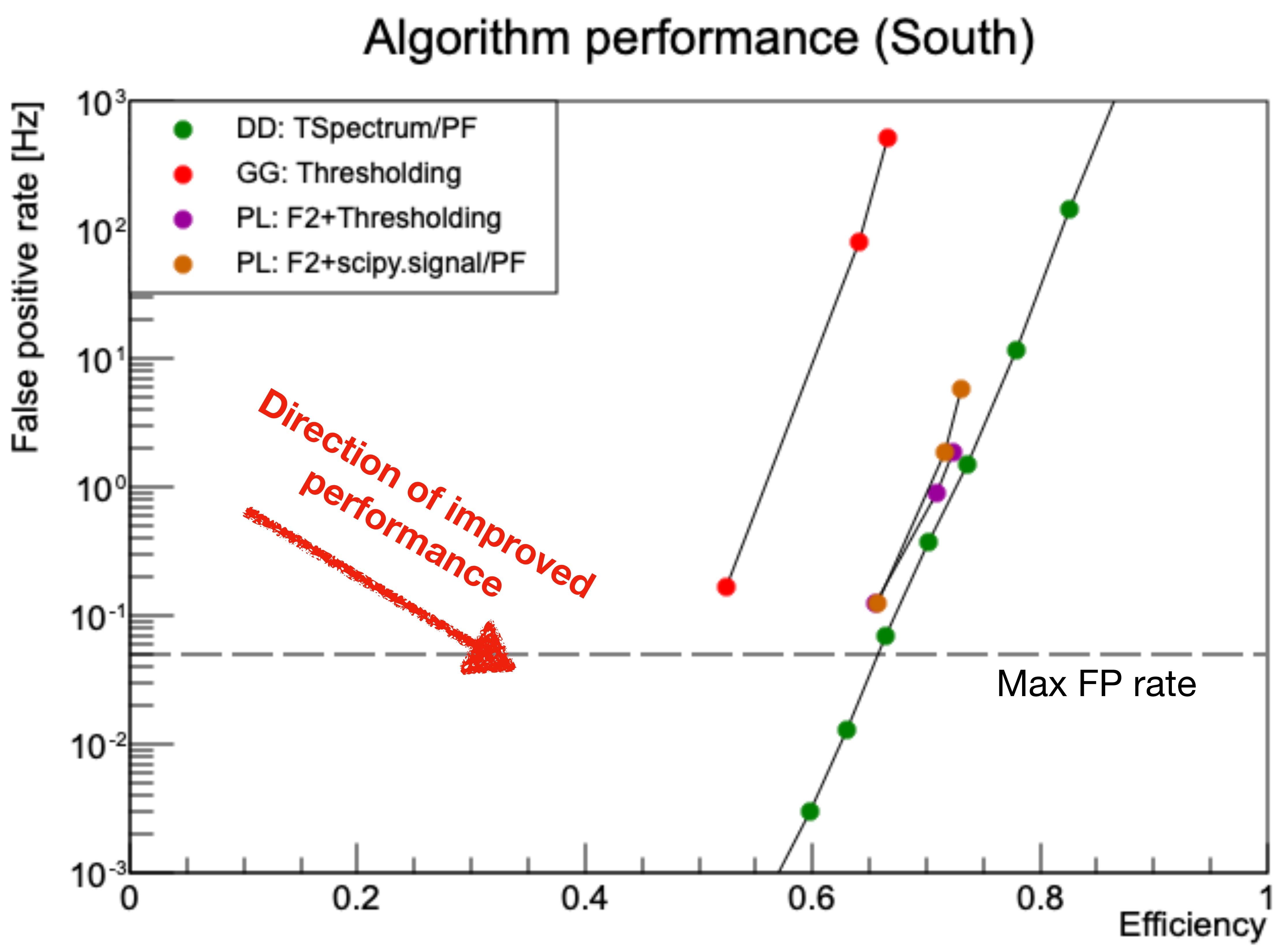

Peak counting: Performance

- 1st measure of quality: identification of electrons vs rate of false positives due to baseline noise
  - NOTE: This is not used as triggering algorithm, the « FP rate » is only applied for ~1ms around each trigger.
  - Maximum allowed FP rate set such that « natural » 2-peak event rate much larger than the one induced by baseline noise in 21h test physics data
- 2nd measure of quality: capacity to separate peaks next to each other

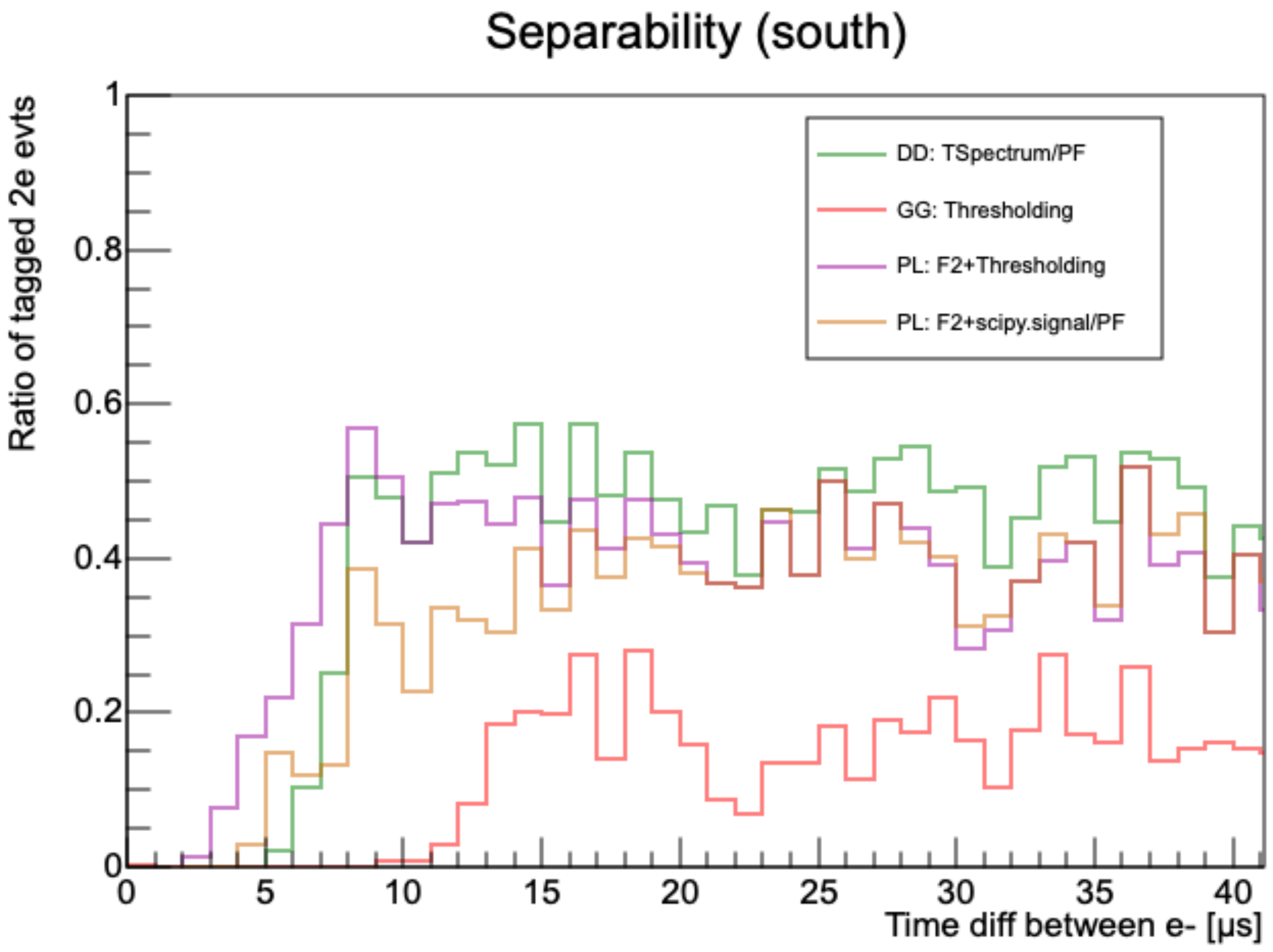

Peak counting: Performance

- 1st measure of quality: identification of electrons vs rate of false positives due to baseline noise
  - NOTE: This is not used as triggering algorithm, the « FP rate » is only applied for ~1ms around each trigger.
  - Maximum allowed FP rate set such that « natural » 2-peak event rate much larger than the one induced by baseline noise in 21h test physics data
- 2nd measure of quality: capacity to separate peaks next to each other

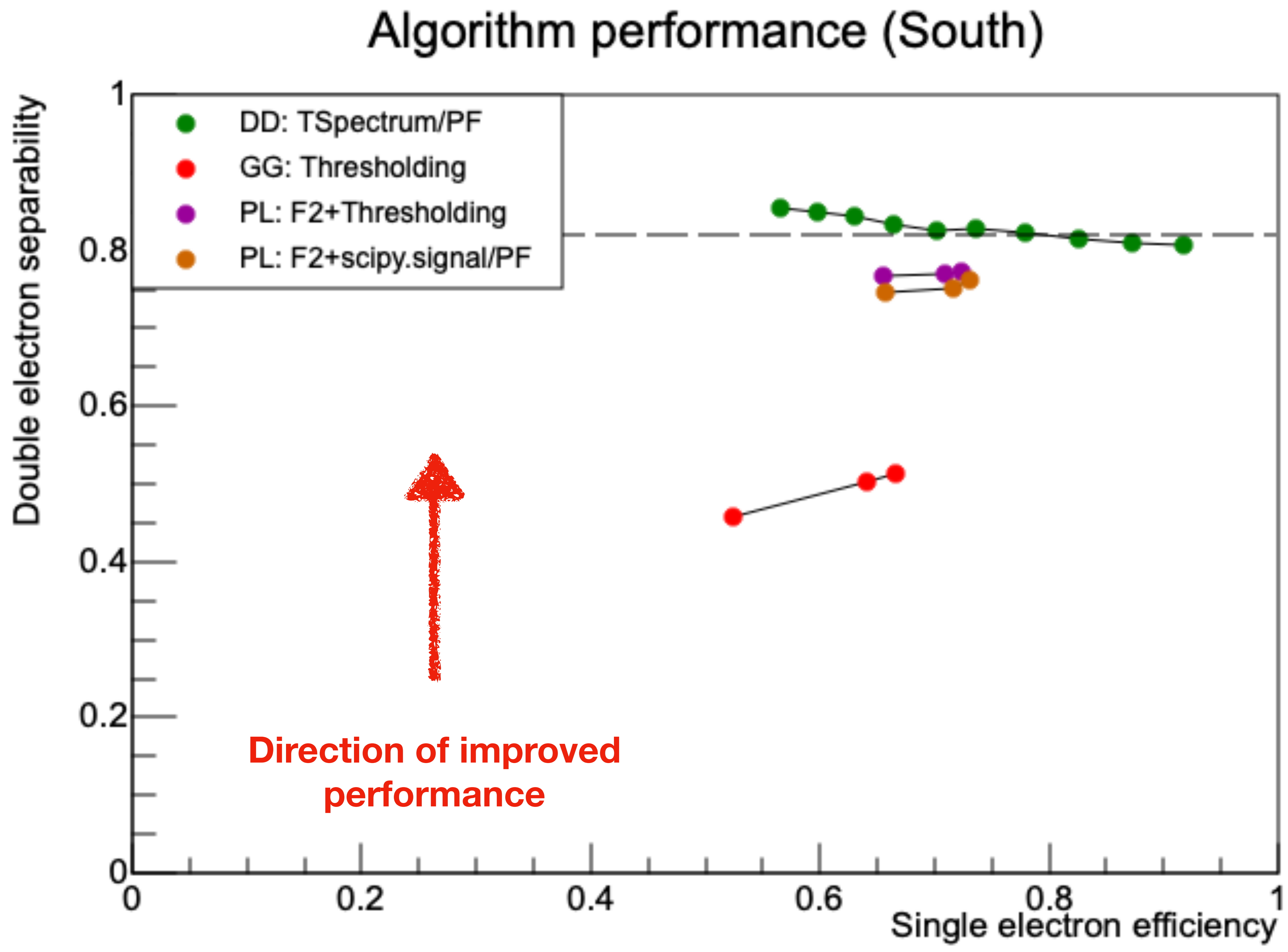

Use 3rd algorithm : double deconvolution & ROOT's TSpectrum

Peak counting: Time separation power

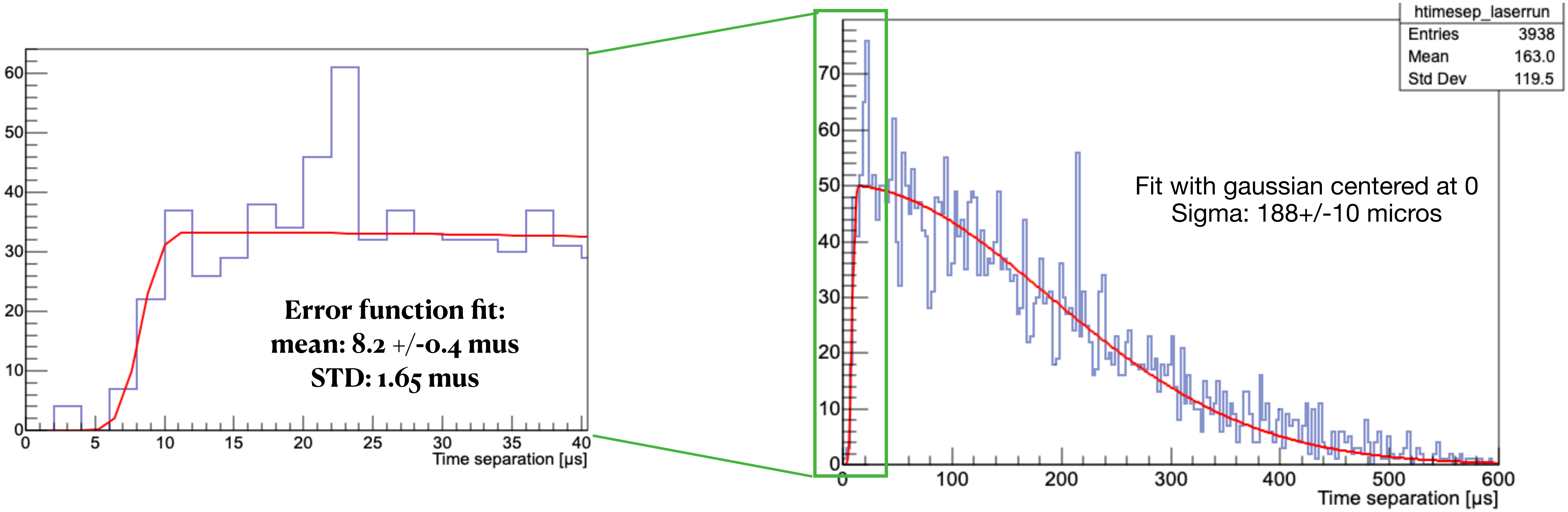

- Laser produces surface events, with fixed diffusion: 2-peak time separation laser data should follow gaussian centered at 0. Can use it to characterise algorithm
- Algorithm splits 95% of peaks if 10 microseconds away from each other

PSD cuts

Pulse Shape Discrimination

- Spurious pulses generated in the electronics do not have characteristic shape of physical pulses

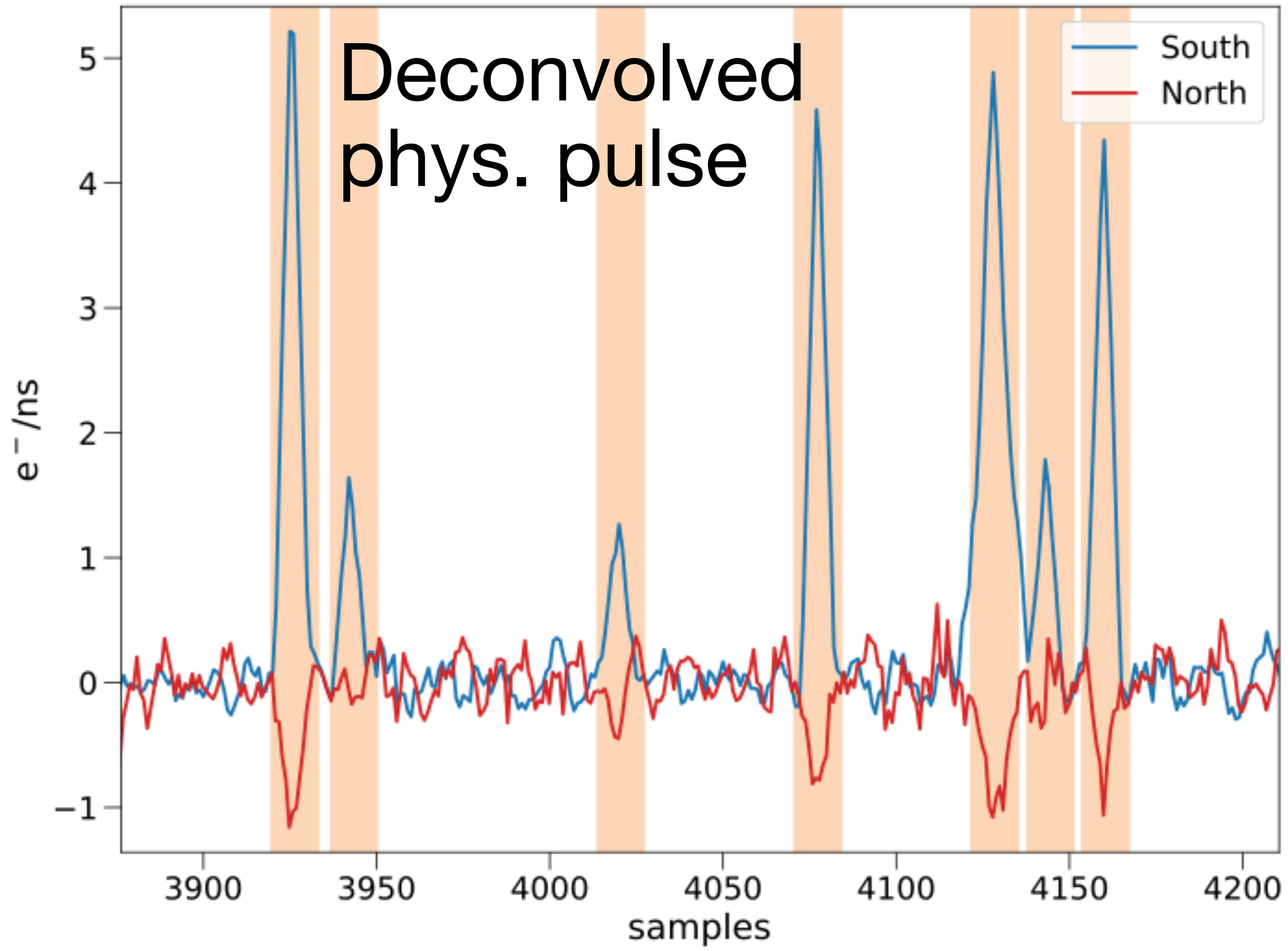

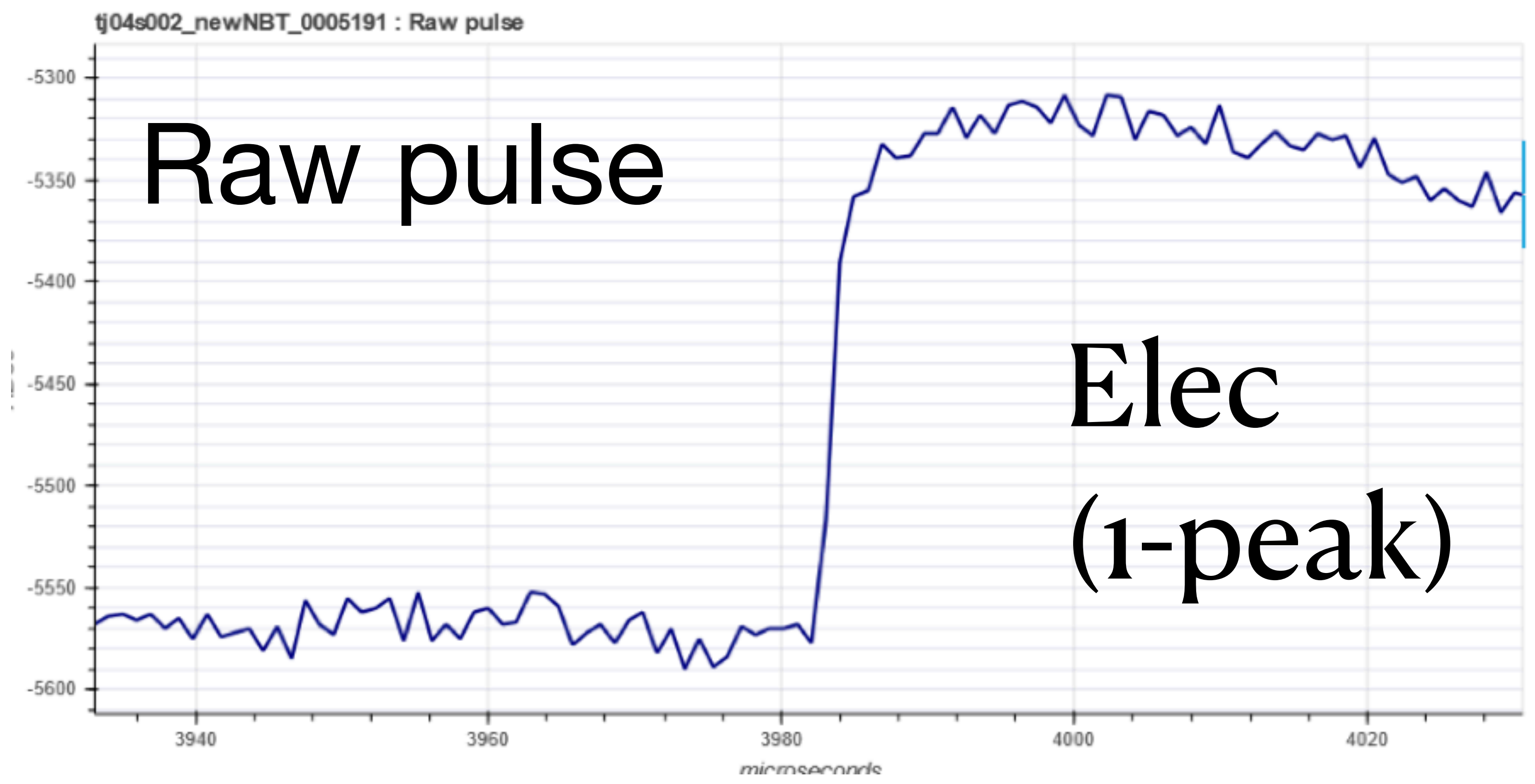

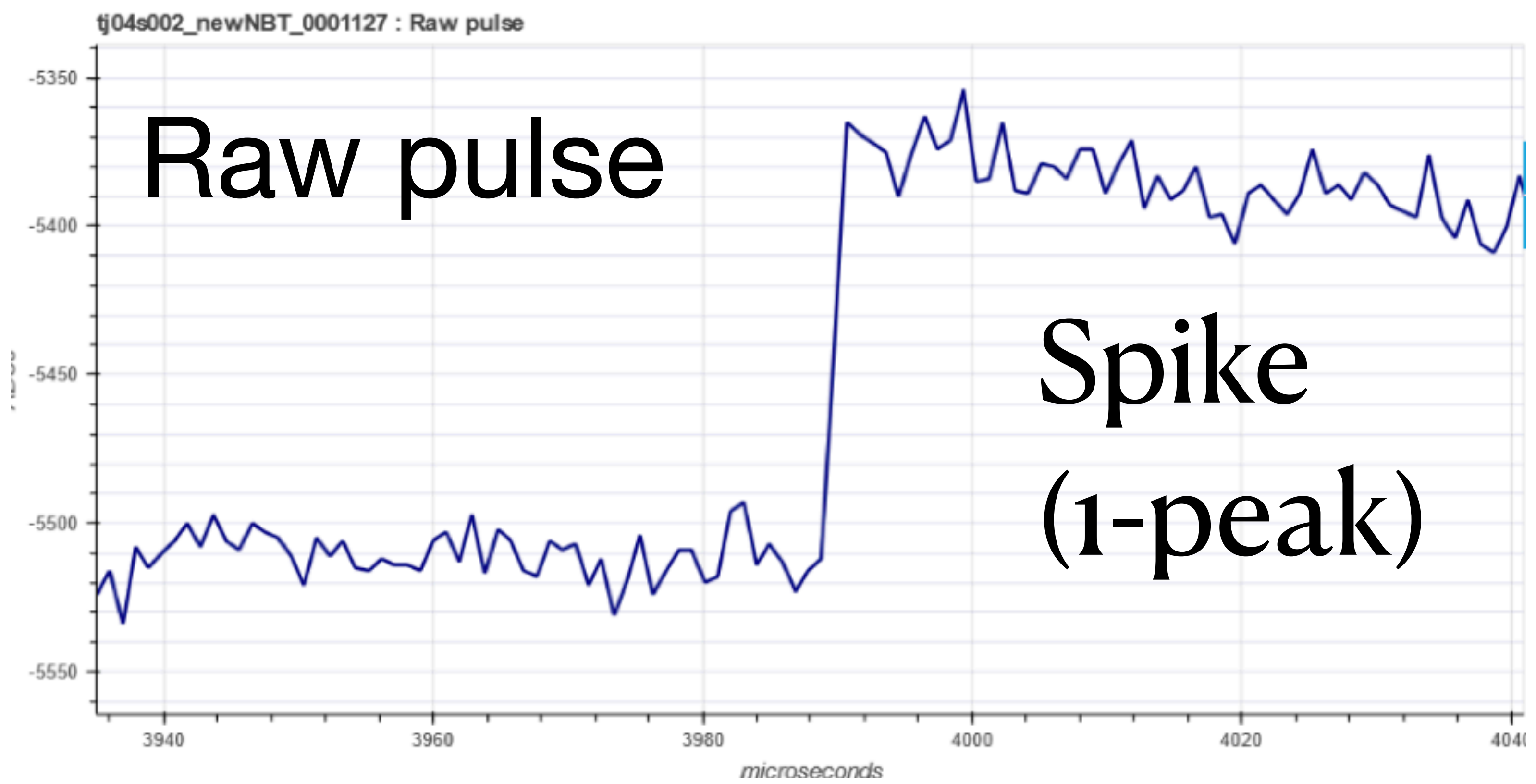

Pulse Shape Discrimination

- Spurious pulses generated in the electronics do not have characteristic shape of physical pulses
- Use Crosstalk (Ampl_North/Ampl_South) and Spikiness (MaxDerivative/Ampl) as variables to discriminate both populations
- Cuts are chosen by comparing single-peak events from laser calibrations with those from test physics data

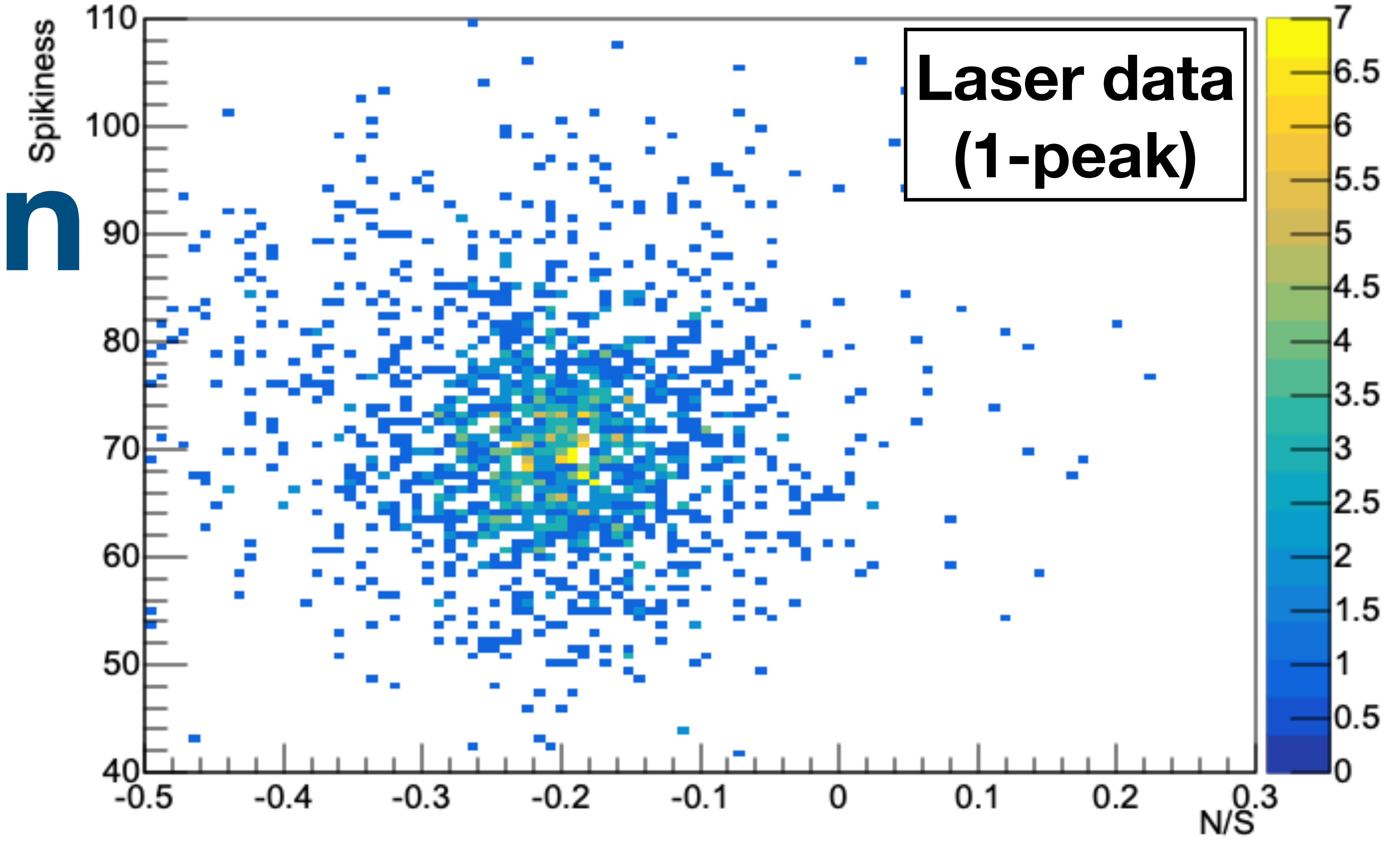

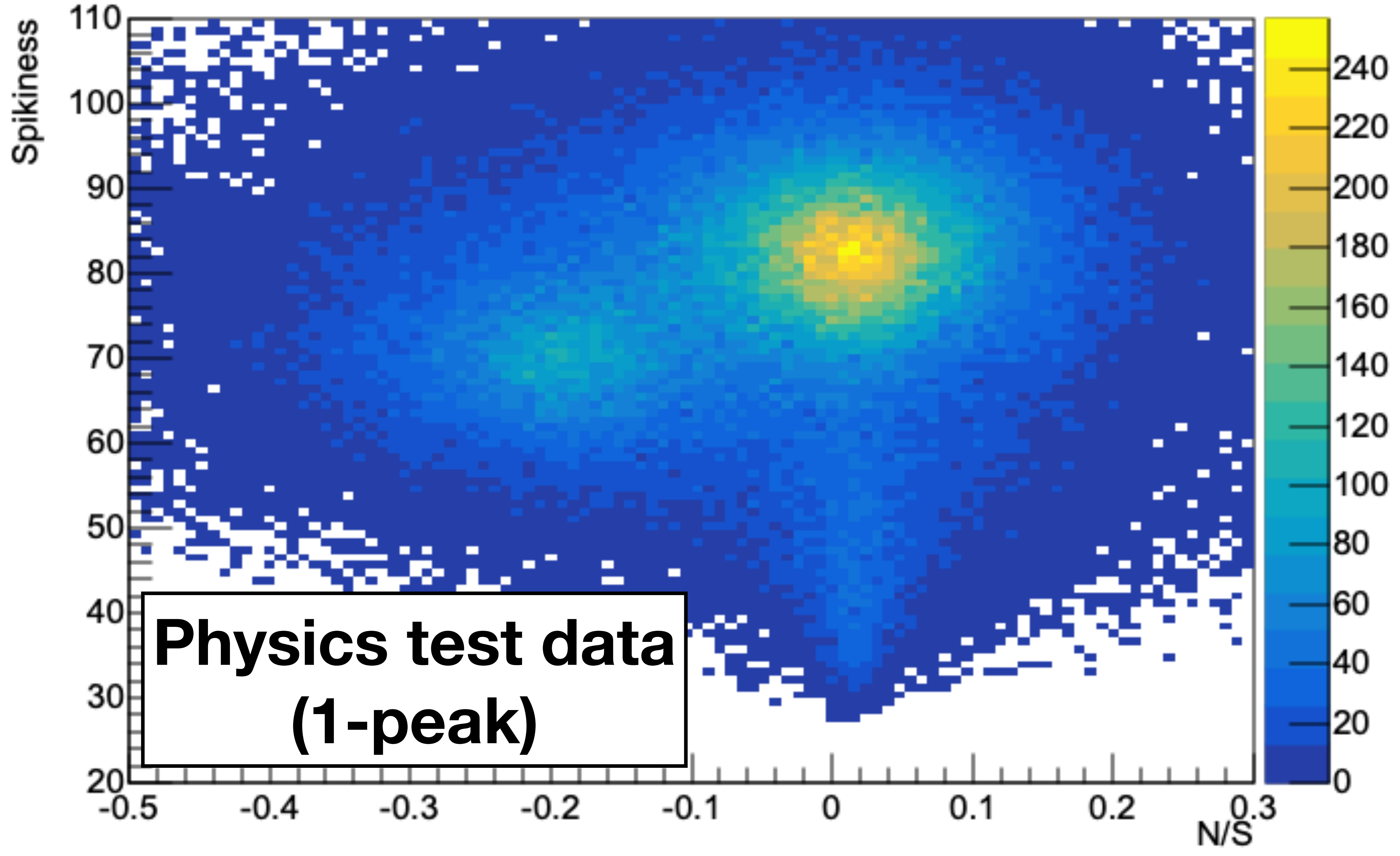

Pulse Shape Discrimination

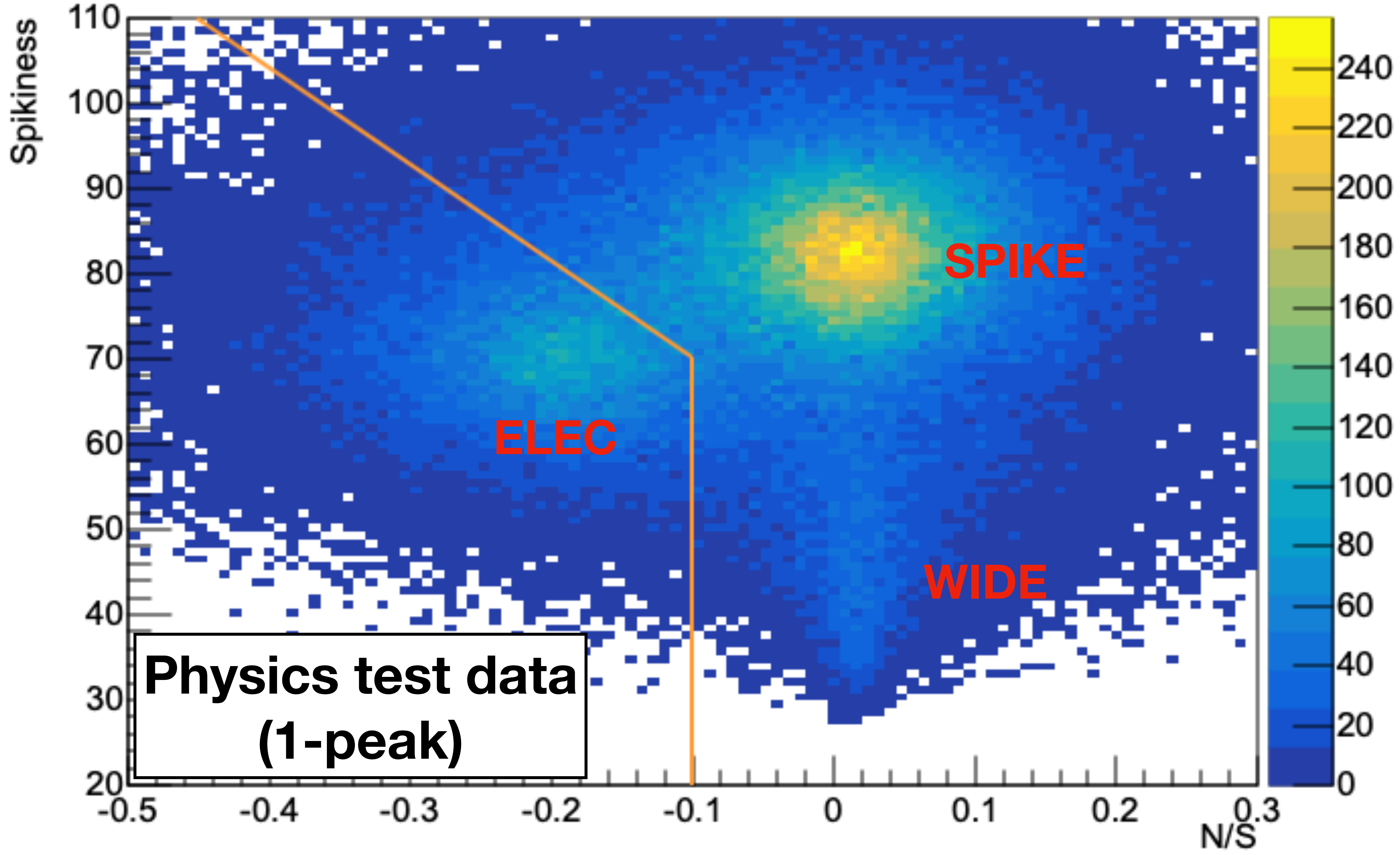

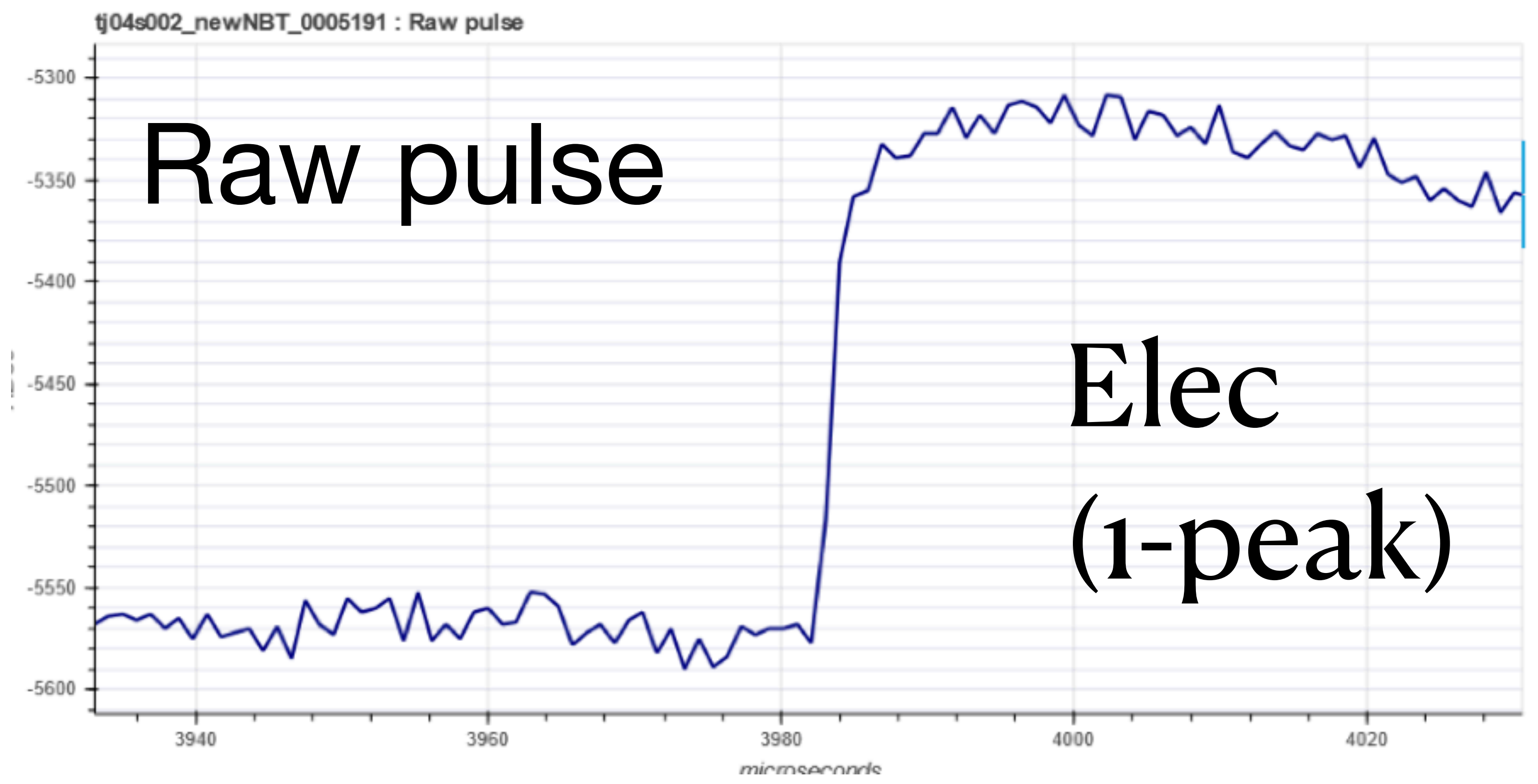

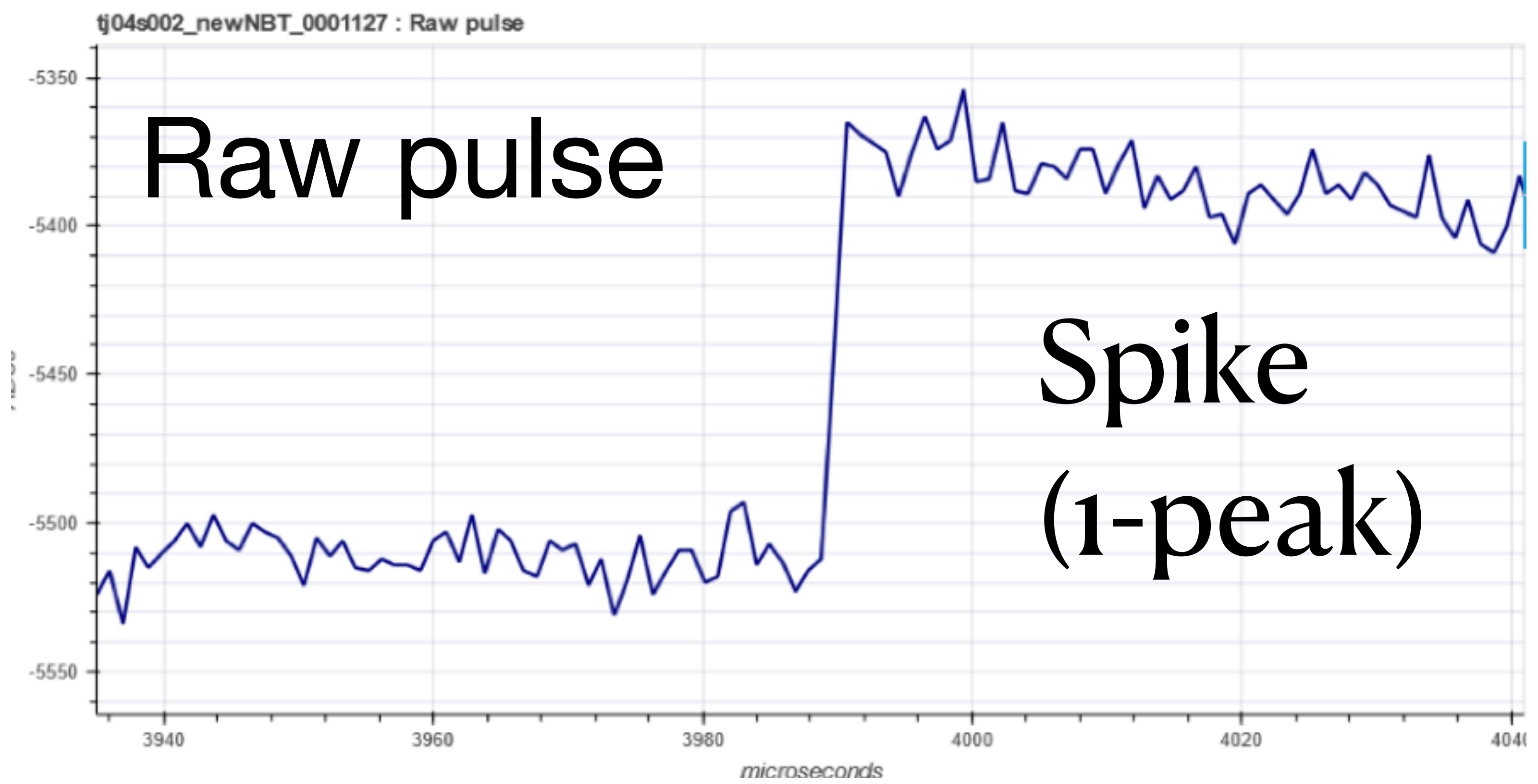

- Fisher discriminant cut is used against « spikes », simple crosstalk cut is used against « wide pulses »
- Keeps 77% of physical events, and rejects ~95% of spurious pulses

Time separation

New diffusion variable

- As we go to lower amplitudes / fewer primary electrons, risetime becomes « poorly defined », and worse at separating surface and volume events
- New variable tested: time separation between first and last peak found

CONTEXT: instead of doing a risetime cut to remove surface events, use knowledge of distribution of new diffusion variable to perform a background subtraction

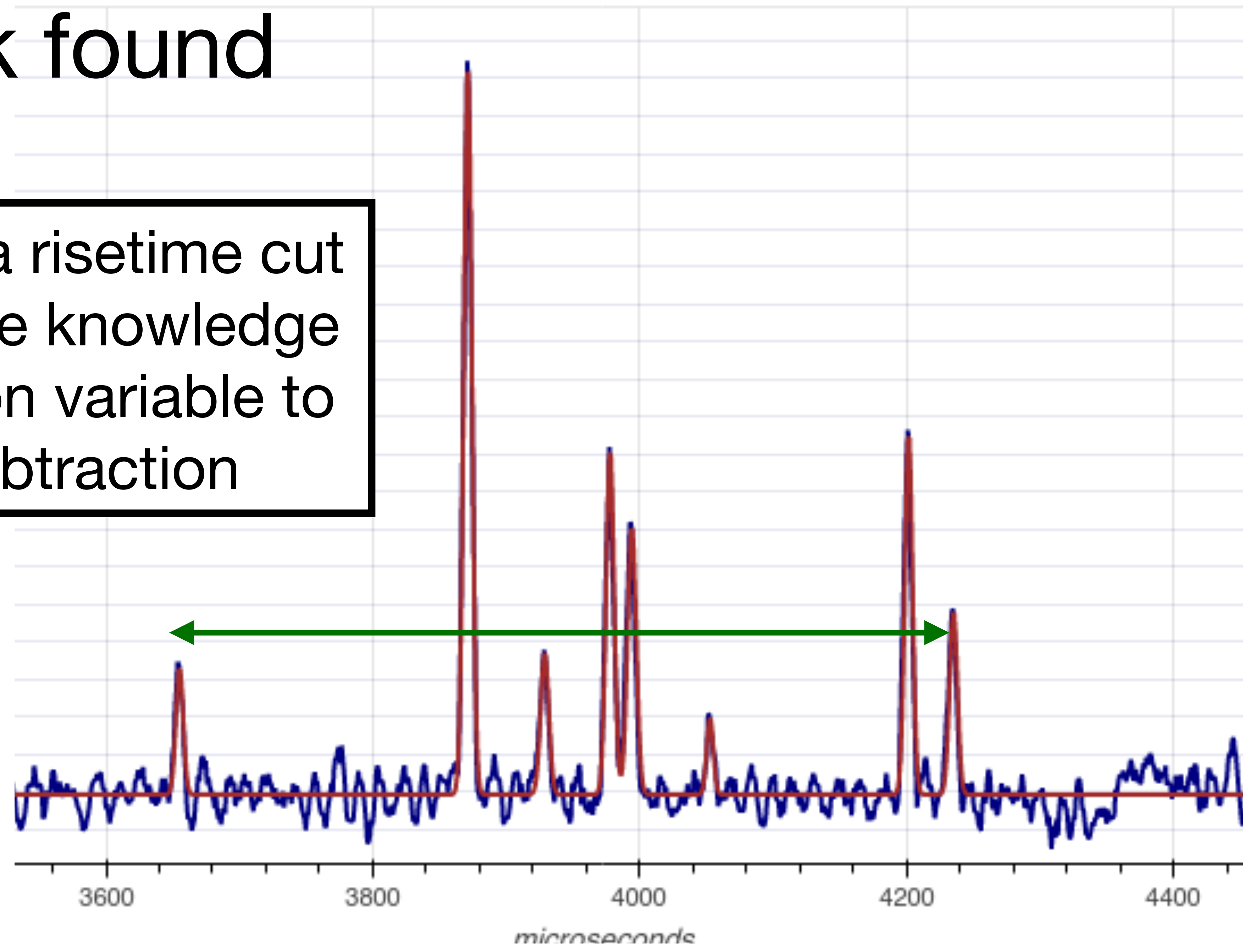

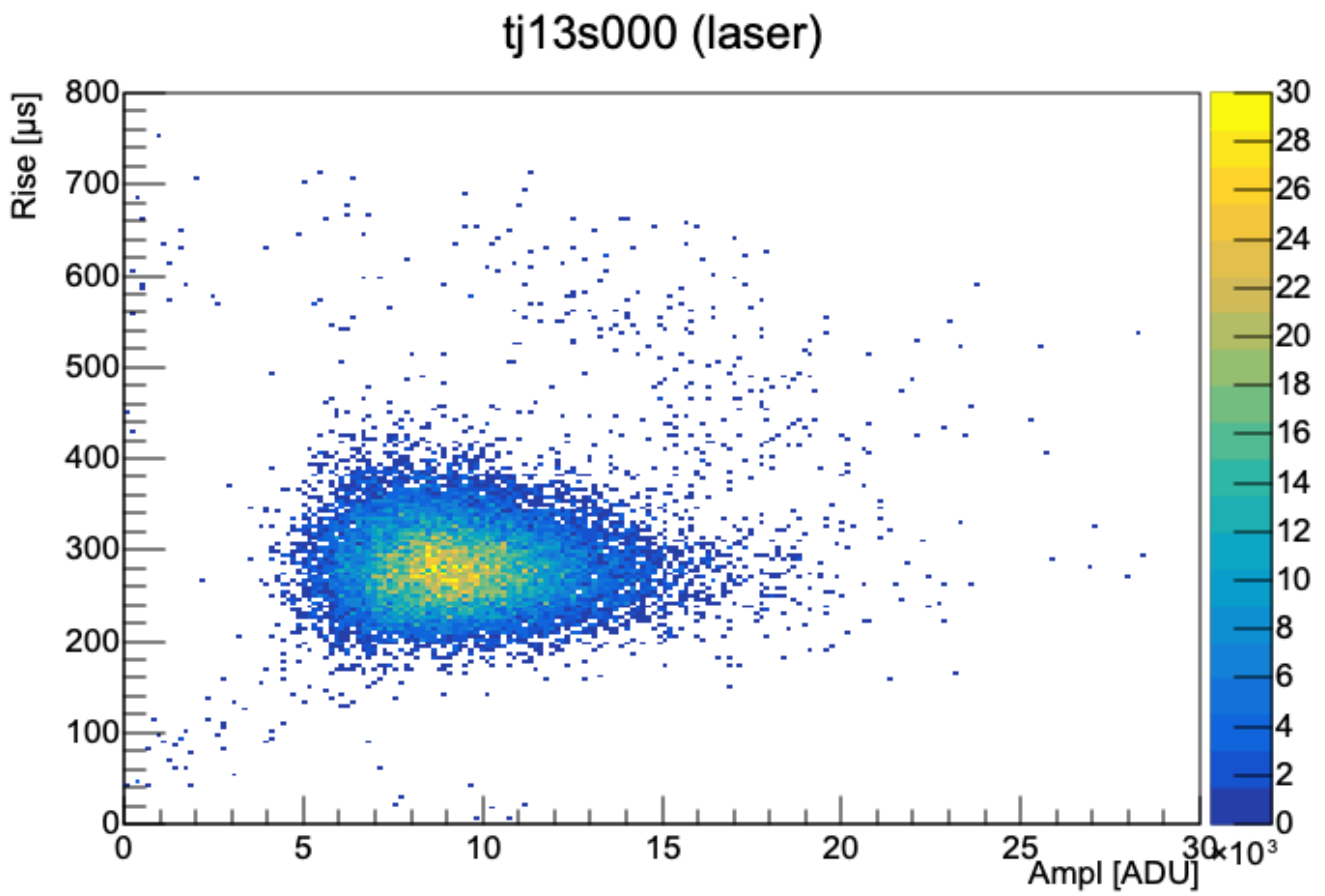

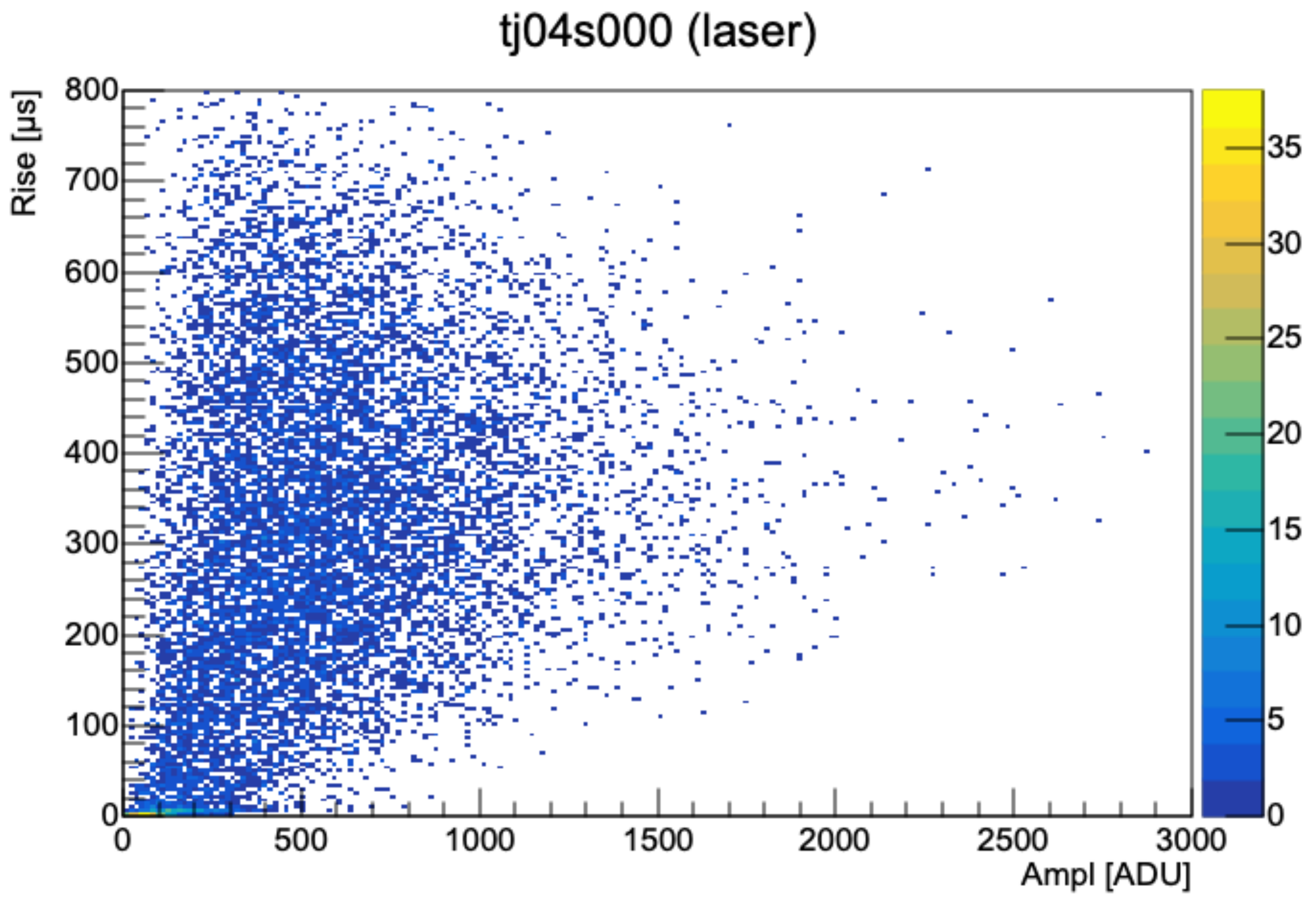

Toy model for time separation distribution

- For **n** primary electrons, draw **n** arrival times from a gaussian (standard deviation given by calibrations, and whether we're interested in surface or volume events). Order their arrival times;
- Give each electron a chance to be detected based on attachment and algorithm single-peak finding efficiency;
- Give each set of consecutive electrons a chance to « overlap » and be counted as only one peak based on the calibrated time separation power of the algorithm (plus some corrections in case of multiple overlaps in a row)

Effect of overlapping peaks

Added effect of overlaps to toy model for 3-peak and 4-peak events. Much stronger effect on volume events than (intuitively) expected!

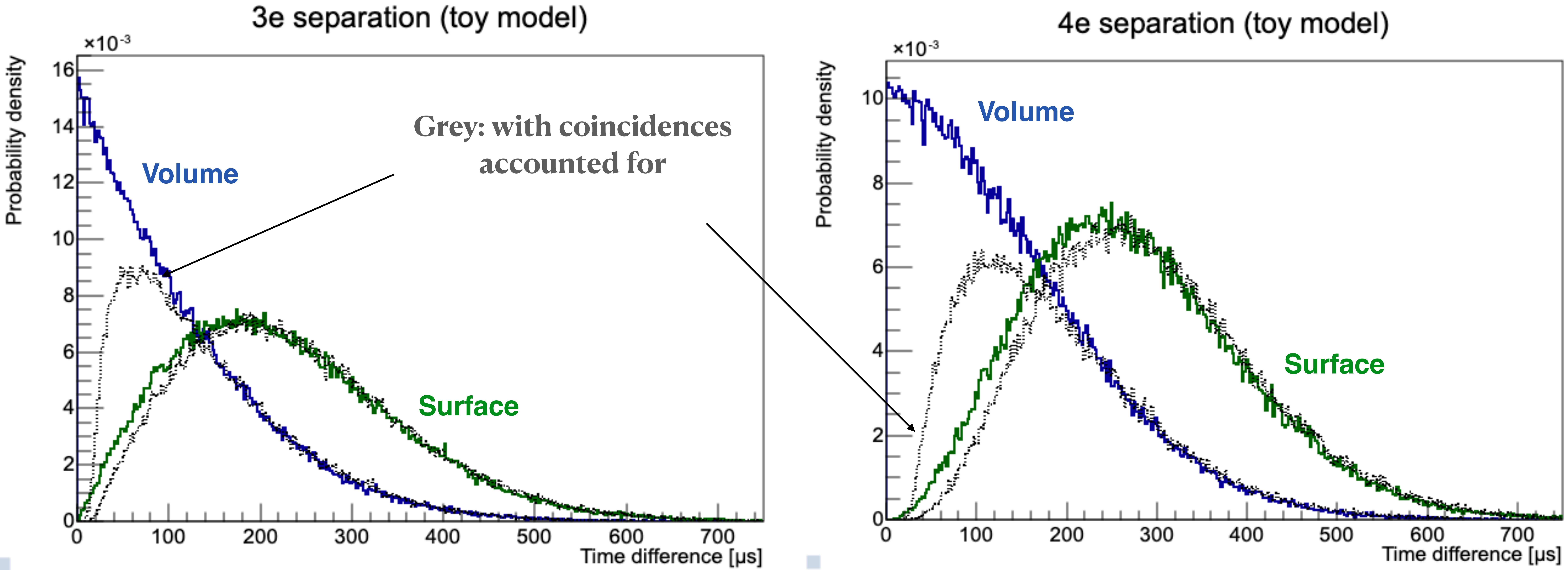

Laser data

- 2-peak, 3-peak, 4-peak laser data match 135 mus surface diffusion toy model perfectly!
  - Although note 2-peak data was used to calibrate the mean e- diffusion time and the algorithm time separation power

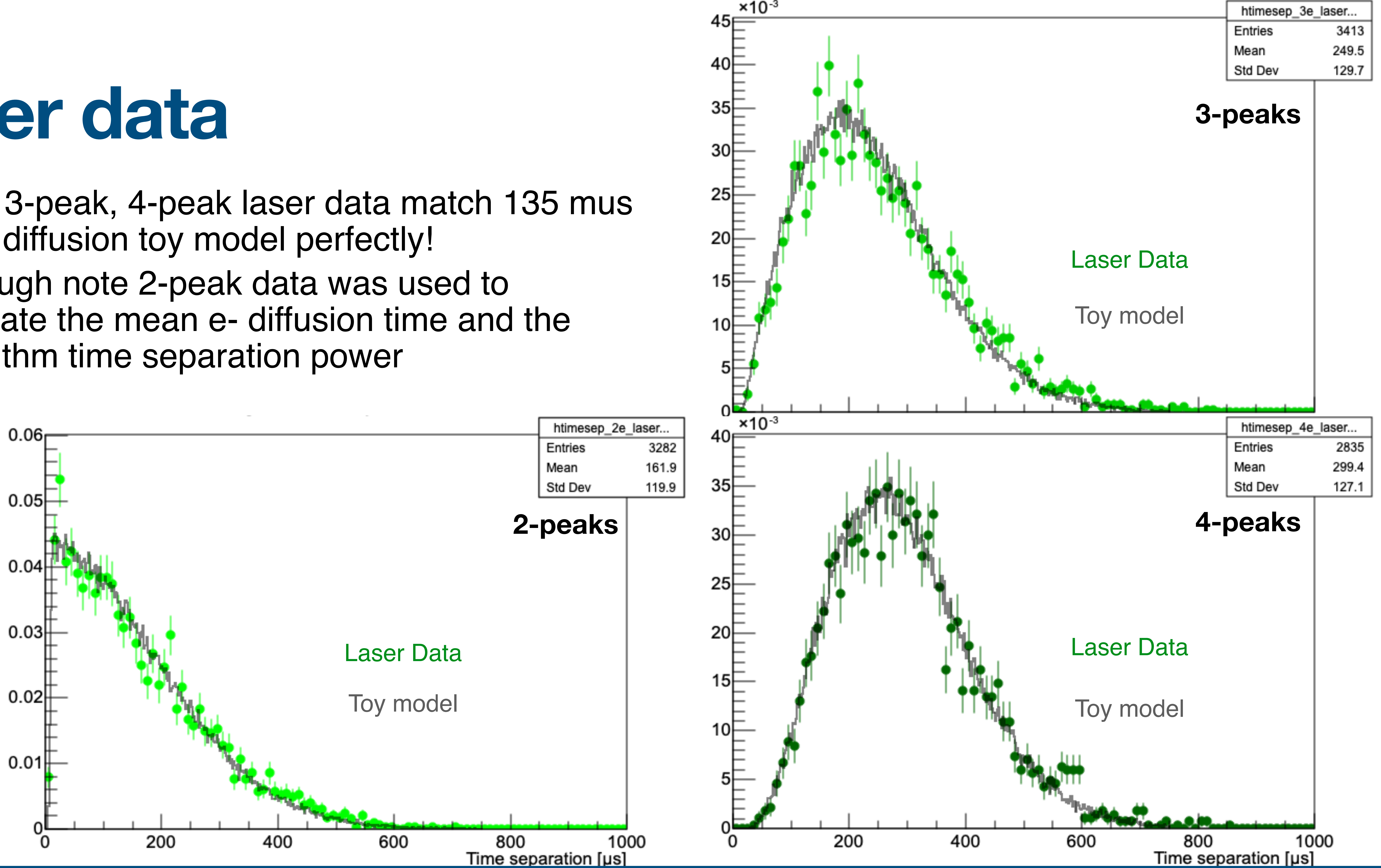

Volume diffusion time calibration

Fit Ar37 2.8 keV (source of volume events) risetime data with a series of gaussians with increasing width for increasing risetimes. Since the radii distribution of volume events in spherical symmetry is known, can convert the recovered distribution of diffusion values into a radius vs diffusion relation

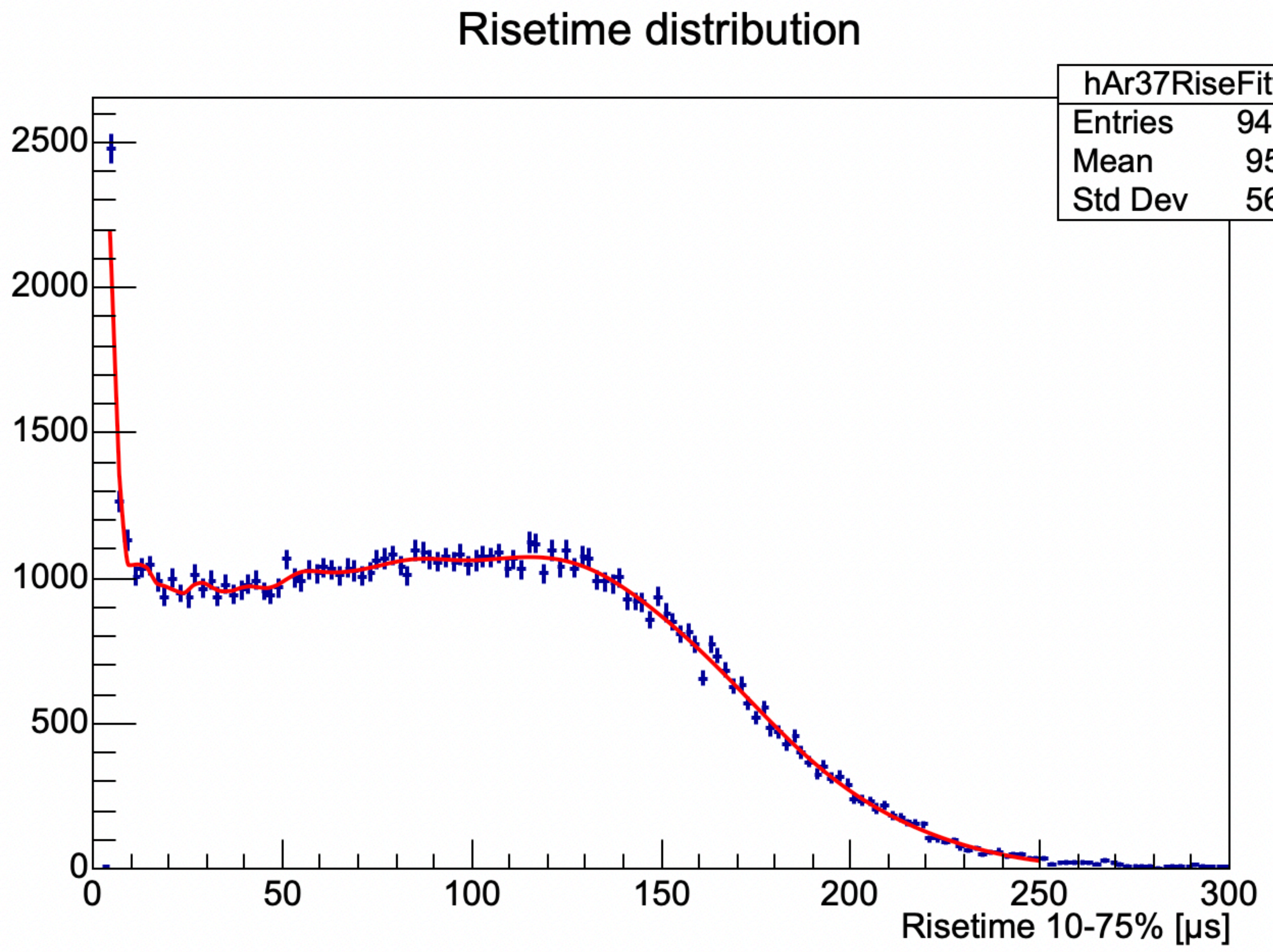

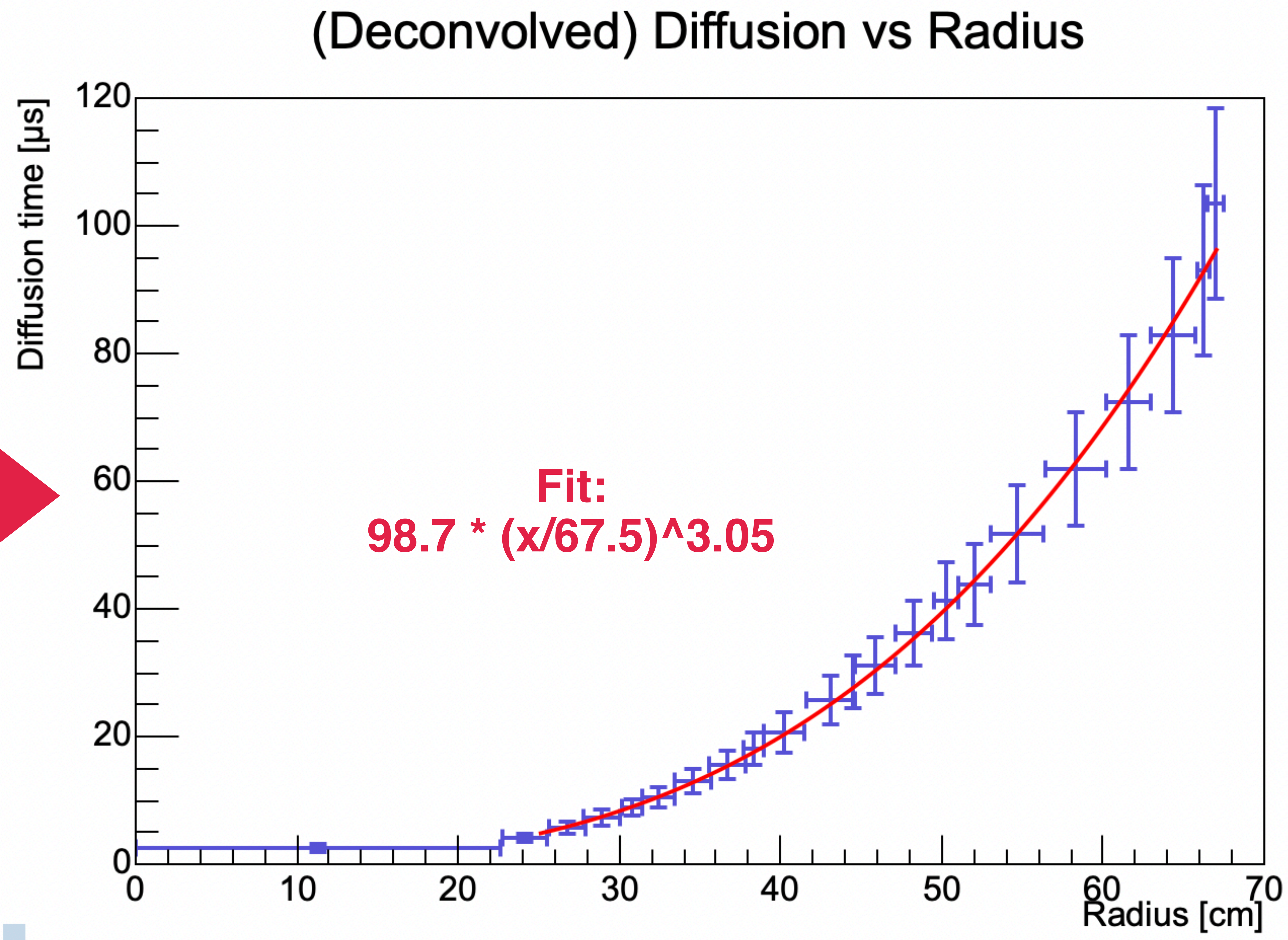

Ar37 data

- 270 eV peak from Ar37 produces some low-peak events
- Tail matches model, but data has more events at low time separation than model… even ignoring effect of algo. separation power

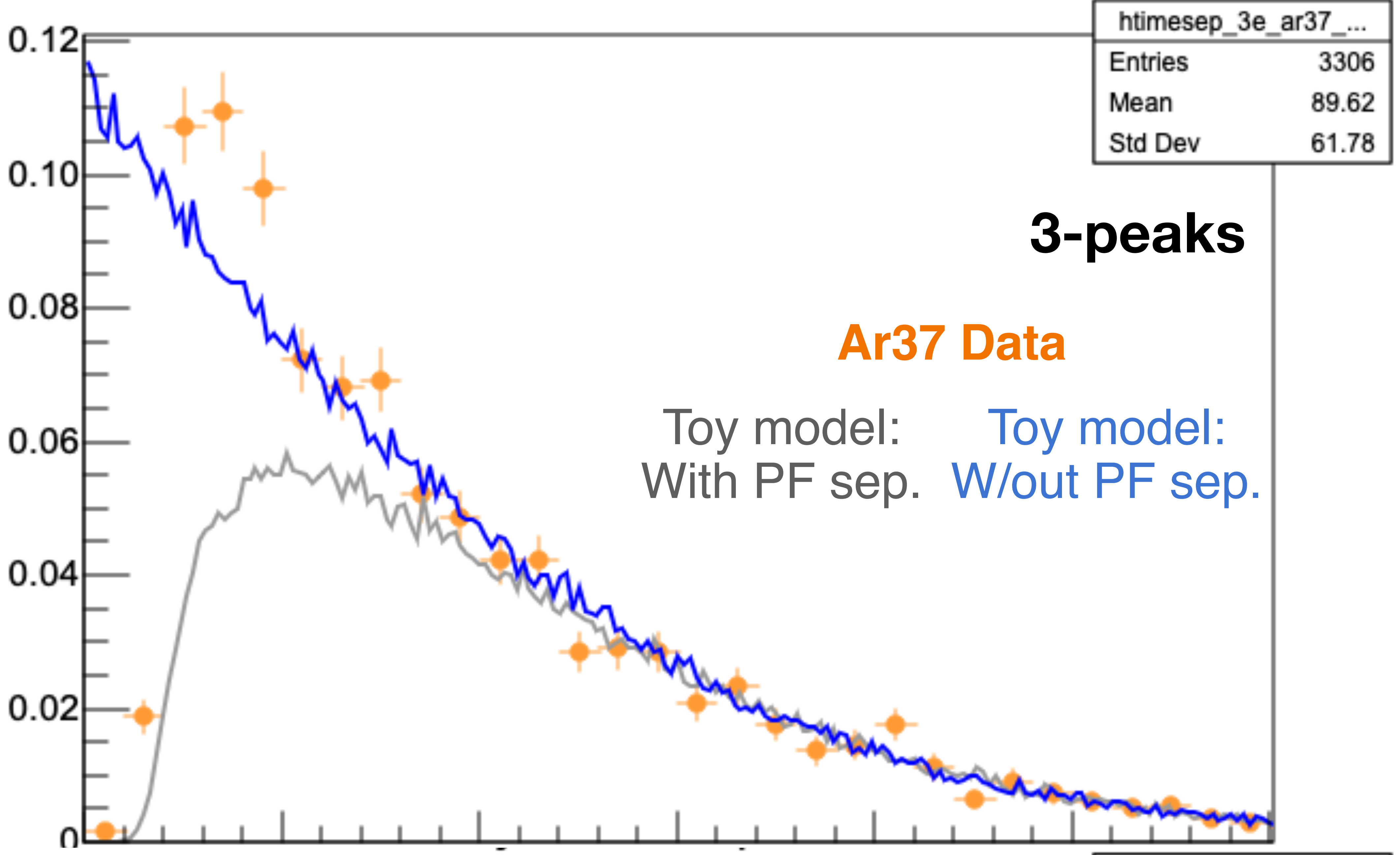

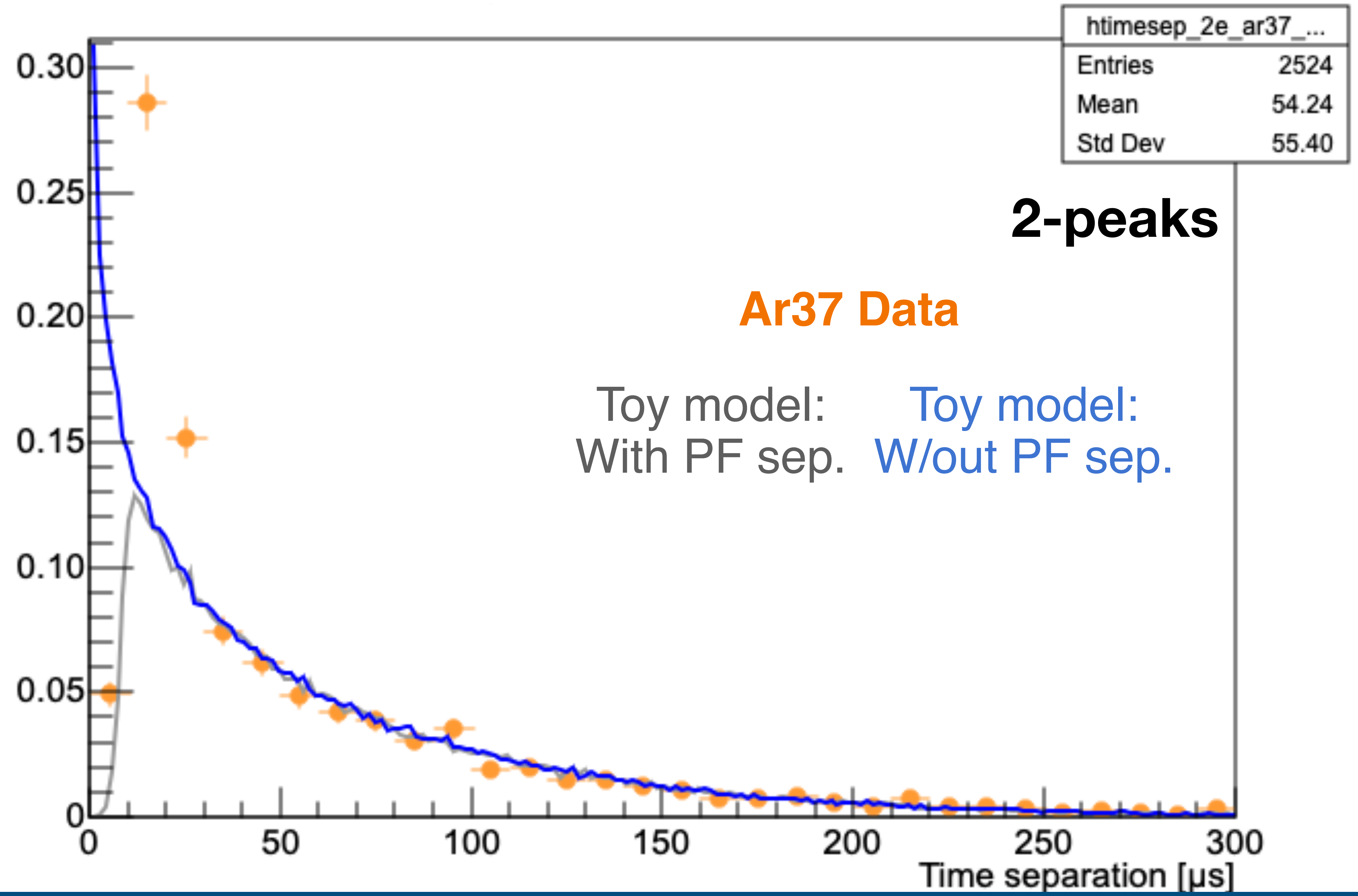

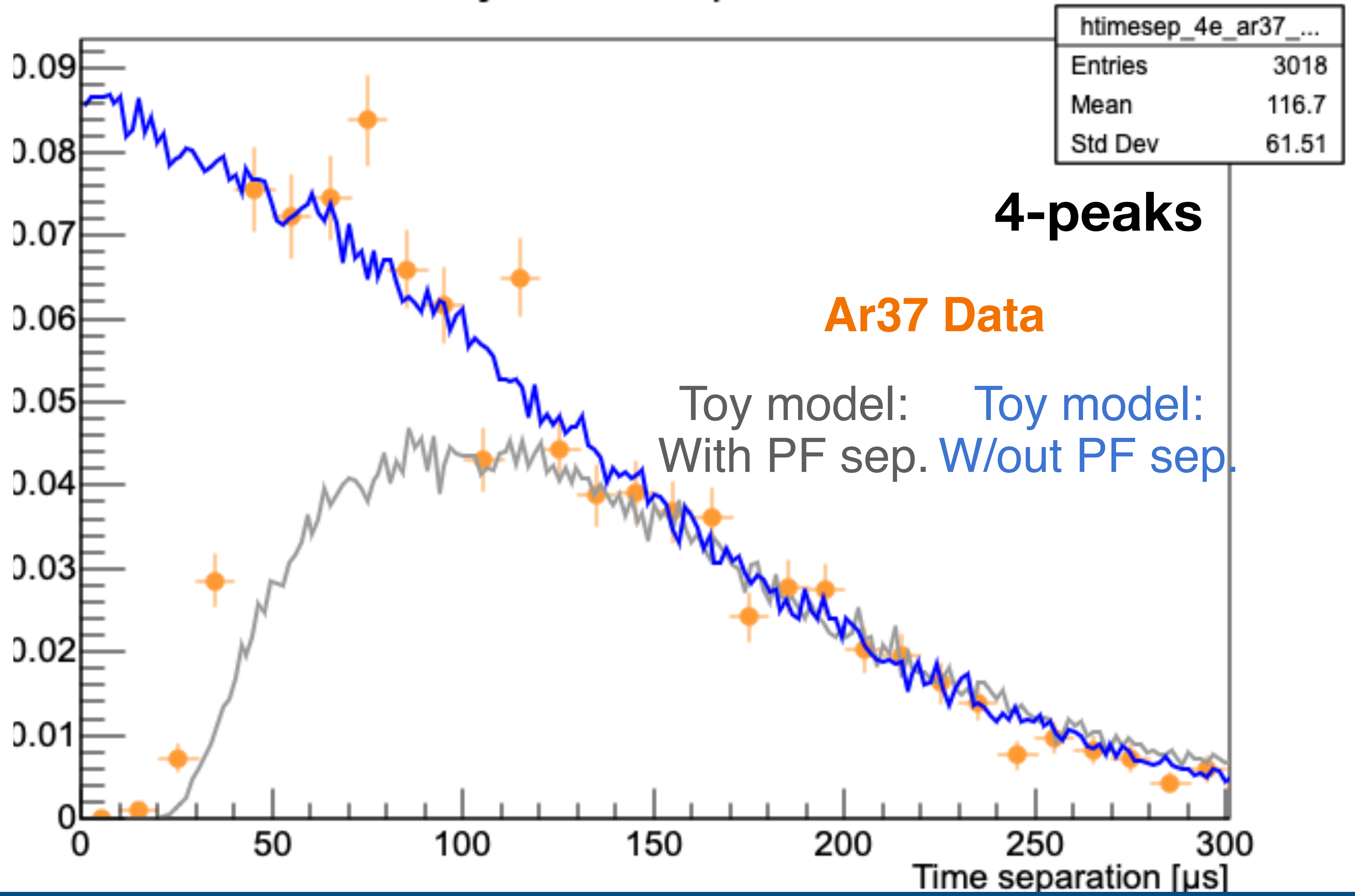

- Due to the larger diffusion time for surface events, overlapping peaks were rare, so they did not affect the time separation distribution of 2, 3, 4-peak events
- For volume events, an event with has a higher chance of being reconstructed as having less peaks than primary electrons when the electrons overlap: *the distribution of, e.g., 2e- events reconstructed as 2-peak is not the same as a 8e- events reconstructed as 2-peak!*

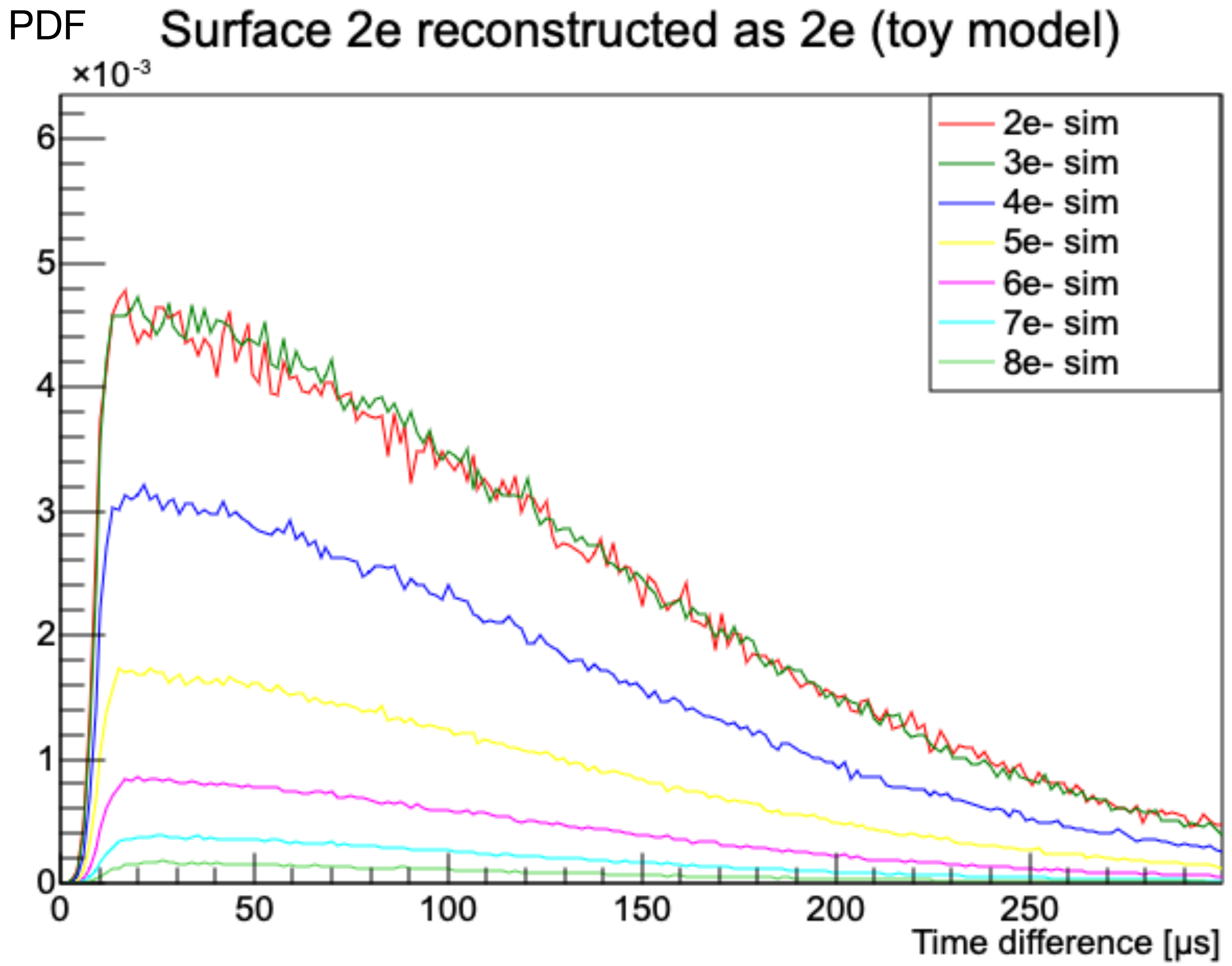

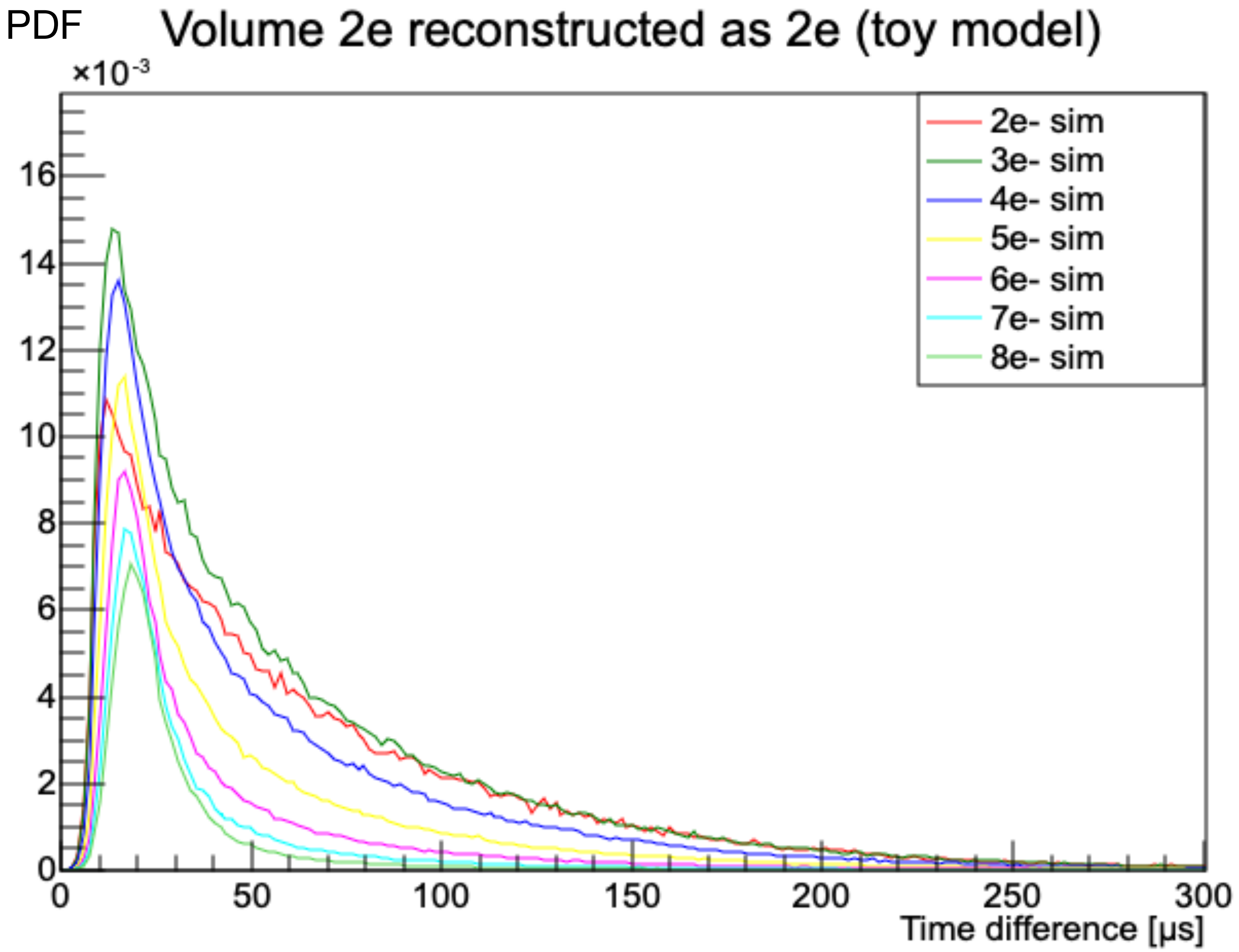

Ar37 data

- 2-peak, 3-peak, 4-peak Ar37 data match volume diffusion model very well, even though none of them were used to calibrate it!
- Agreement of model with both surface and volume data will allow for background subtraction in physics run

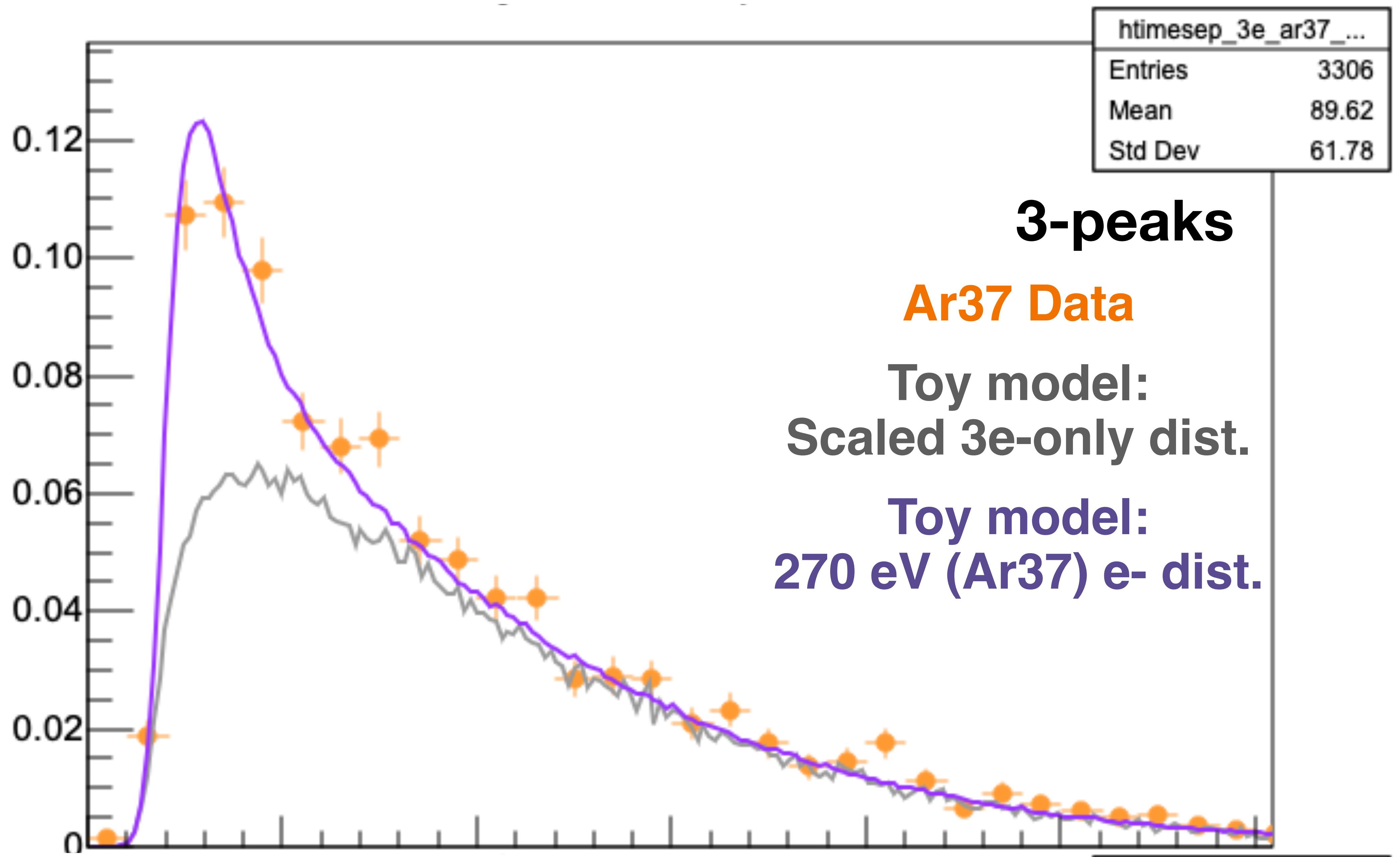

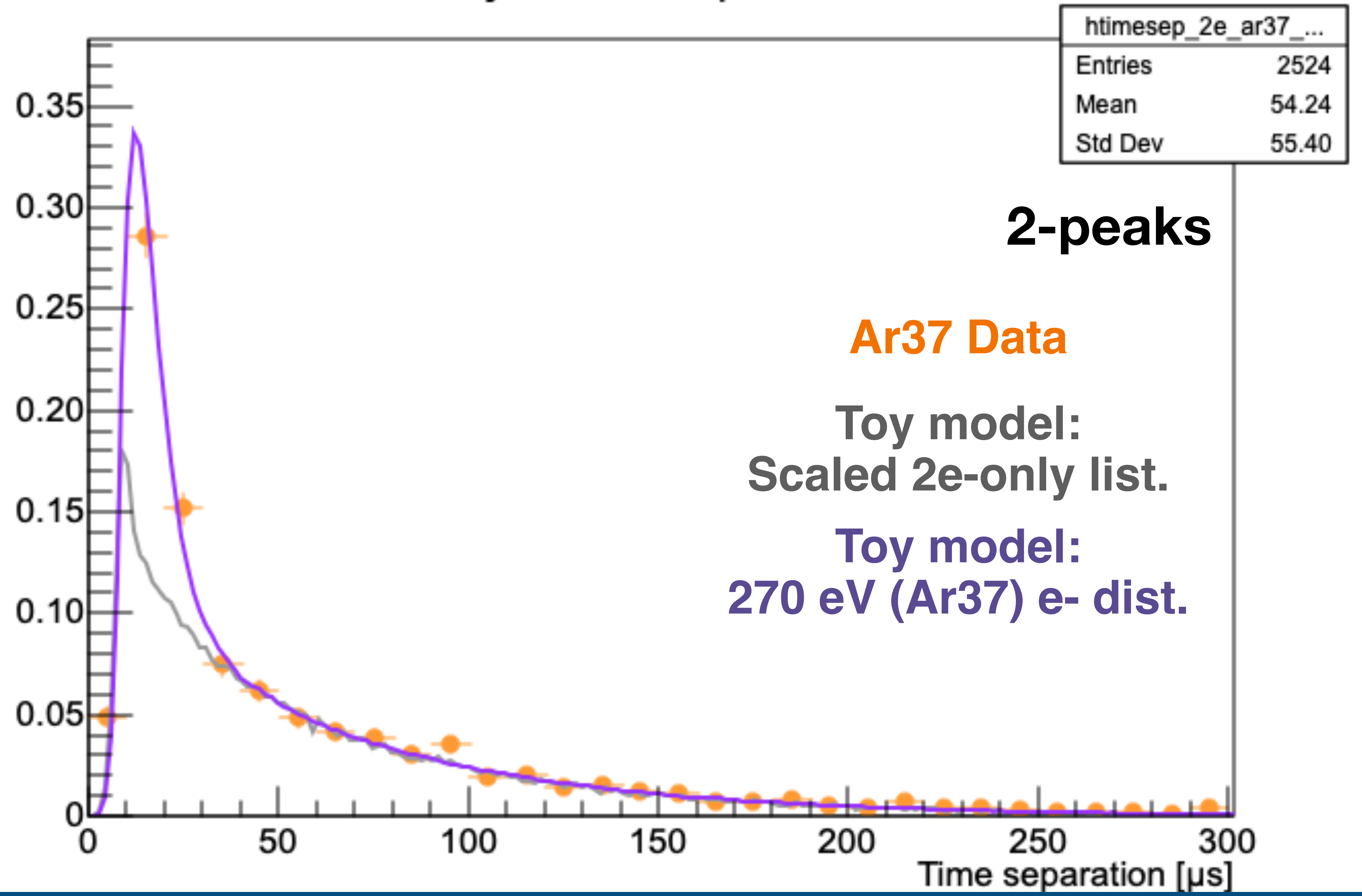

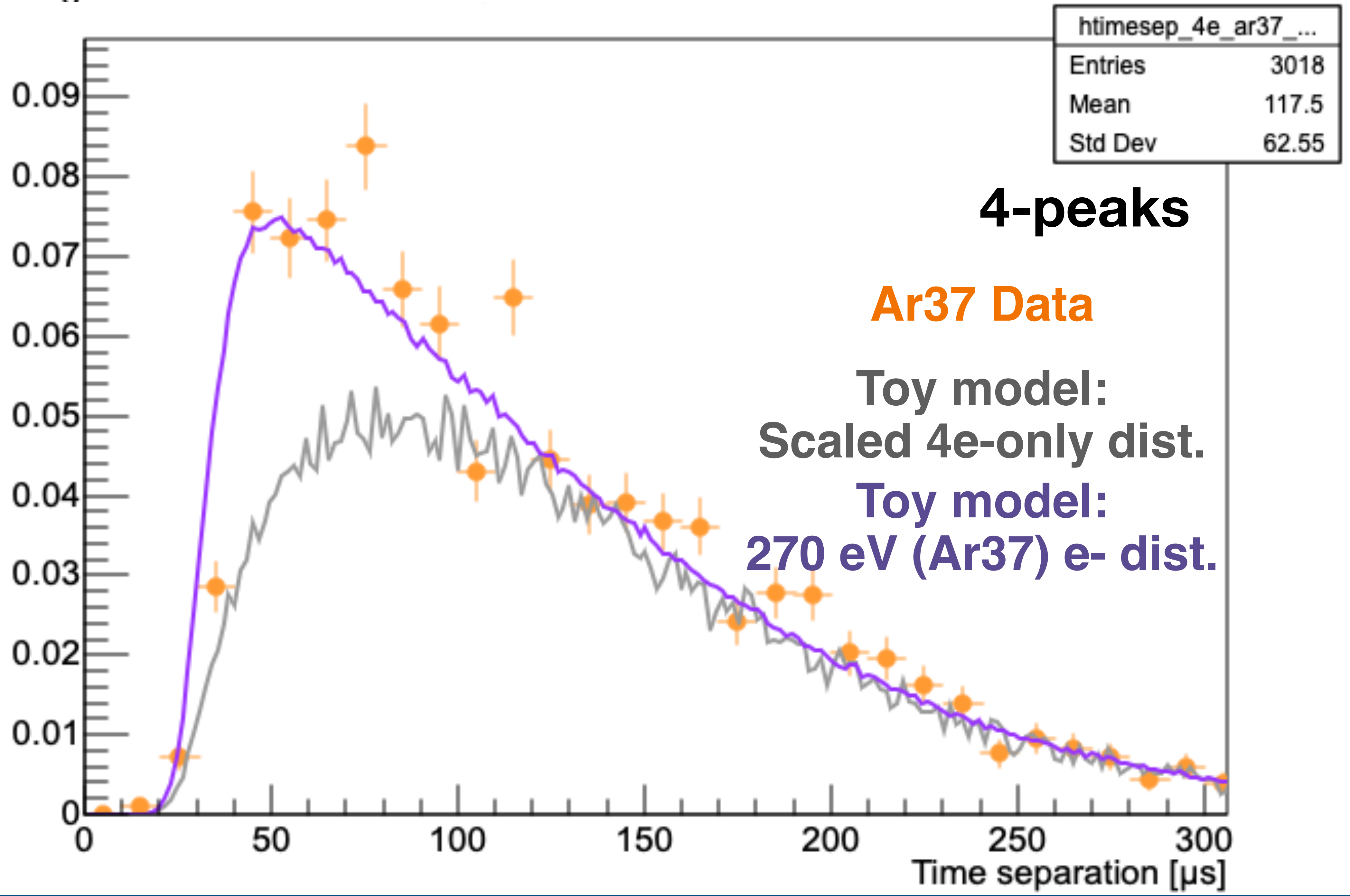

Summary

Summary

- New ACHINOS sensor developed for large SPCs, tested during commissioning run of S140 at LSM with 135 mbar of CH_4
- Large time dispersion of primary electrons allows electron counting, despite avalanche statistics
- Multi-channel operation of anode allows rejection of non-physical pulses through crosstalk
- After calibration with laser and Ar37 data, simple model of dispersion and peak counting algorithm performance reproduces data well

Thank you for your attention!

Extra slides

Dark Matter: beyond WIMPS?

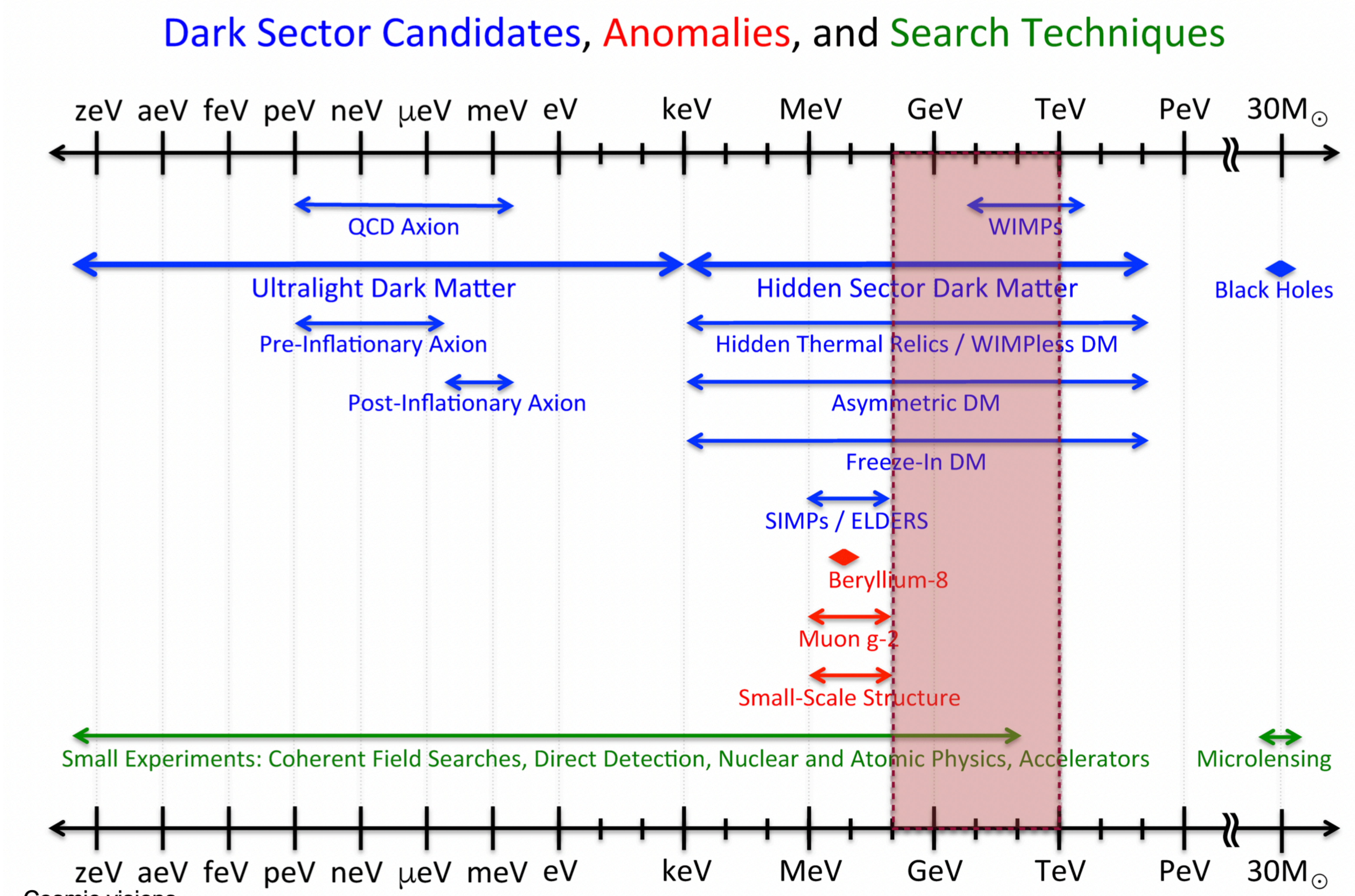

Cosmic visions
arXiv:1707.04591

Cosmogenic activation of copper

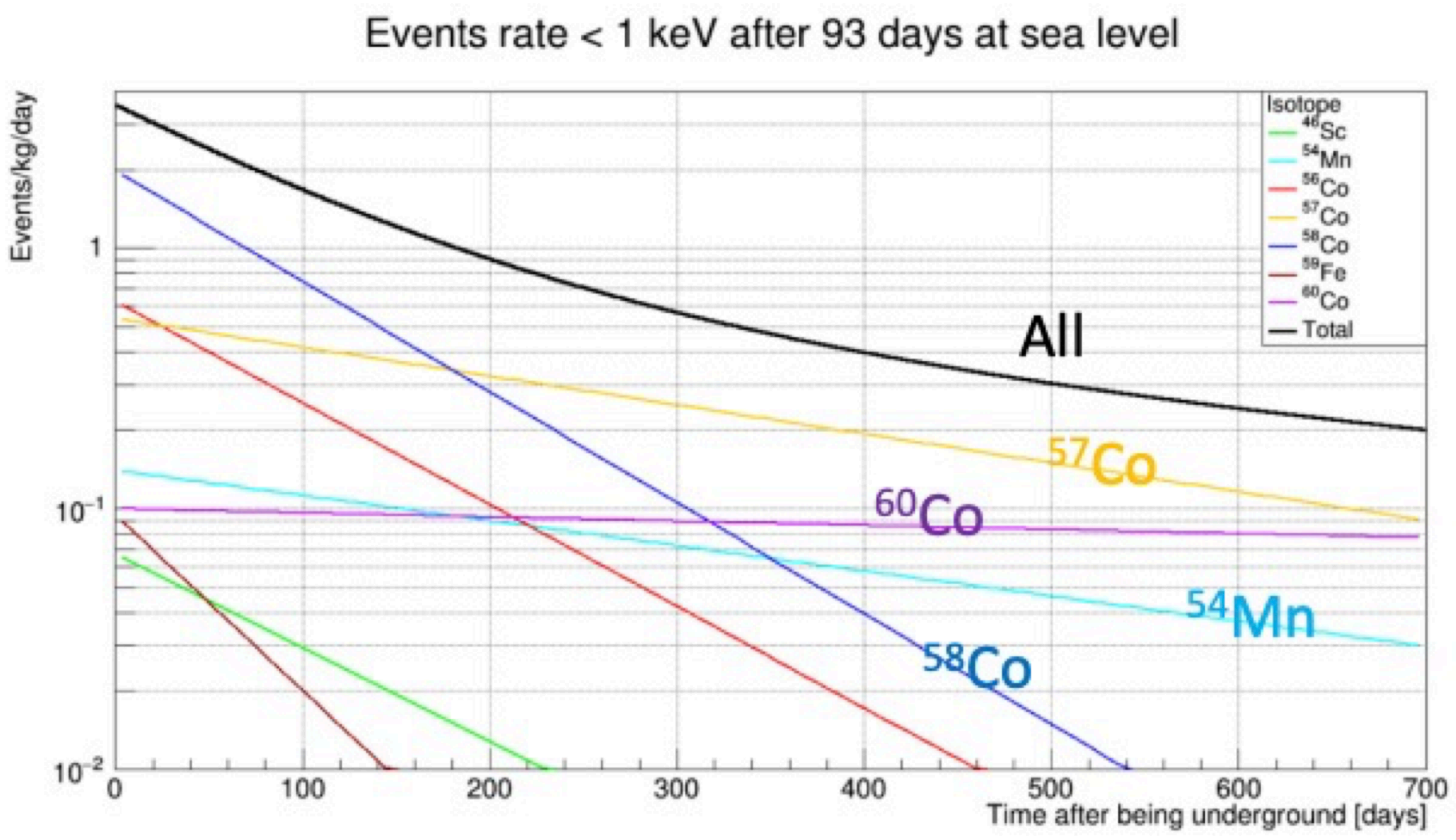

4 dru at t = 0

0.4 dru at t = 1 year

S140: Improvements

Background reduction

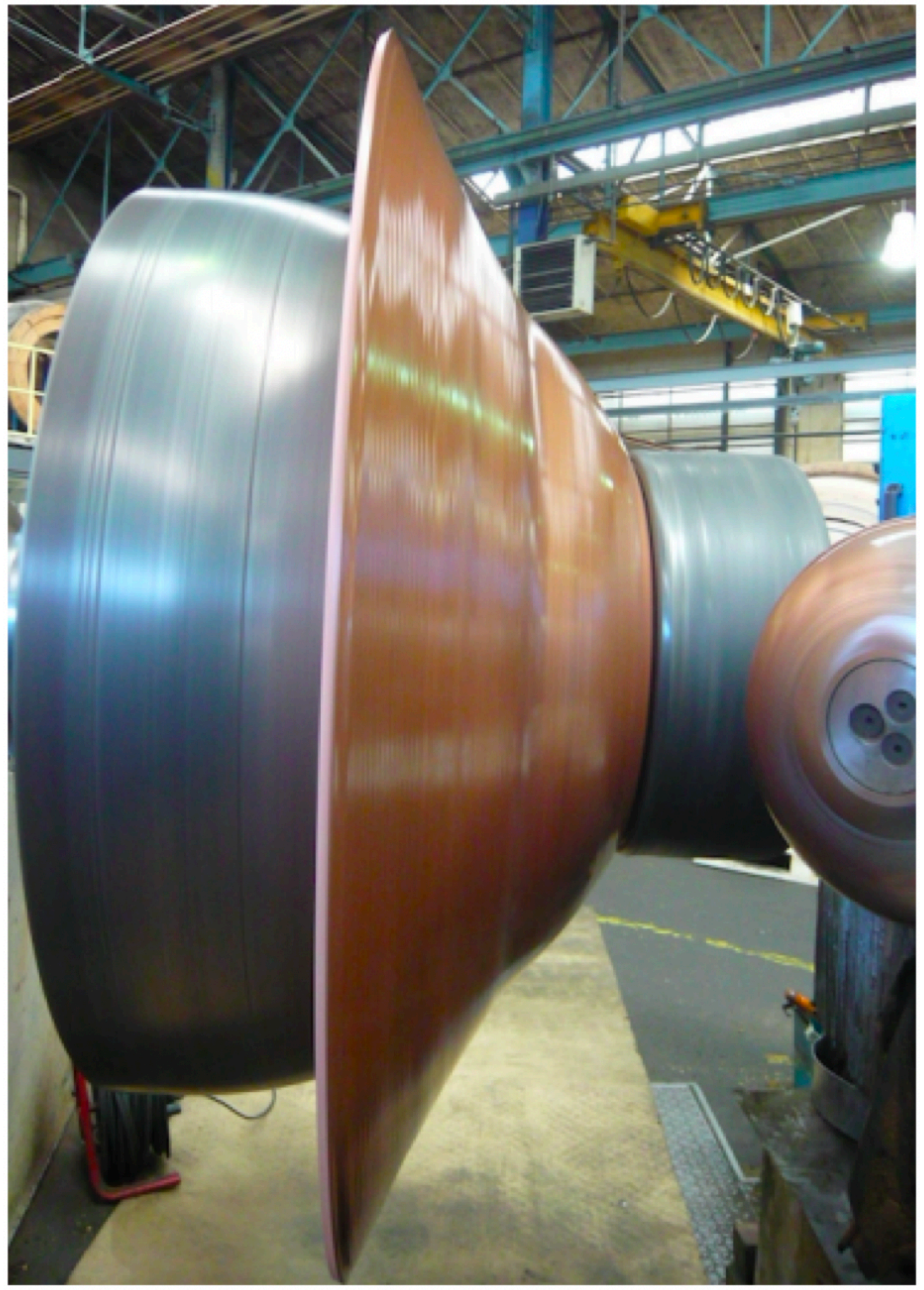

- 2 hemispheres of C10100 (4.5N) copper, electron-beam welded together
- XIA alpha counter estimated ~30 mBq/kg ^{210}Pb in copper bulk (collaboration with XMASS)

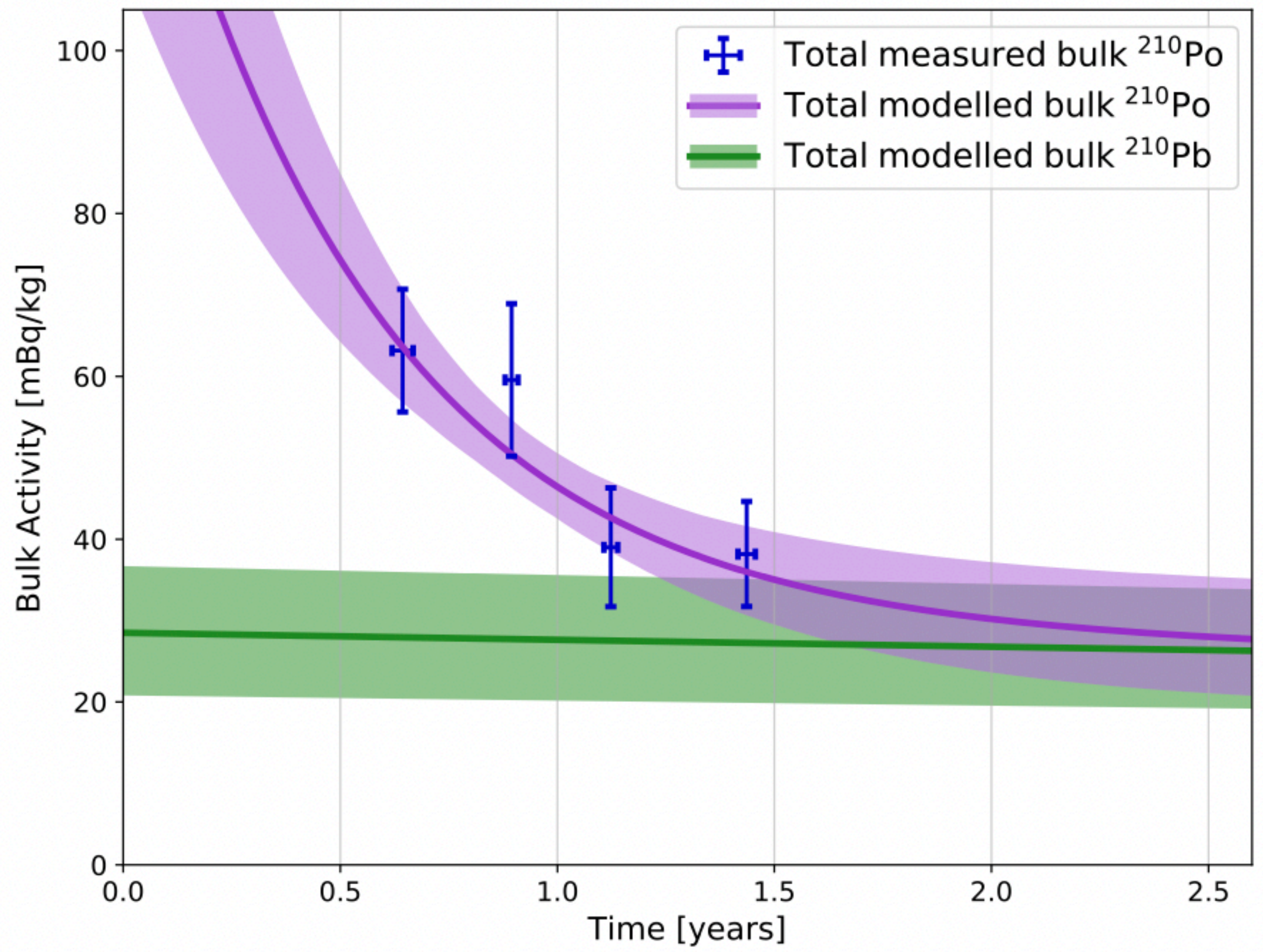

Present in copper

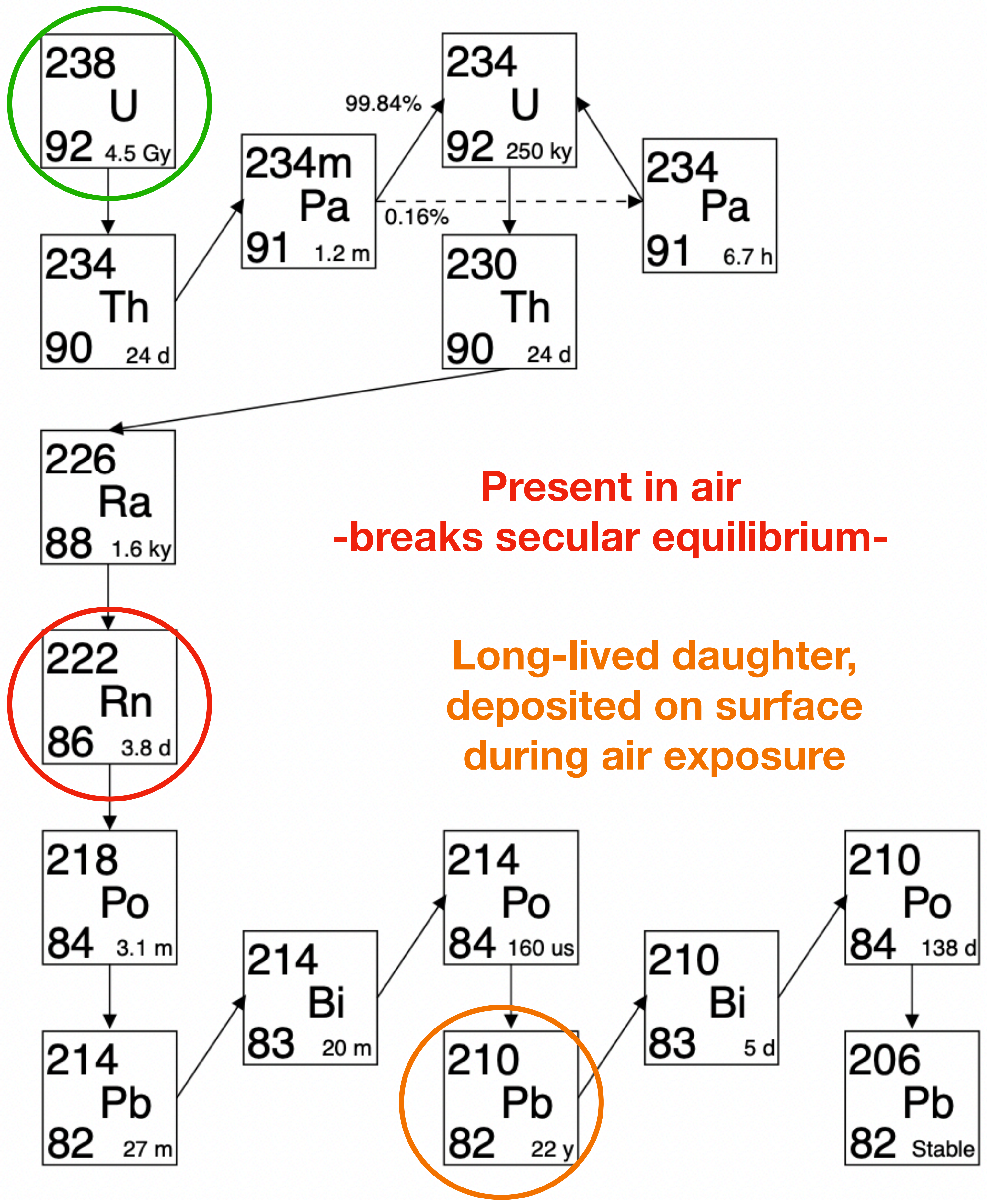

Present in air
-breaks secular equilibrium-

Long-lived daughter, deposited on surface during air exposure

L. Balogh et al, Nucl.Instrum.Meth.A 988 (2021)

S140: Improvements

Background reduction

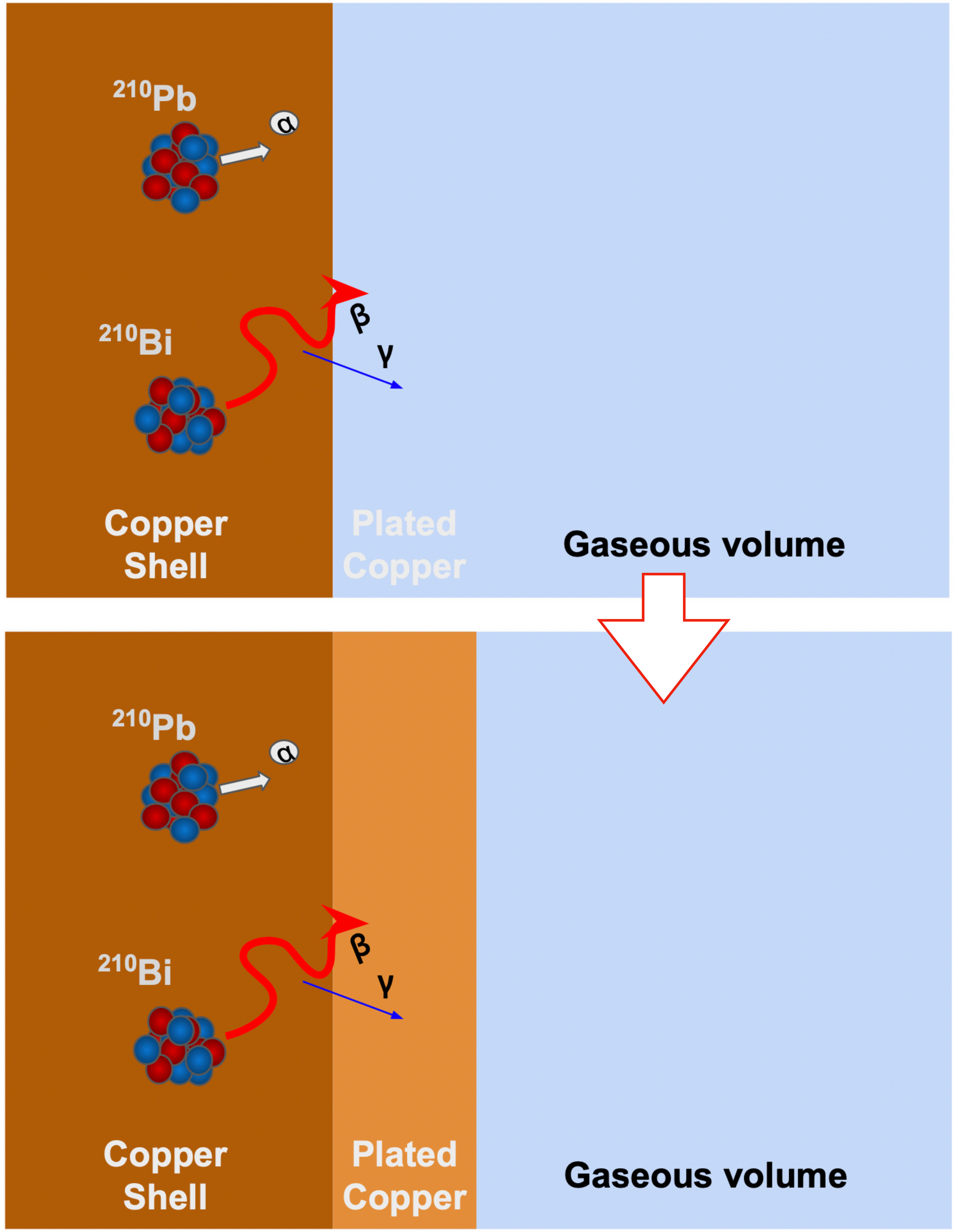

L. Balogh et al, Nucl.Instrum.Meth.A 988 (2021)

S140: Improvements

Background reduction

- Background: Bremsstrahlung X-rays from ^{210}Pb and ^{210}Bi β-decays in (and on) the copper
- Plating 0.5mm of ultra-pure copper on inner surface of detector expected to reduce background under 1 keV by factor 2.6, and total rate by factor 50

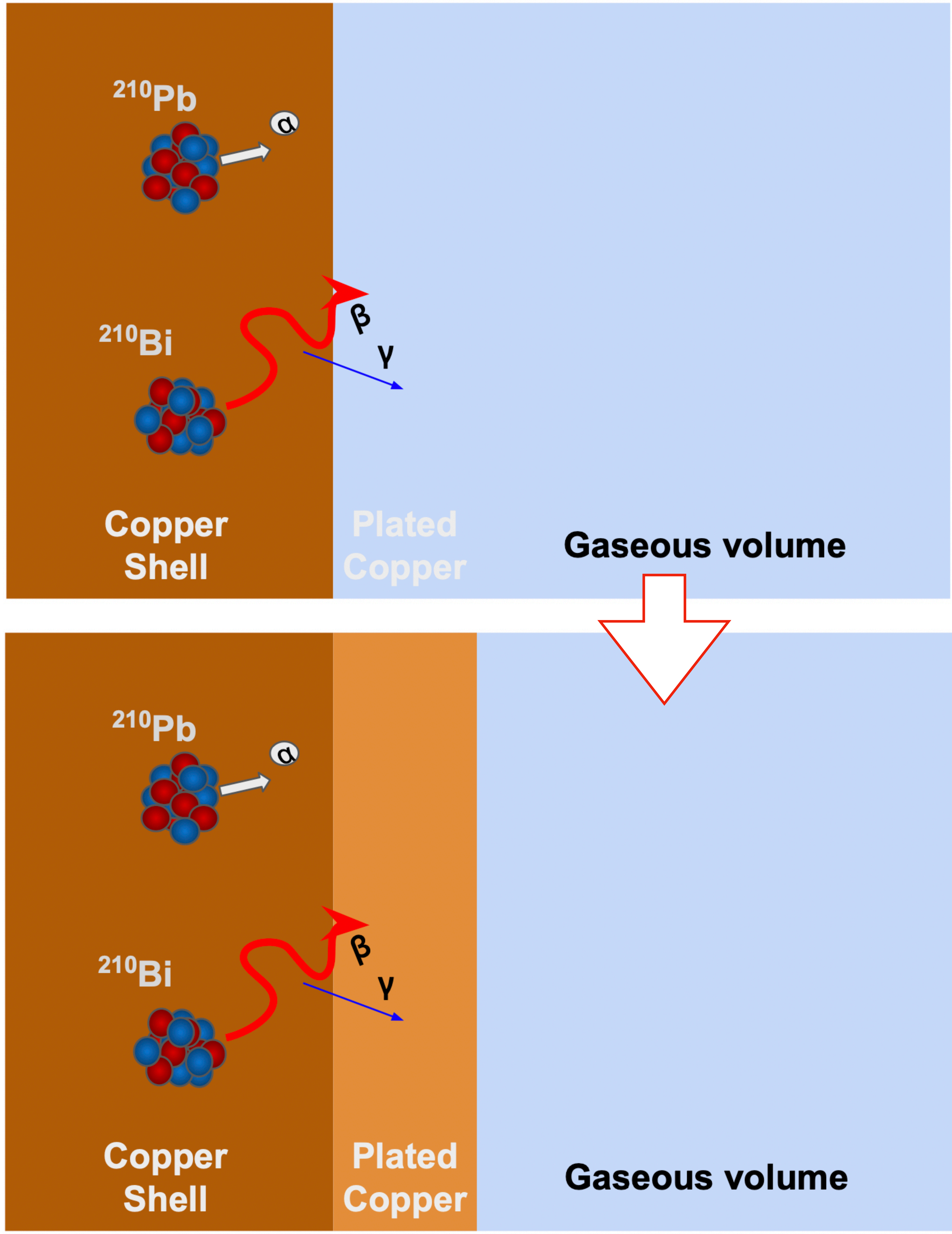

L. Balogh et al, Nucl.Instrum.Meth.A 988 (2021)

S140: Improvements

Background reduction

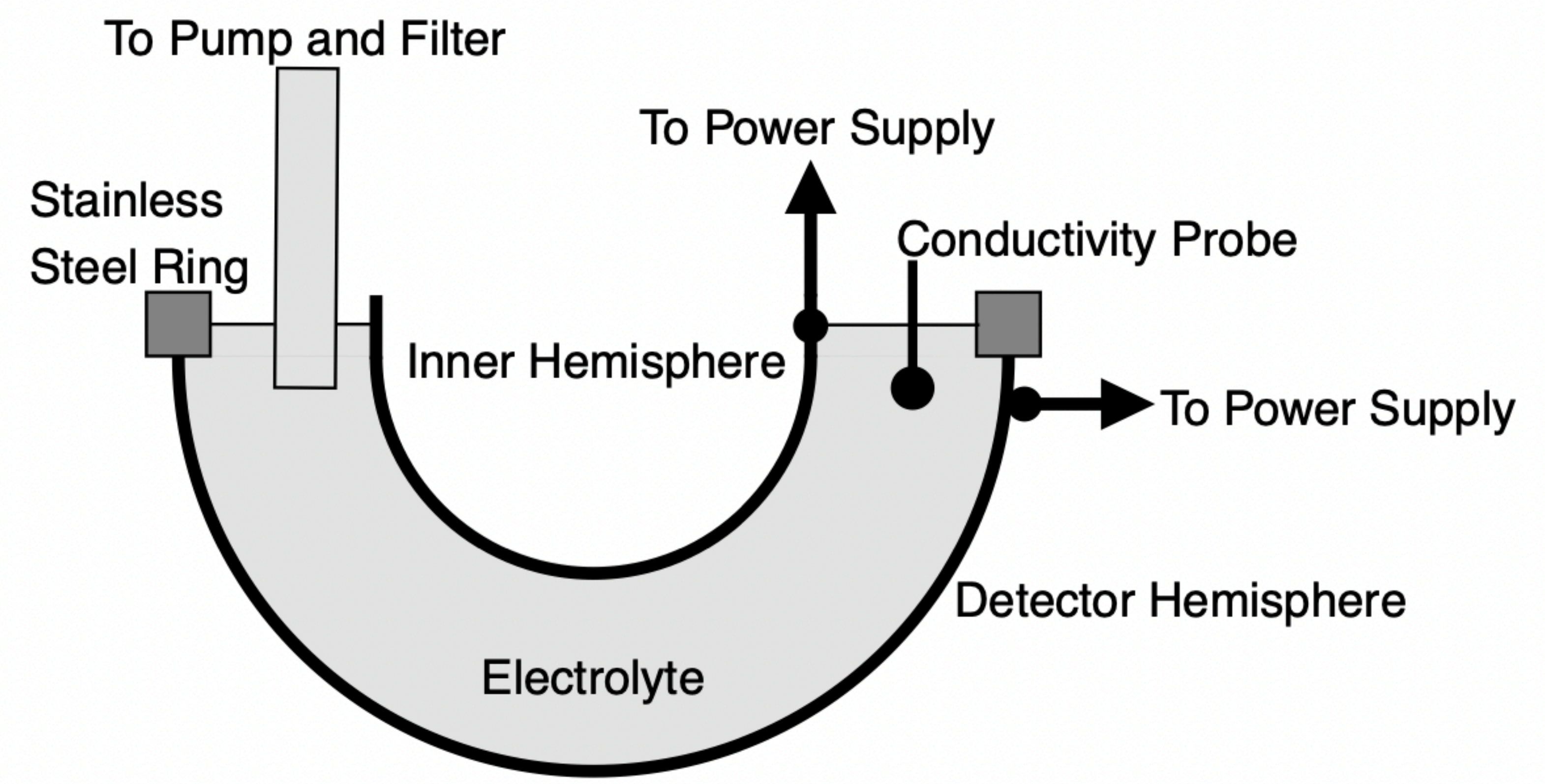

- Background: Bremsstrahlung X-rays from ^{210}Pb and ^{210}Bi β-decays in (and on) the copper
- Plating 0.5mm of ultra-pure copper on inner surface of detector expected to reduce background under 1 keV by factor 2.6, and total rate by factor 50
- Intervention successfully carried out at LSM in collaboration with PNNL

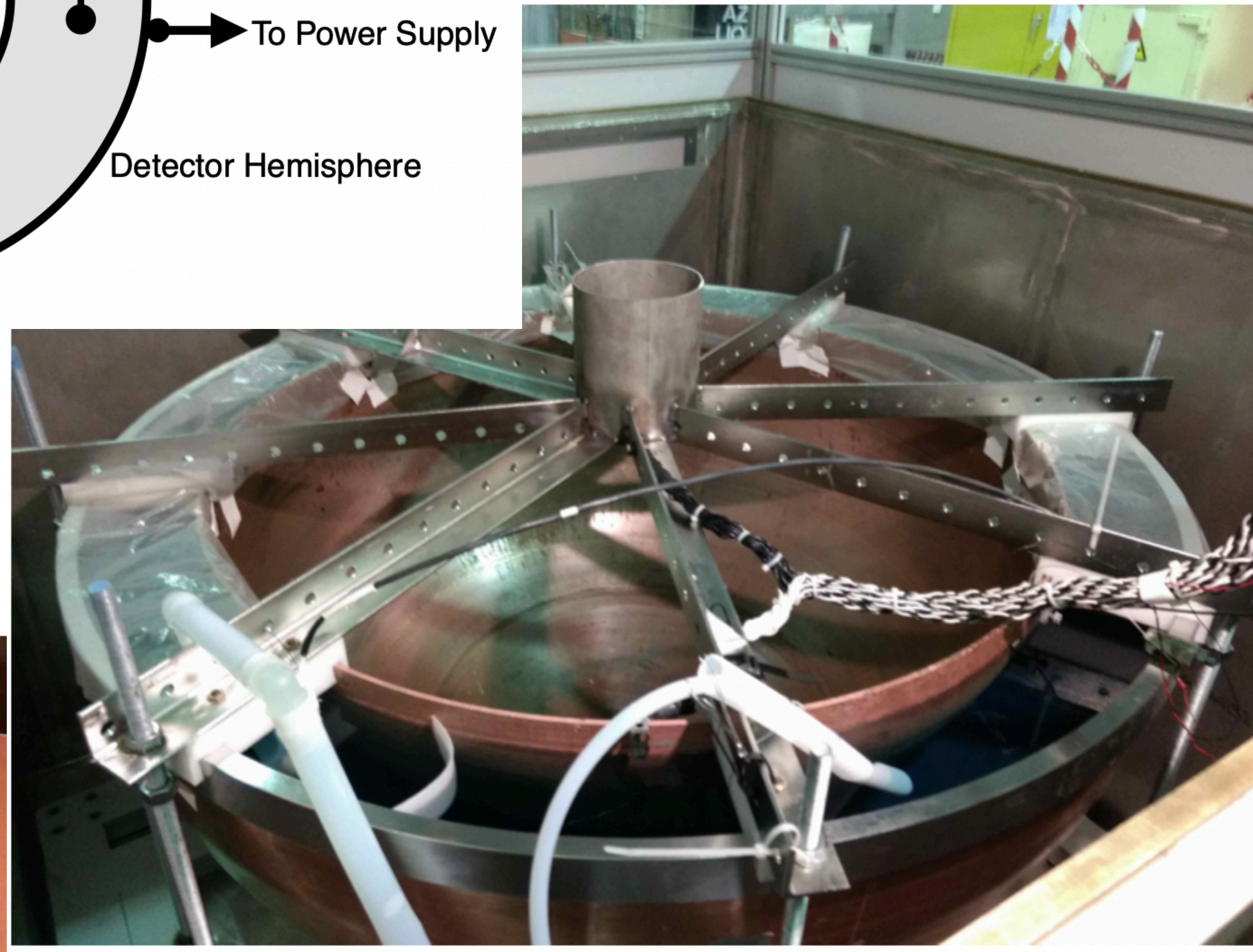

L. Balogh et al, Nucl.Instrum.Meth.A 988 (2021)

S140: Improvements

Calibrations

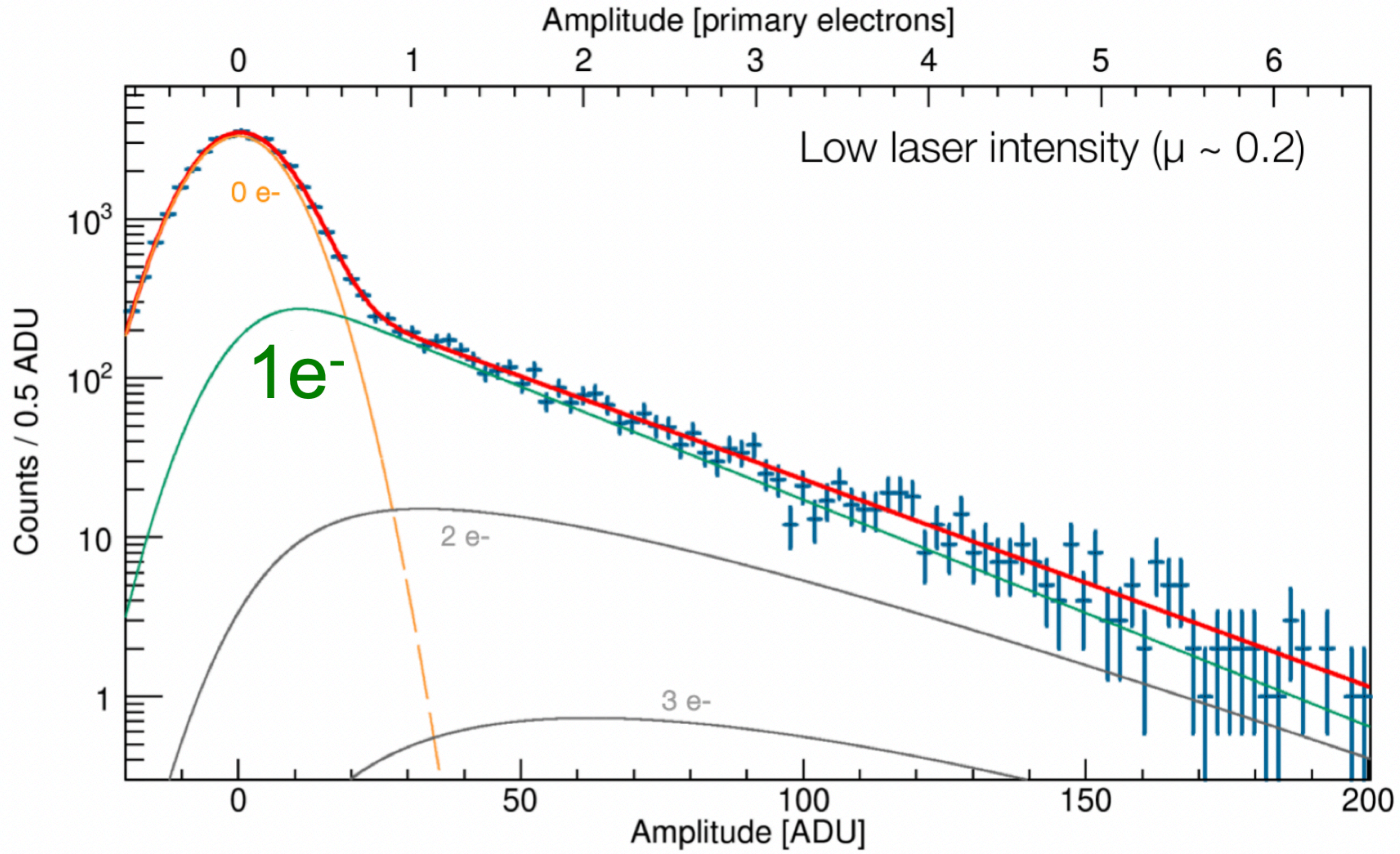

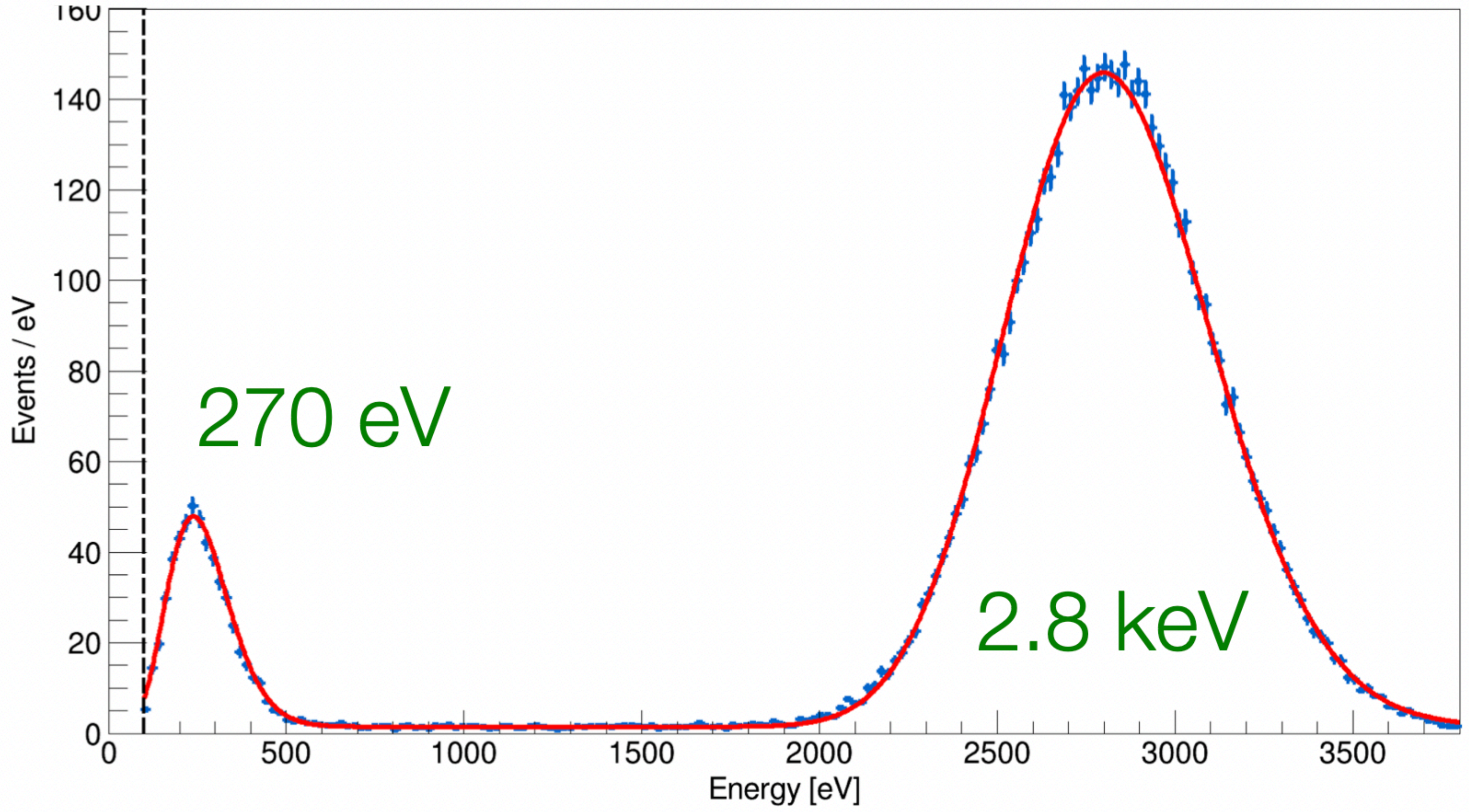

Q. Arnaud et al, Phys. Rev. D 99, 102003 (2019)

S140: Improvements

Calibrations

213nm laser, intensity tuned to extract 1-100 photoelectrons

- Single e- gain calibration
- Drift, diffusion time calibrations
- W calibration, combined with ^{37}Ar source (produced at RMCC)

D.G. Kelly et al, Journal of Radioanalytical and Nuclear Chemistry 318(1) (2018)

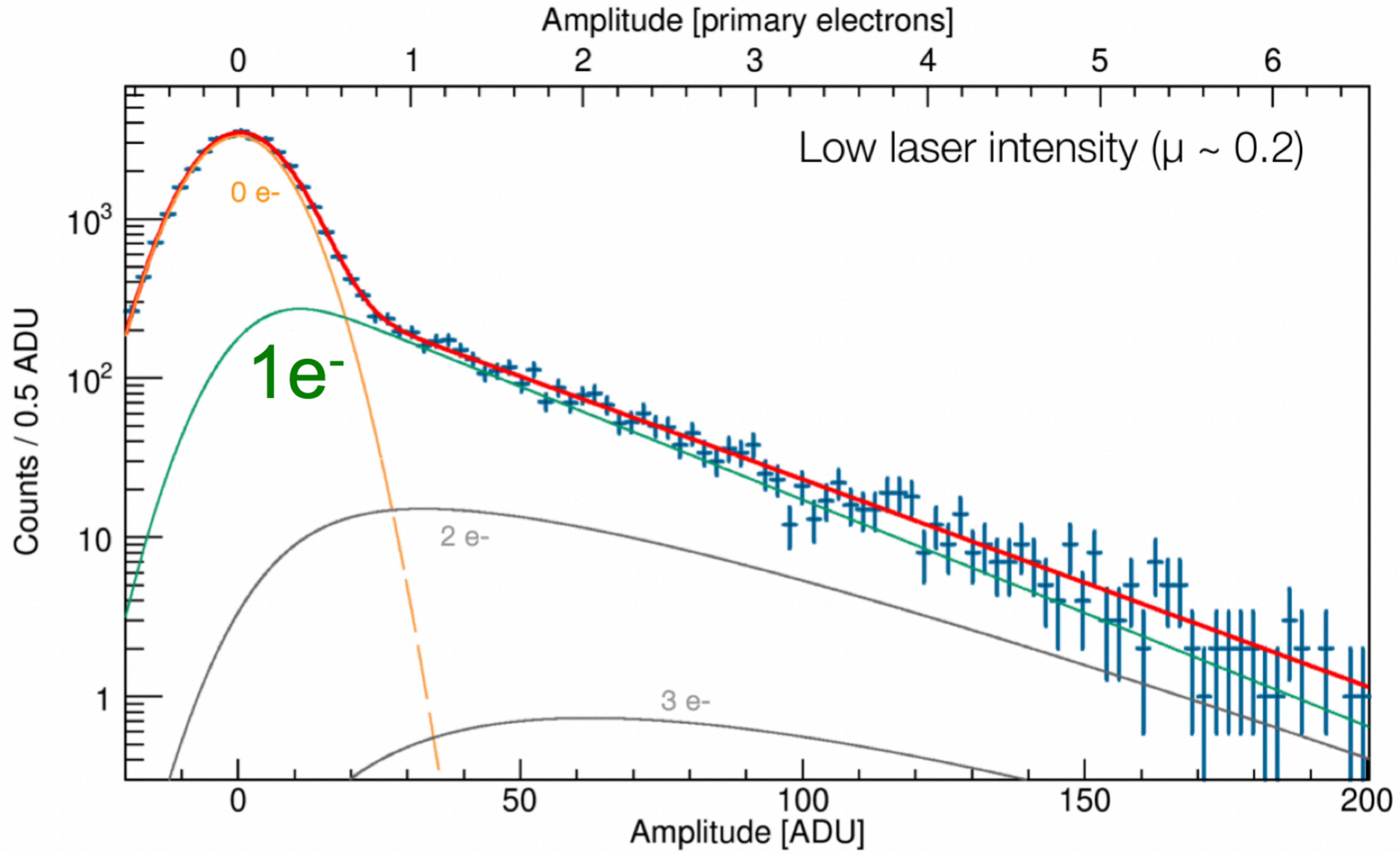

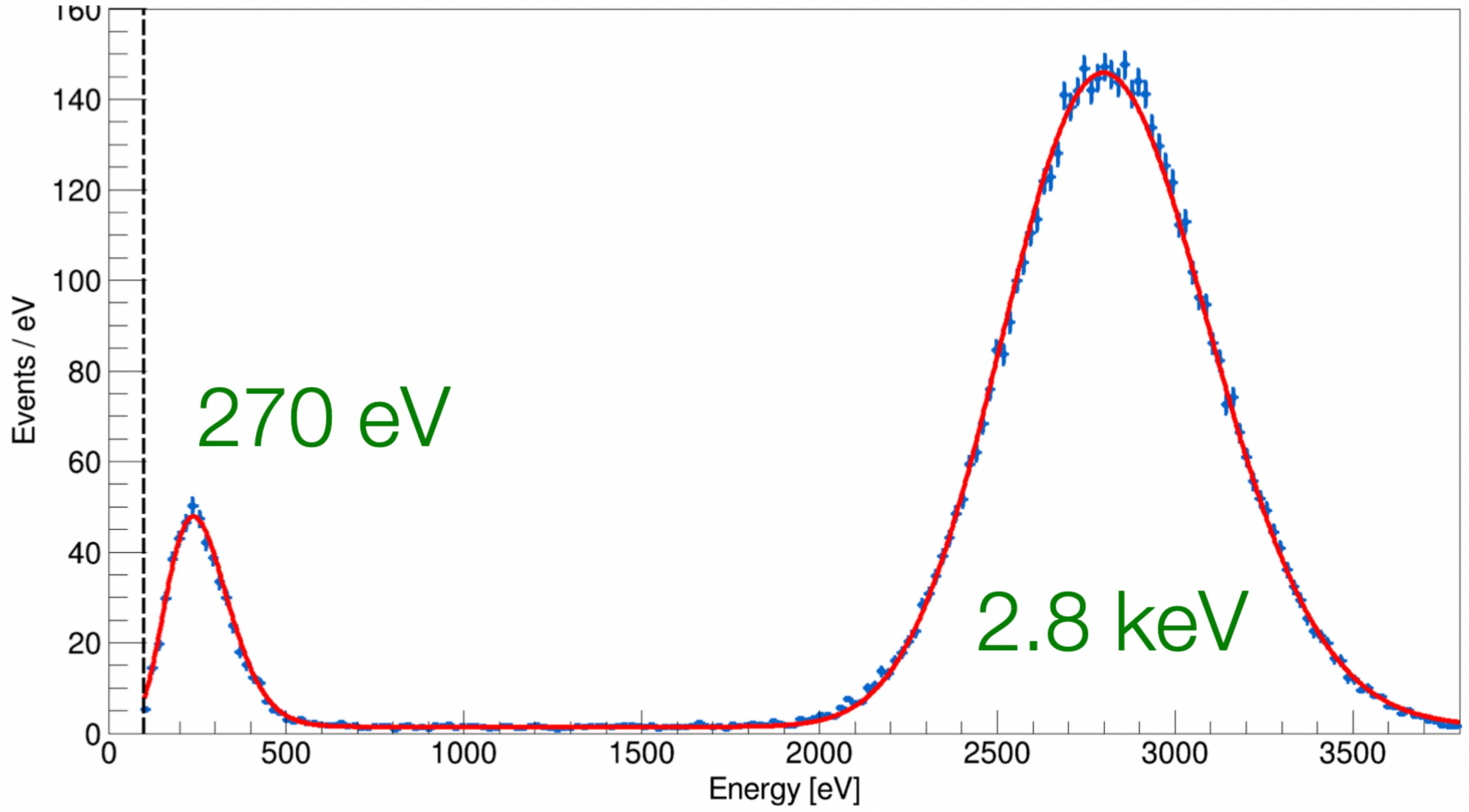

Q. Arnaud et al, Phys. Rev. D 99, 102003 (2019)

S140: Improvements

Calibrations

213nm laser, intensity tuned to extract 1-100 photoelectrons

- Single e- gain calibration
- Drift, diffusion time calibrations
- W calibration, combined with ^{37}Ar source (produced at RMCC)

D.G. Kelly et al, Journal of Radioanalytical and Nuclear Chemistry 318(1) (2018)

- Run monitoring and trend correction

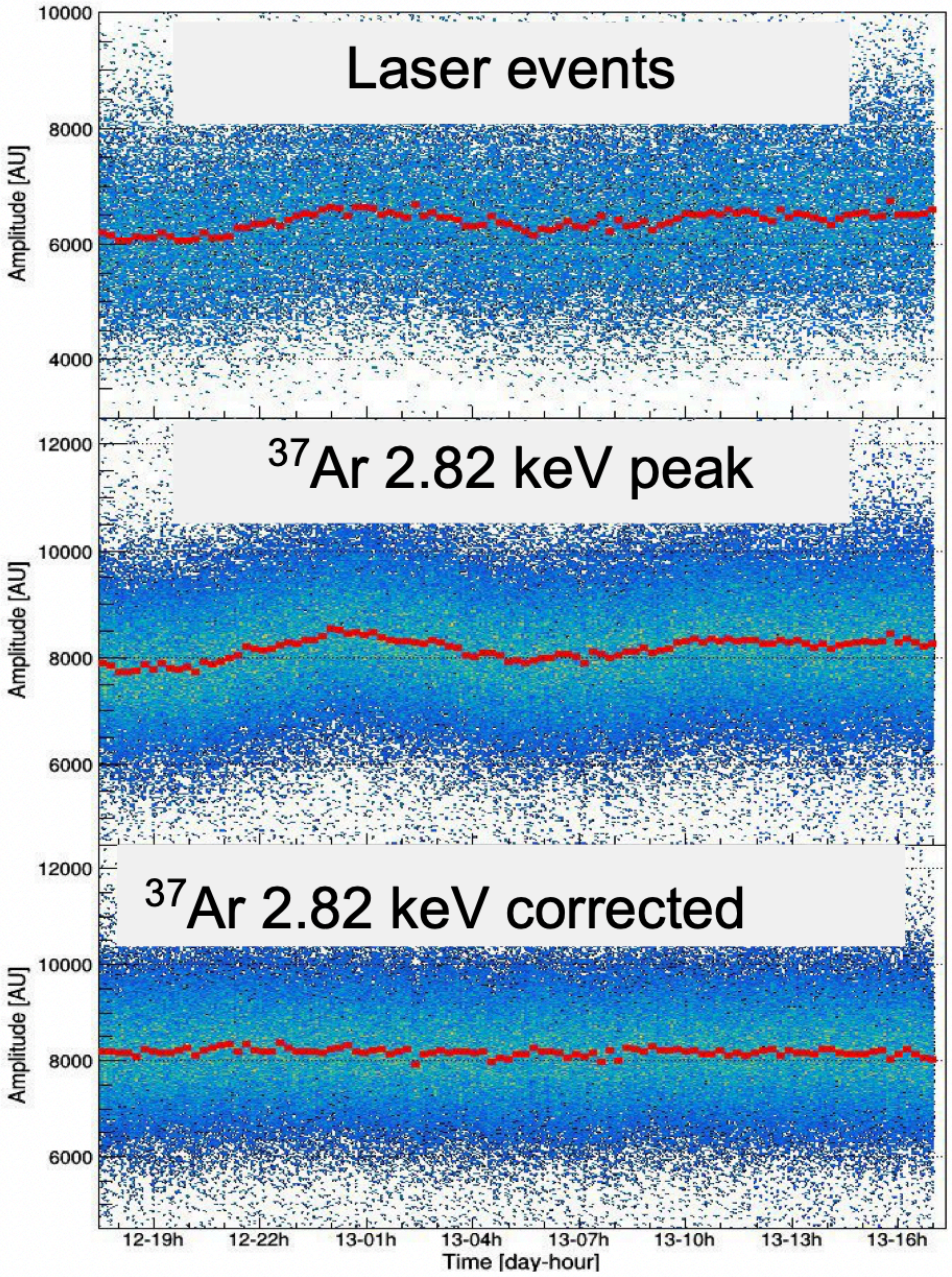

Q. Arnaud et al, Phys. Rev. D 99, 102003 (2019)

Some simulation plots

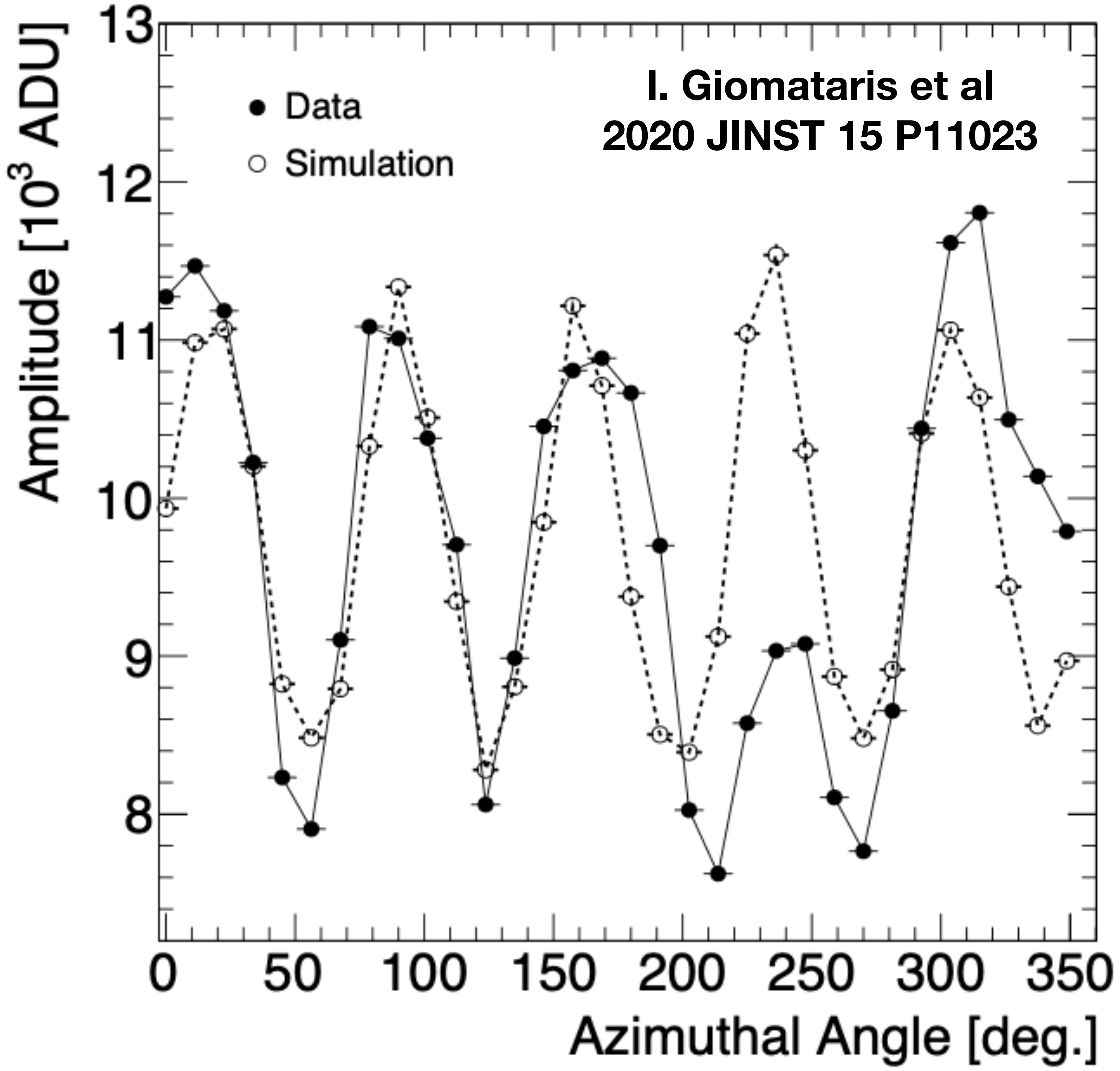

- Reproduction of angular variation of gain observed with Fe55 calibration

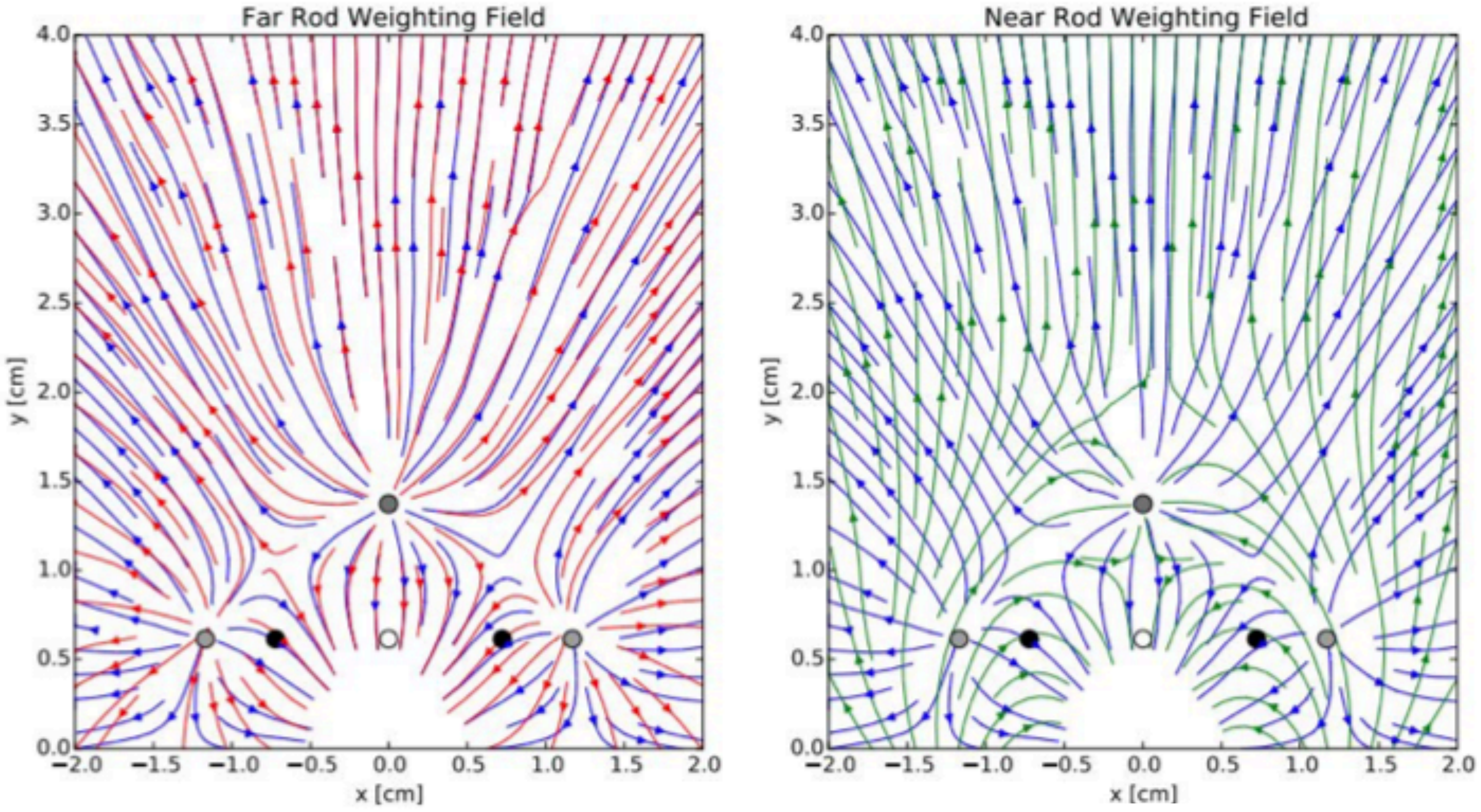

From work described, but not shown, in:

R. Ward et al 2020 JINST 15 C06013

- Weighting fields used to compute induced current on anode / channels

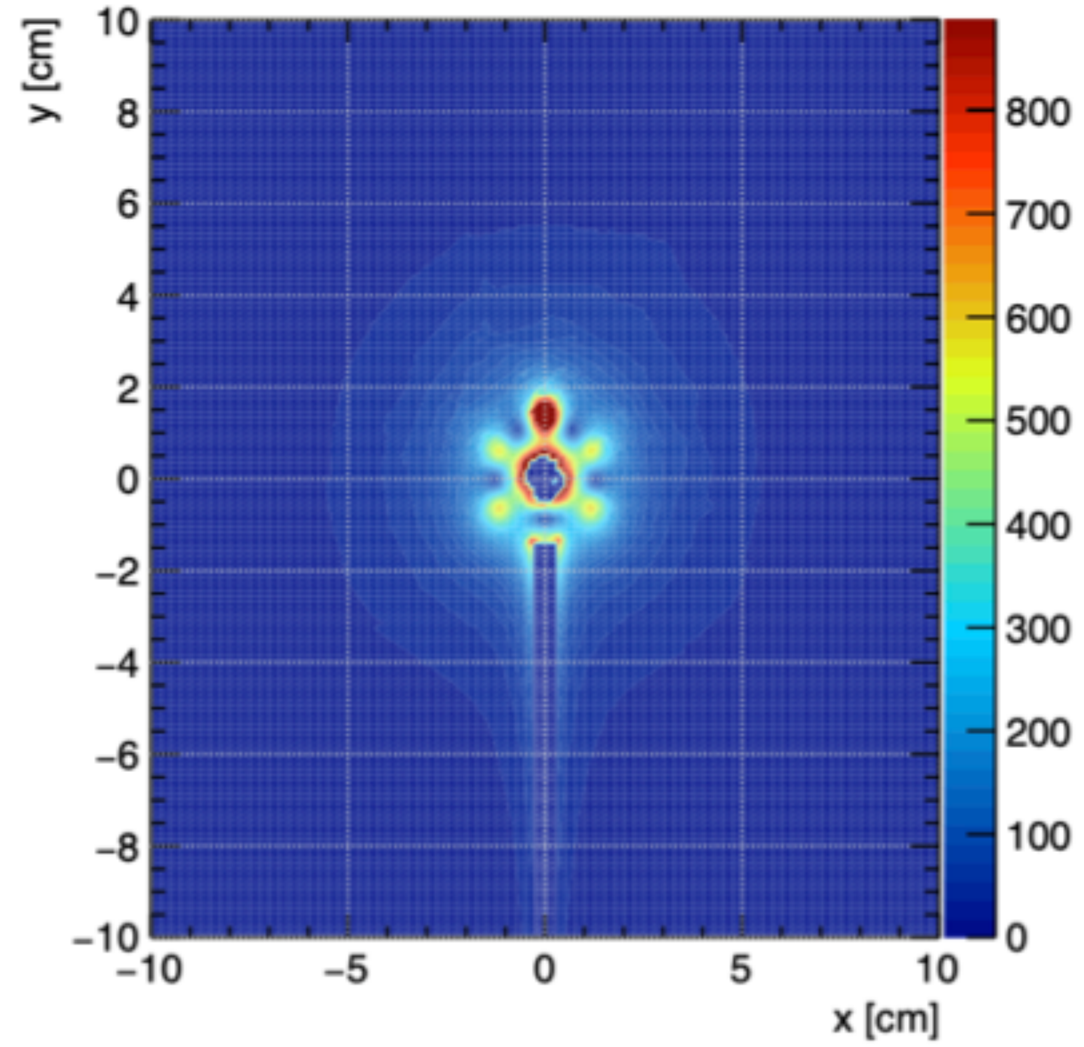

Laser gain calibration

- Fit of laser data provides mean gain, theta of Polya distribution
- Laser trigger (instead of SPC trigger) allows to calibrate trigger efficiency too by implementing it « offline »

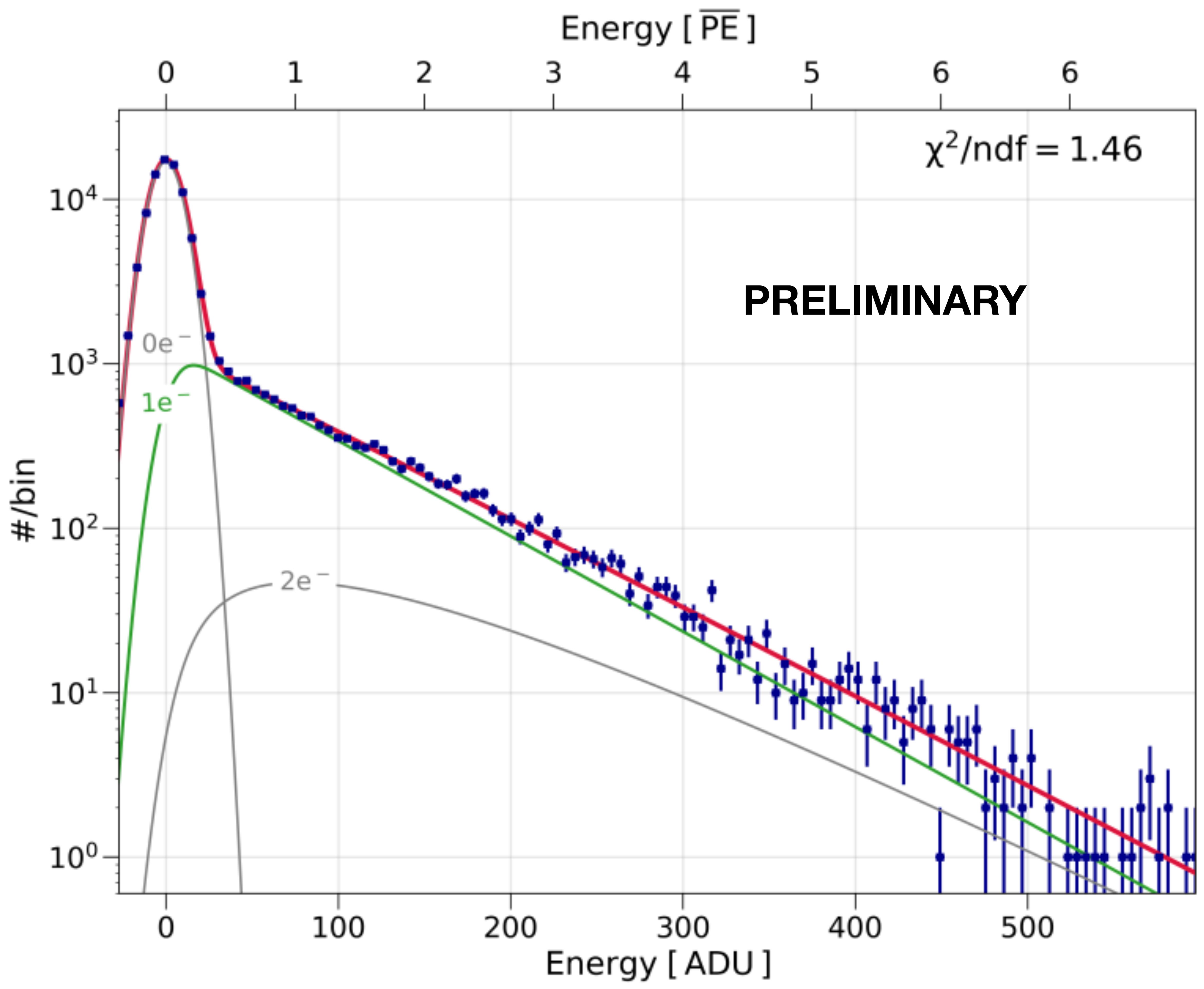

Diffusion calibration

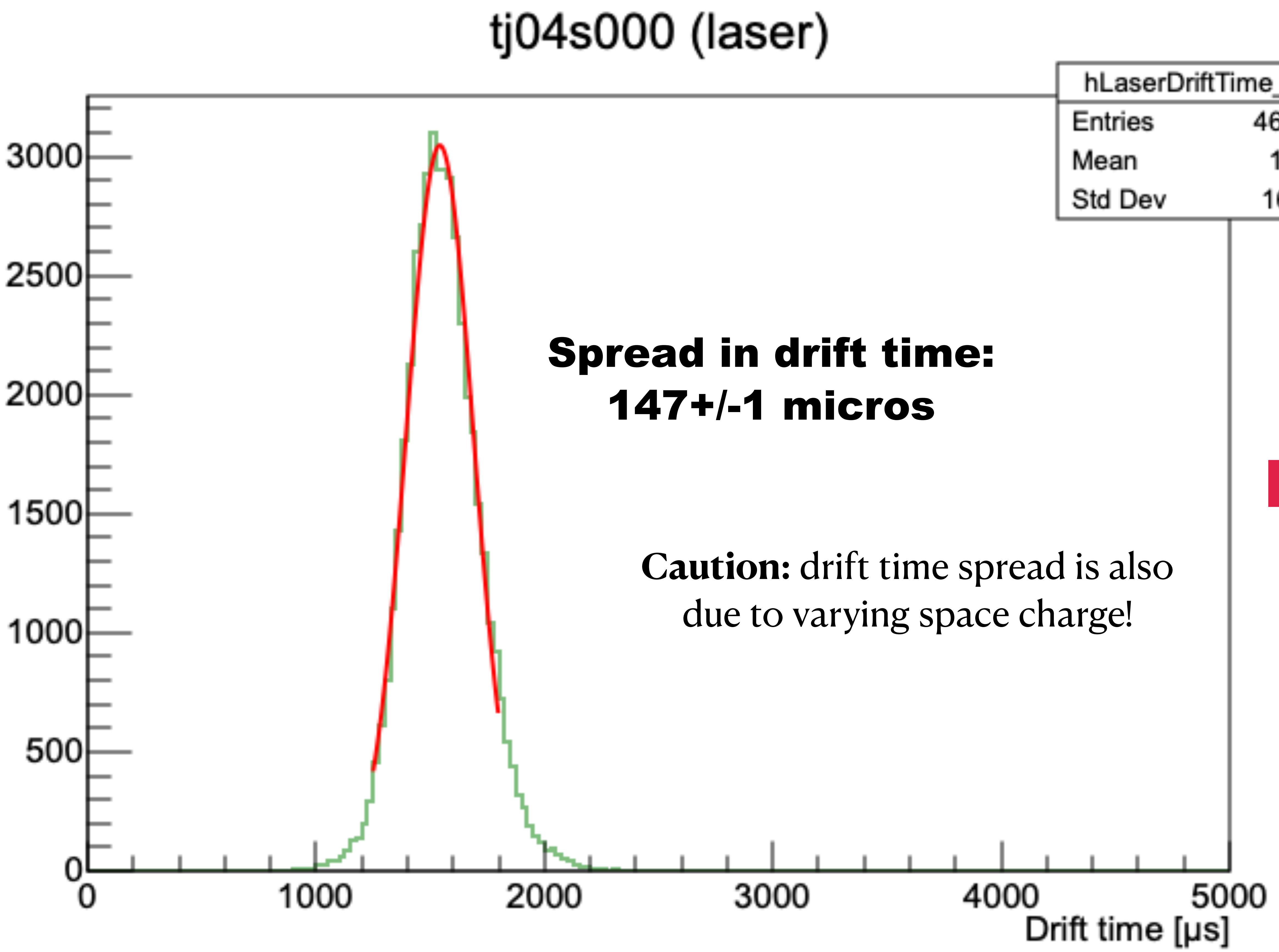

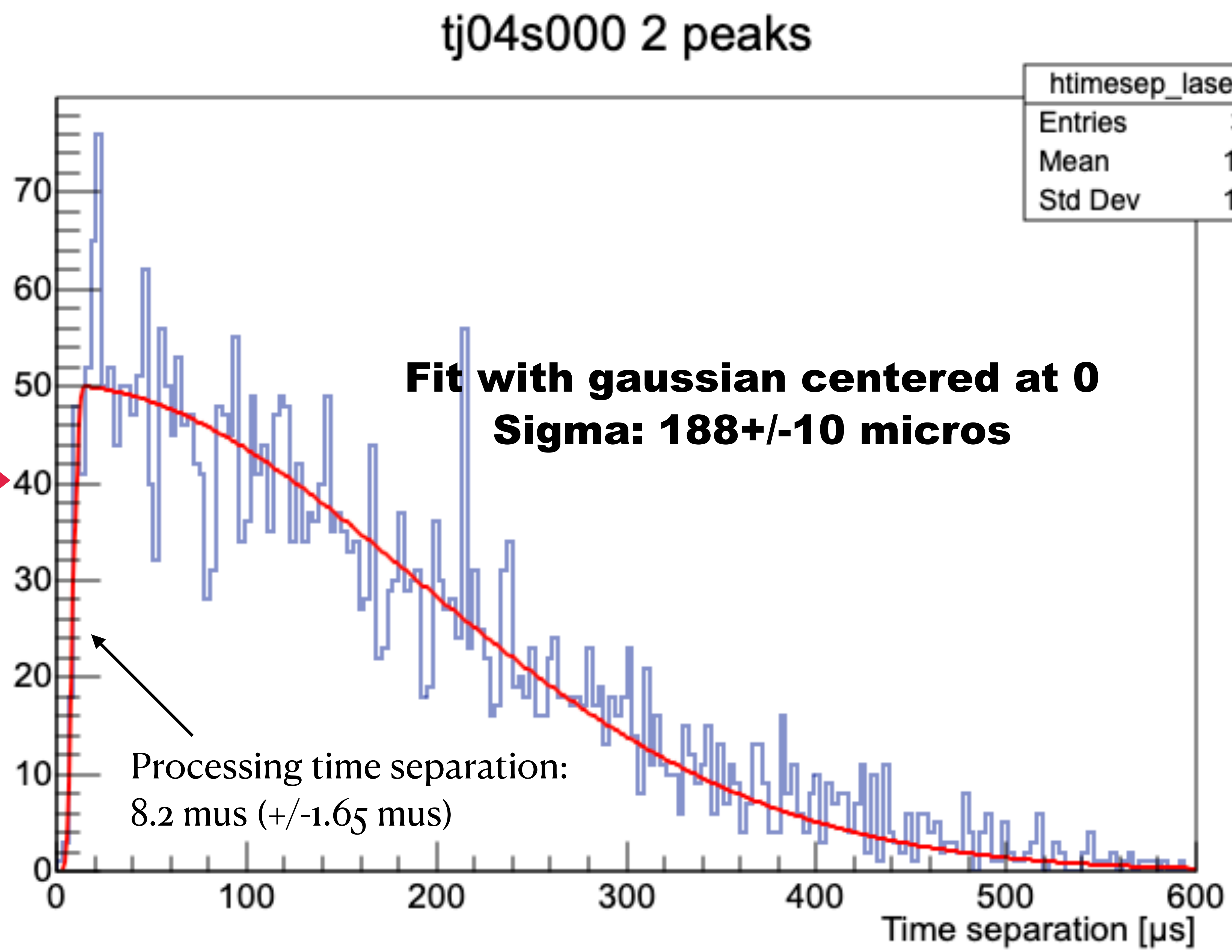

Sanity check:

In laser data, distribution of 2e- events behaves *roughly* as expected: $\mathbf{sigma_{2e}} = \sqrt{(2)} * \mathbf{sigma_{surface}}$

Roughly? Time sep distribution implies $\mathbf{sigma_{surface}}$ = **132** +/**- 7 mus** -> Space charge effect on drift?

Overlapping peaks

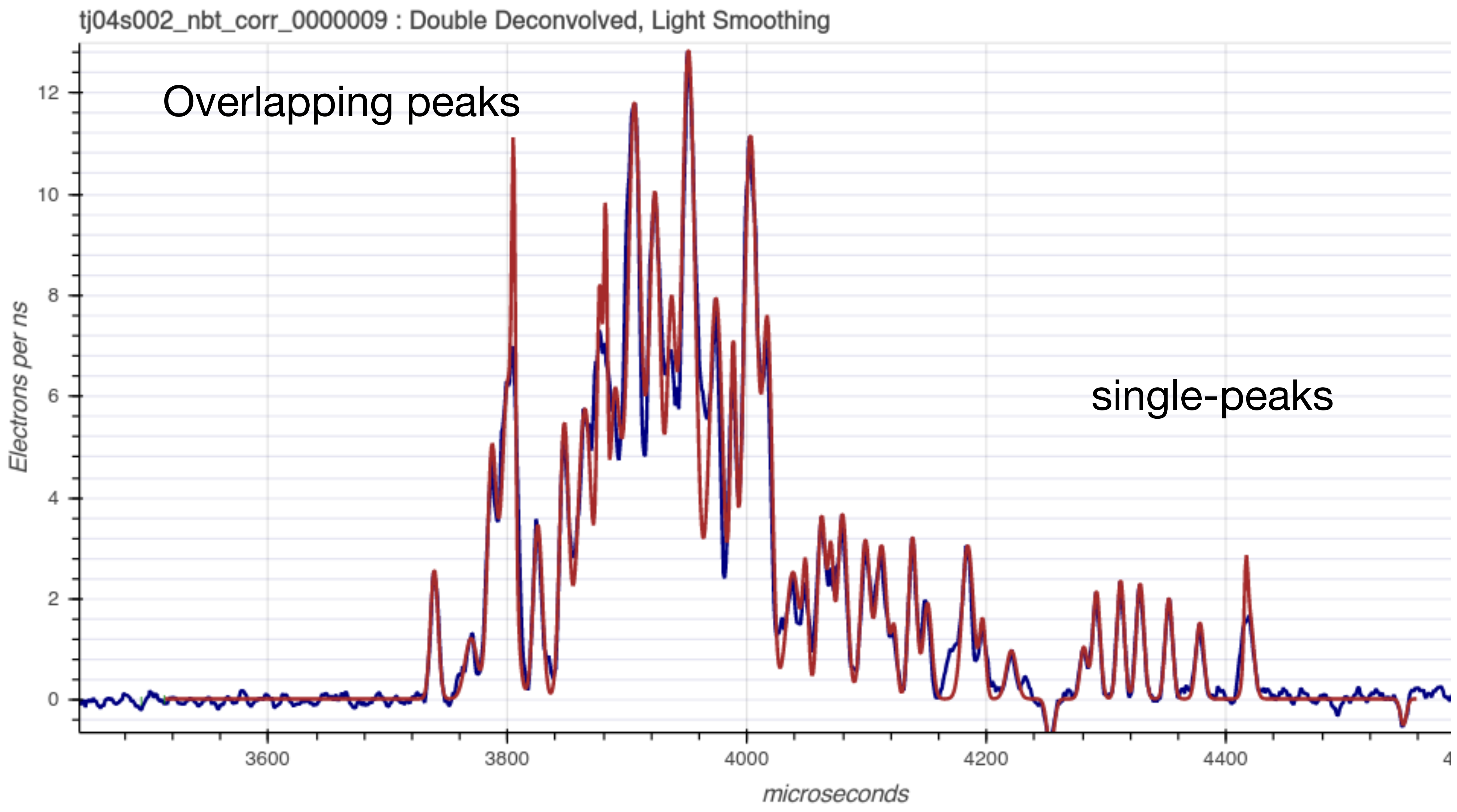

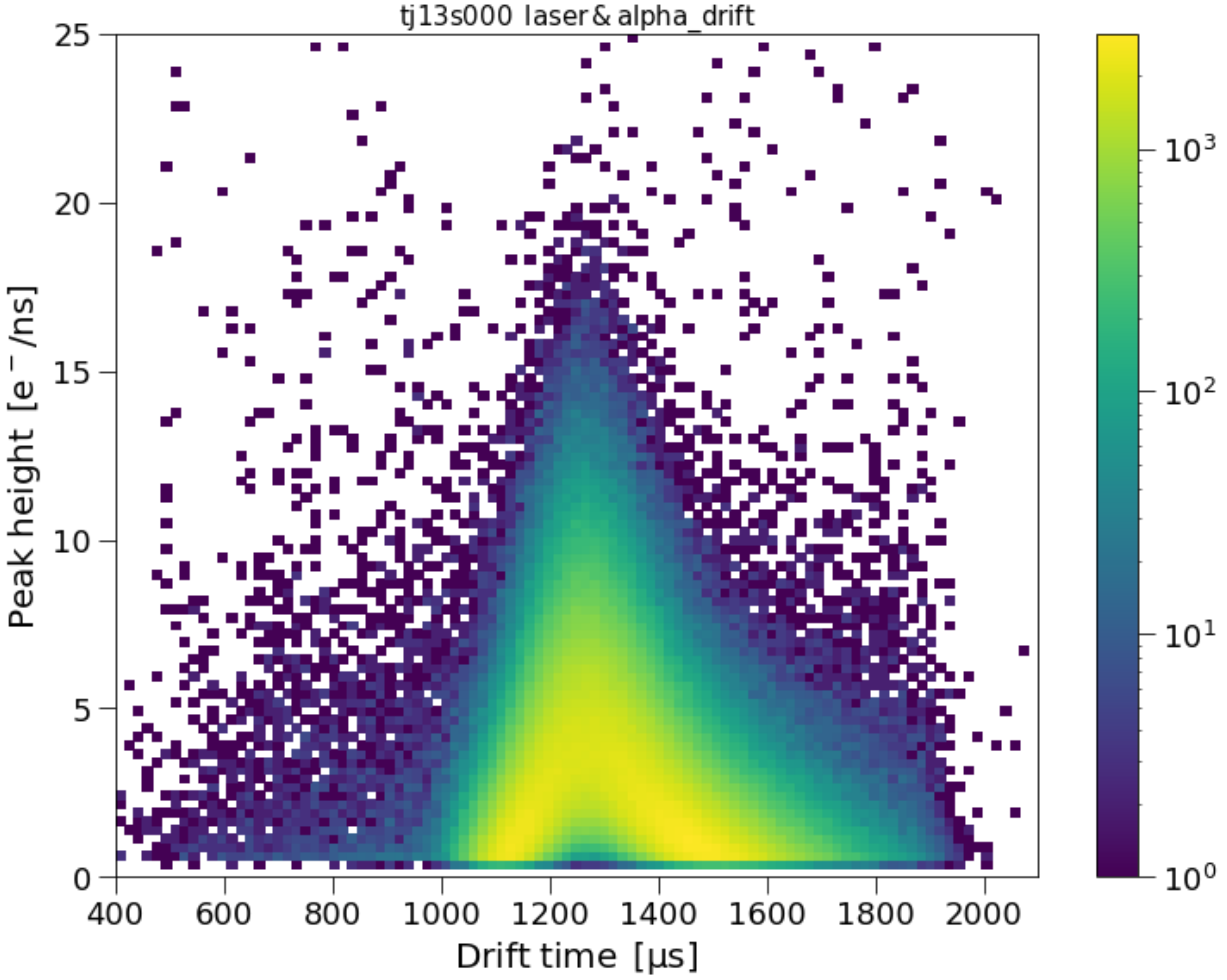

- Effect of overlapping peaks observed at all energies
- Non-intuitive effect: mean peak height depends on position within the time window. This is due to diffusion creating more overlaps in the centre than the « wings »

Random coincidences

- 2, 3, 4-peak alpha-correlated data (when event rate is much higher) match well behaviour of random coincidences, if SAMBA occasionally does not center window around first peak

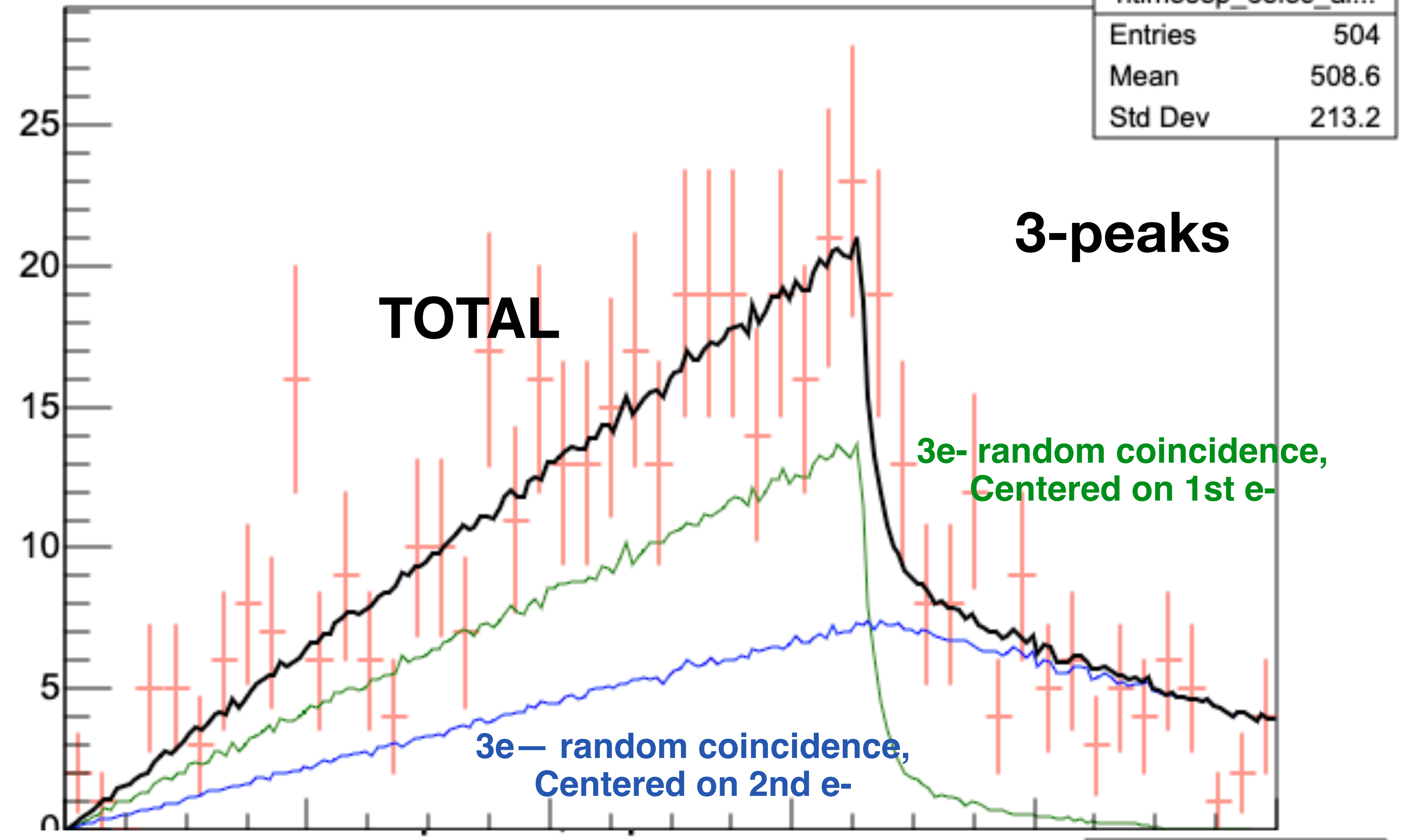

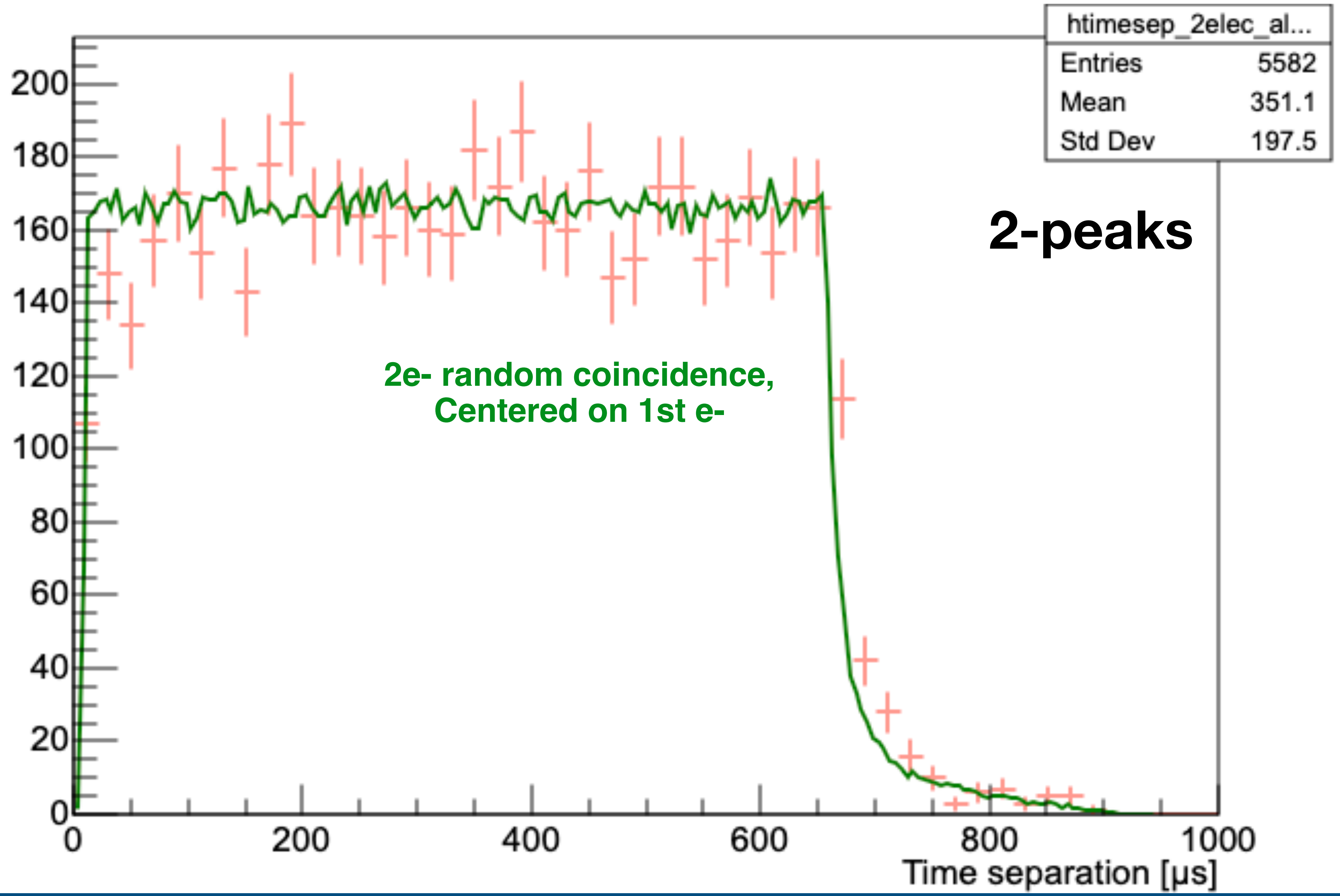

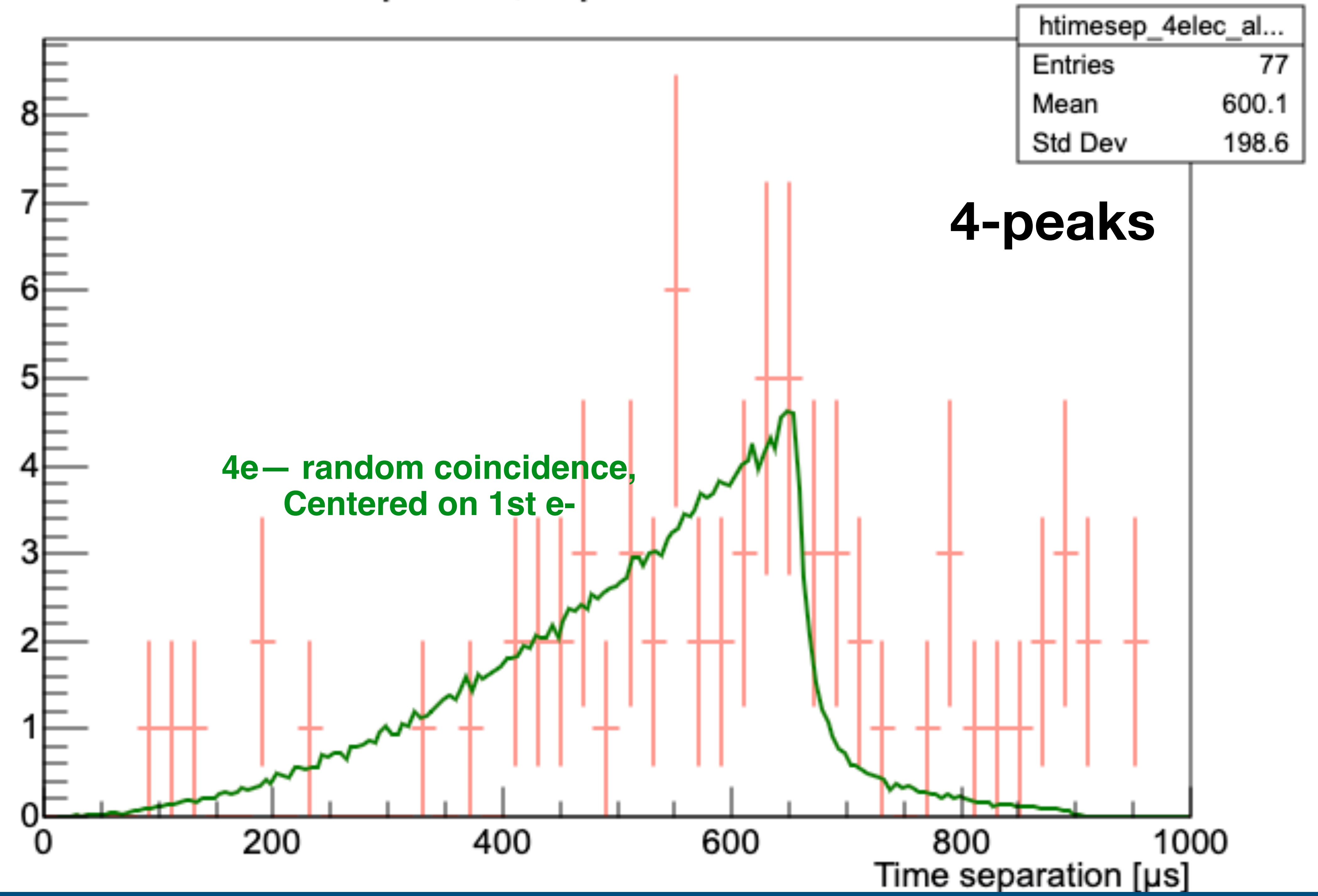

S140: Improvements

Gas quality developments

- Contaminants: O2, H2O, electronegative gases
- Filtering with: Getter, Oxysorb, Custom filter
- Filtering in a gas recirculation system
  - SAES MicroTorr Purifier (MC700 902-F)
  - Incorporated with Residual Gas Analyser
- Incorporation of Carboxen 1000 radon trap cooled with dry ice

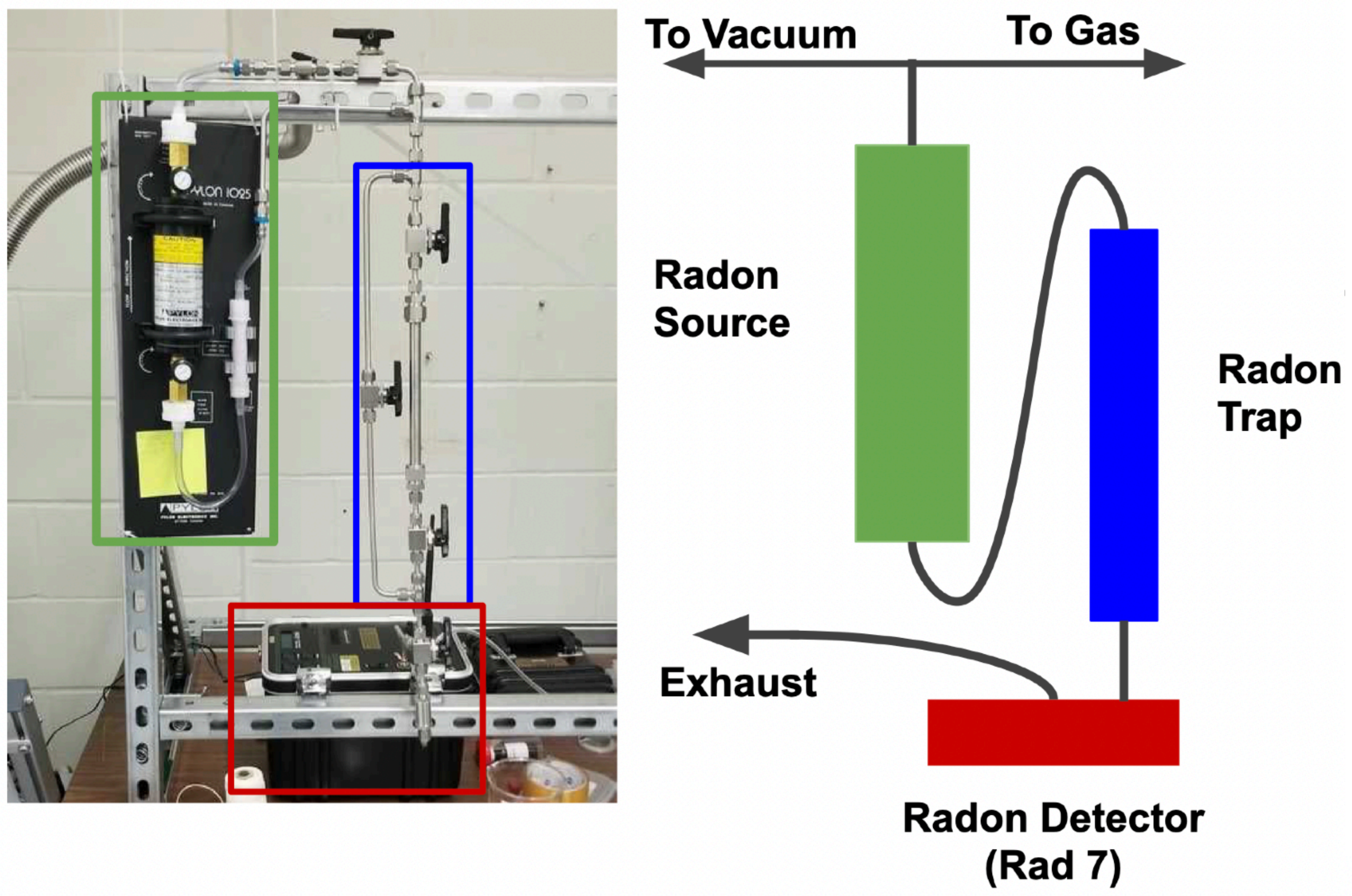

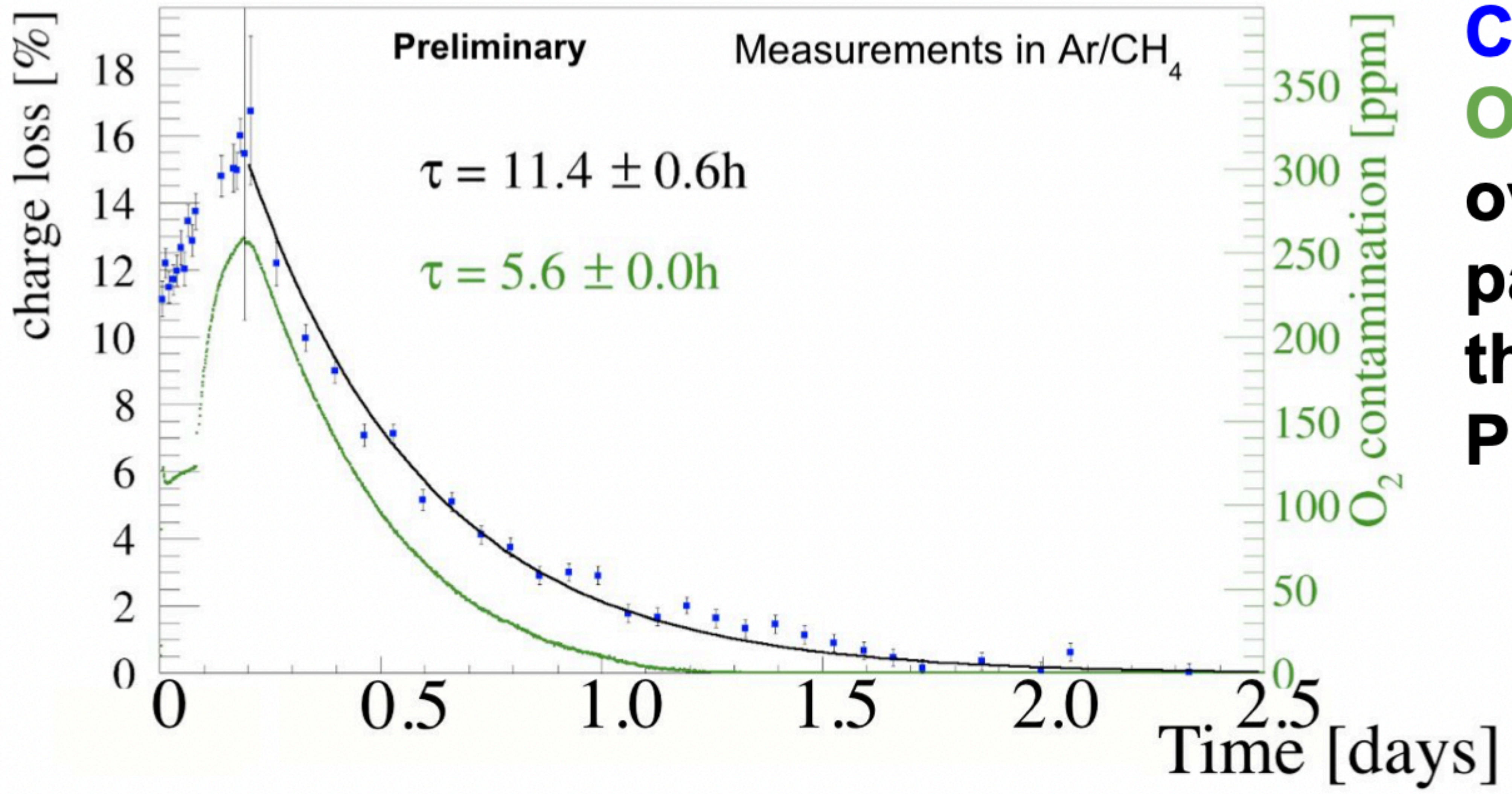

Charge Loss and **Oxygen Concentration** over Time while gas passes circulated through MicroTorr Purifier

QF measurement #1

COMIMAC, LPSC Grenoble

- **QF: ratio of ionisation energy to total energy deposited by incident particle. Must be known down to ~100 eV to set WIMP limits at 0.1 GeV/c² with NEWS-G**

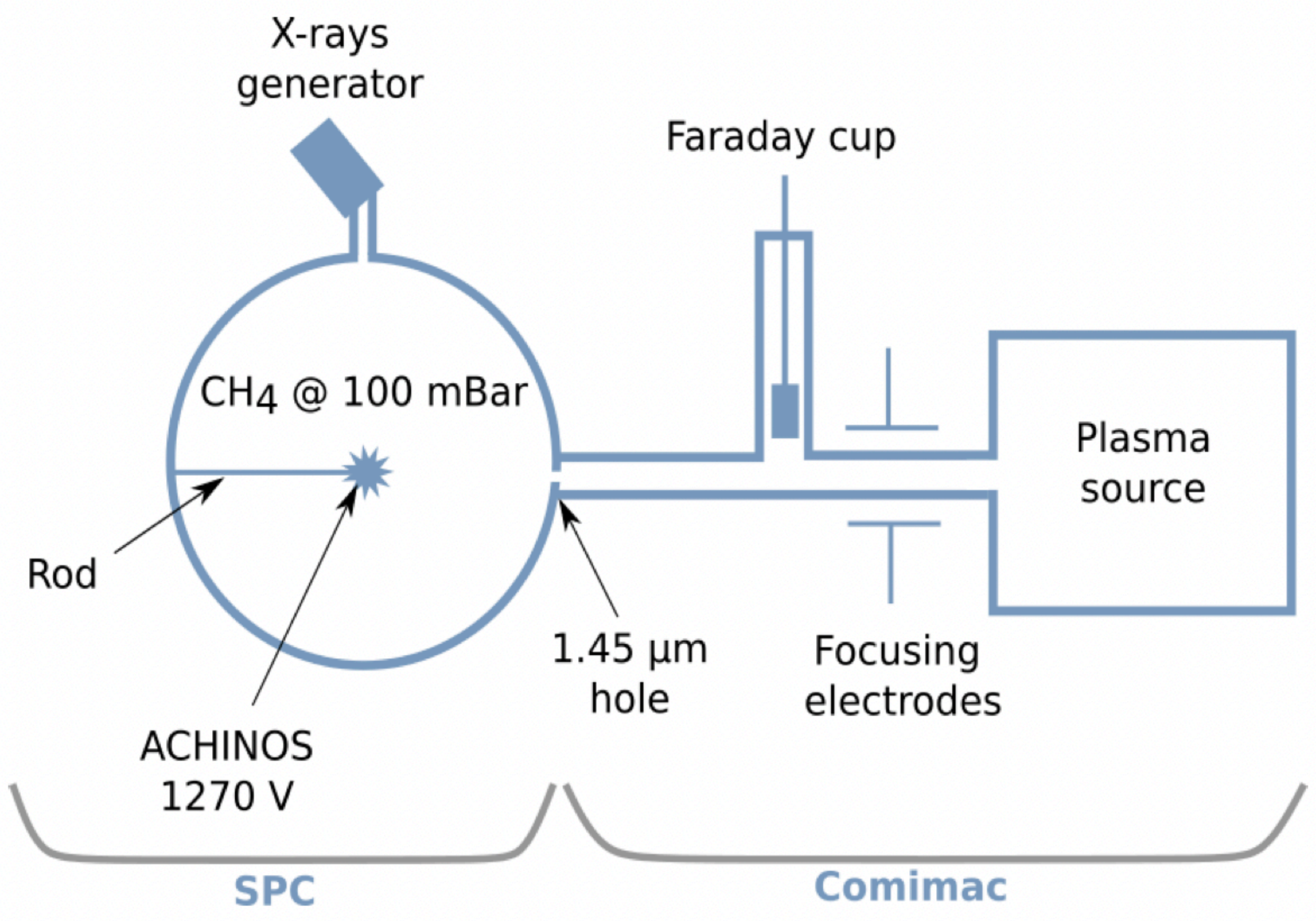

- COMIMAC generates electrons or ions of known energy by accelerating them in electric field
- Ratio between observed signals for electrons and ions used to determine QF in 0.7-50 keV range

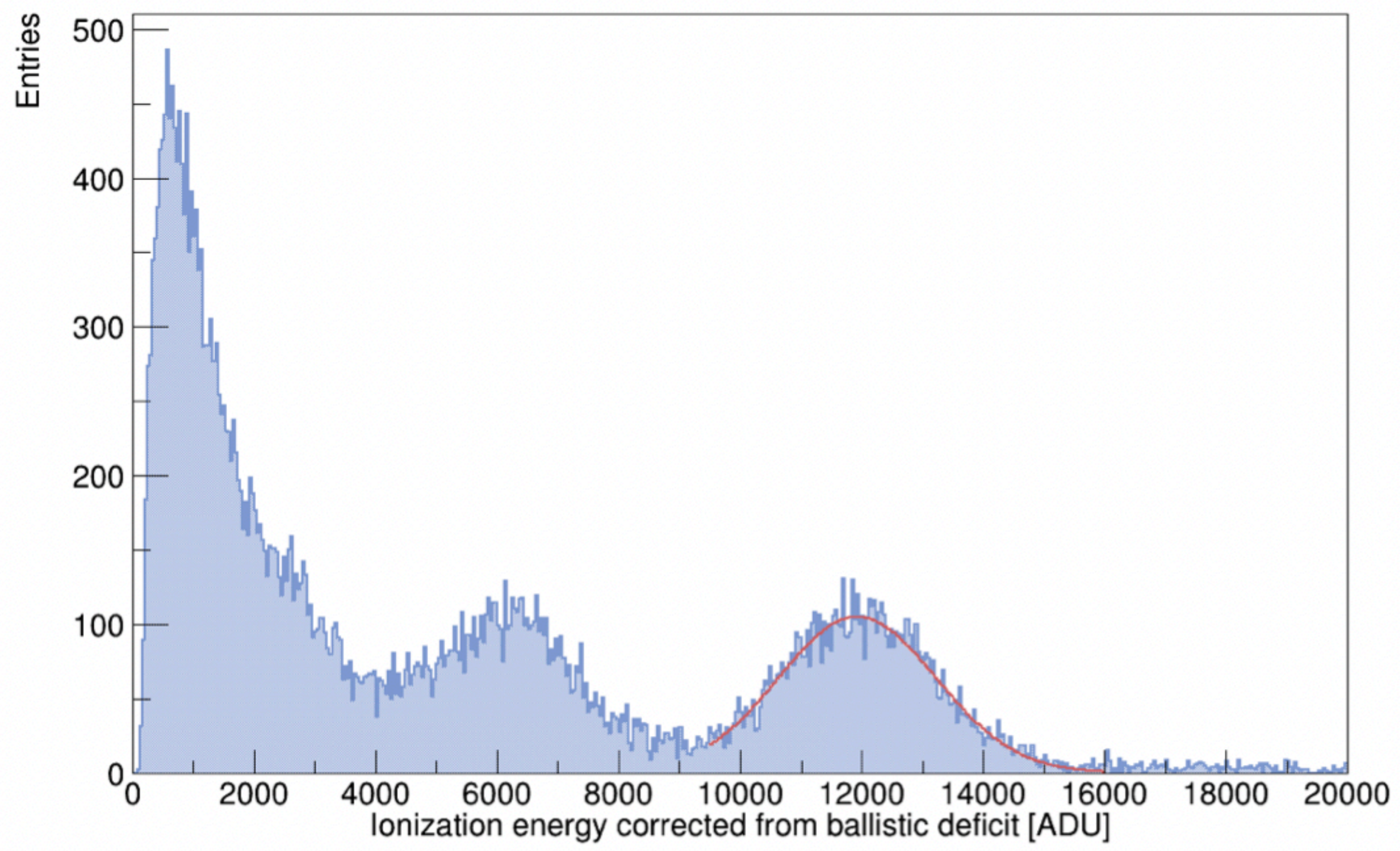

Figure 8: Example of a 5 keV proton spectrum at 1270 V. A Gaussian fit of the proton peak is shown in red.

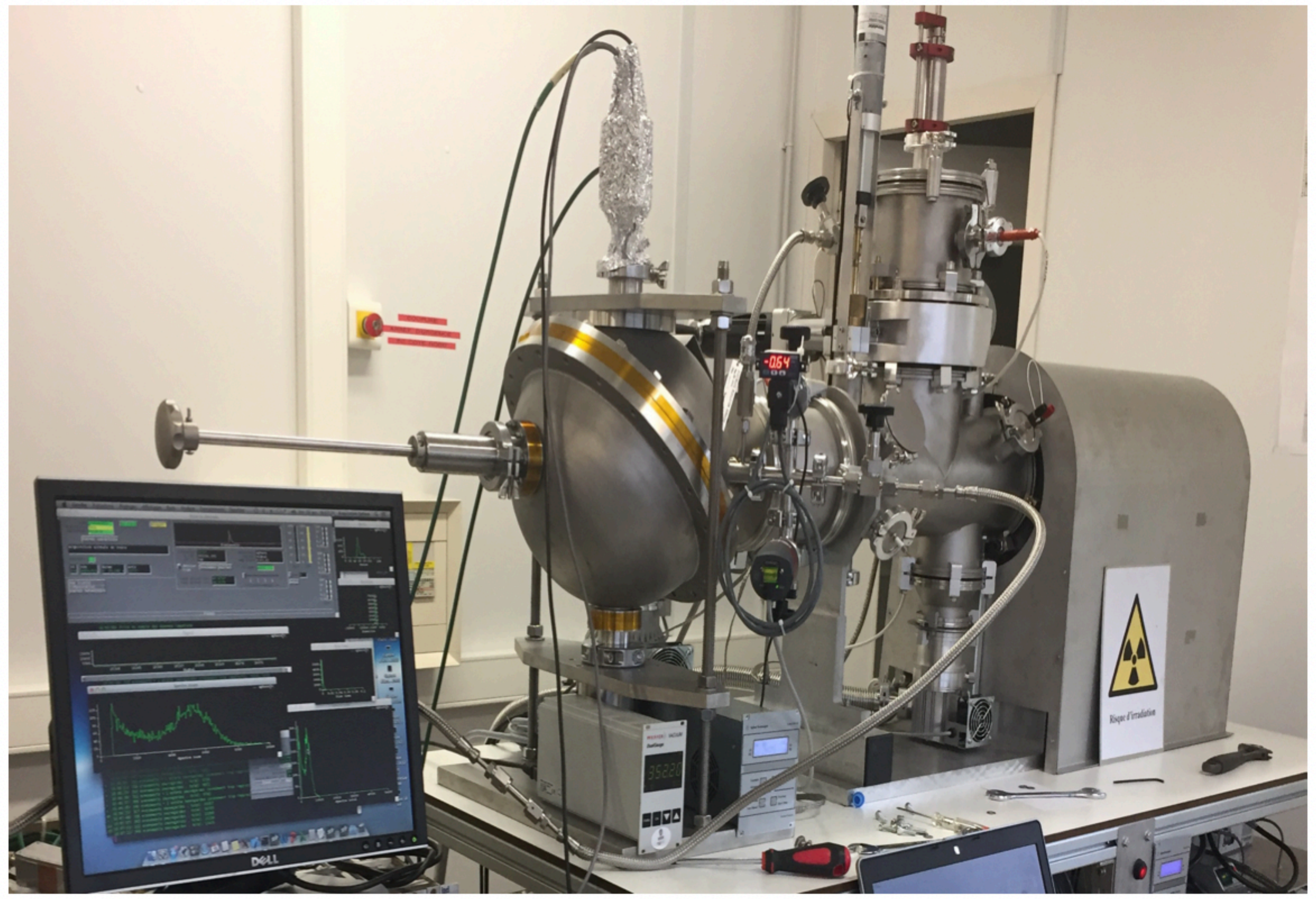

Paper on CH4 QF measurement with COMIMAC currently at internal review stage!

QF measurement #2

545keV neutron beam, TUNL

- Neutron beam of known energy generates recoils on target, emulating WIMP recoil.
- Backing Detector off neutron beam detects scattered neutron. Angle of BD gives energy deposited in recoil through simple kinematics. Different angles are chosen for different energies.
- Comparison with calibration of electronic interactions from ^{55}Fe used to determine QF.

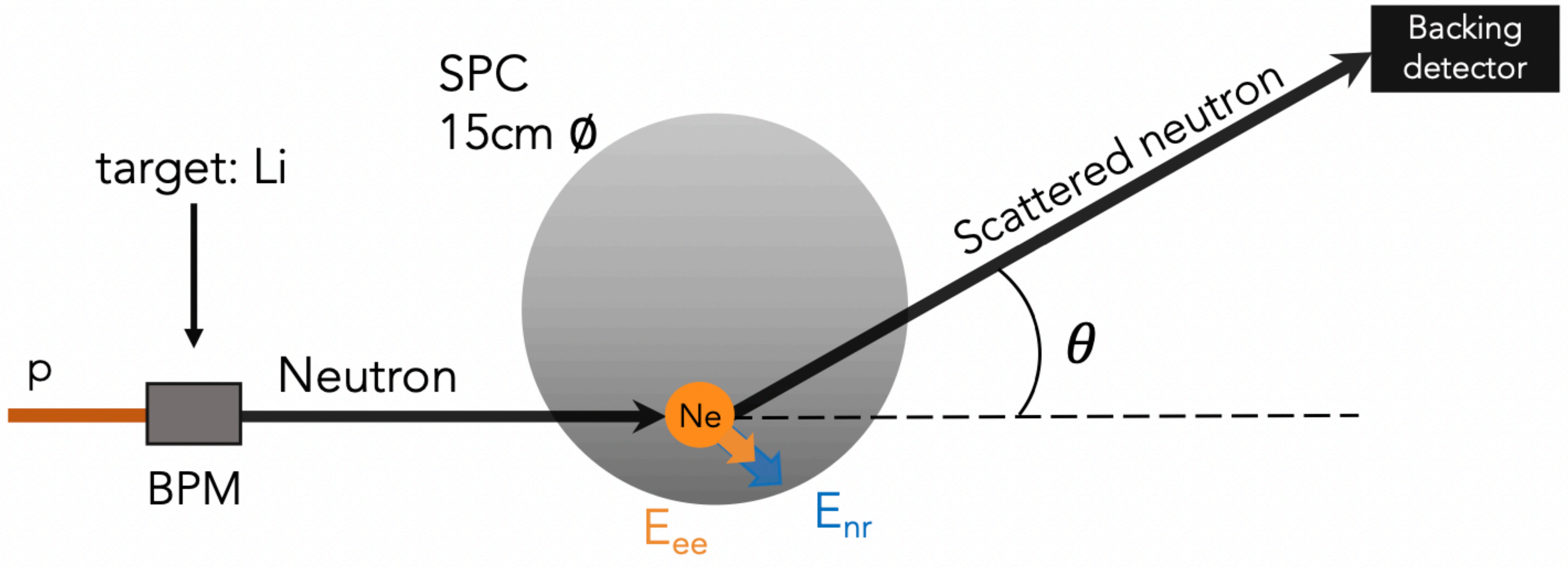

Run	E_{nr} [keV_{nr}]	θ [°]
8	6.8	29.02
7	2.93	18.84
14	2.02	15.63
9	1.7	14.33
10	1.3	12.48
14	1.03	11.13
11	0.74	9.4
14	0.34	6.33

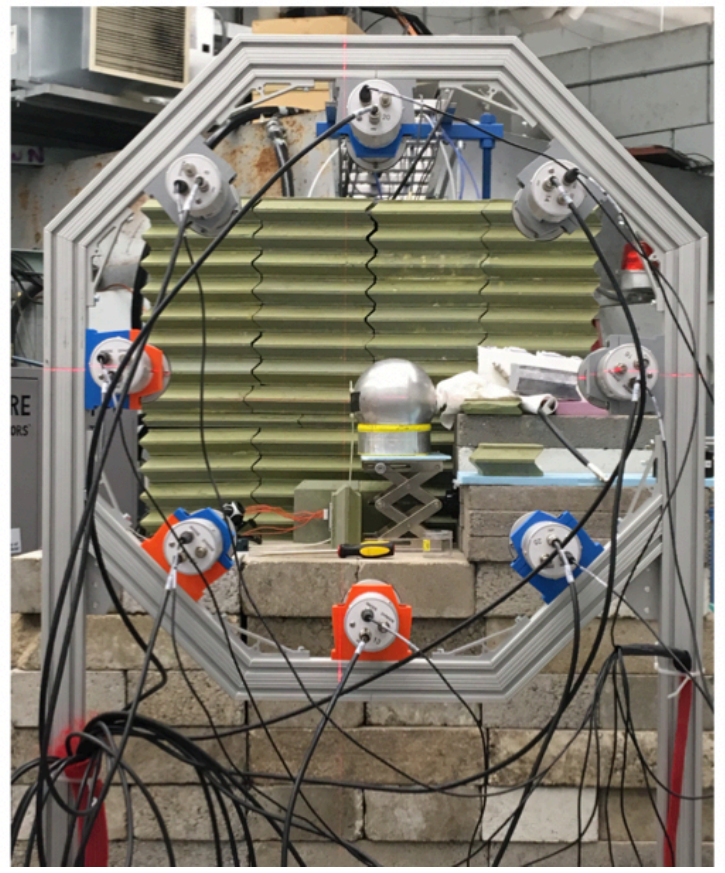

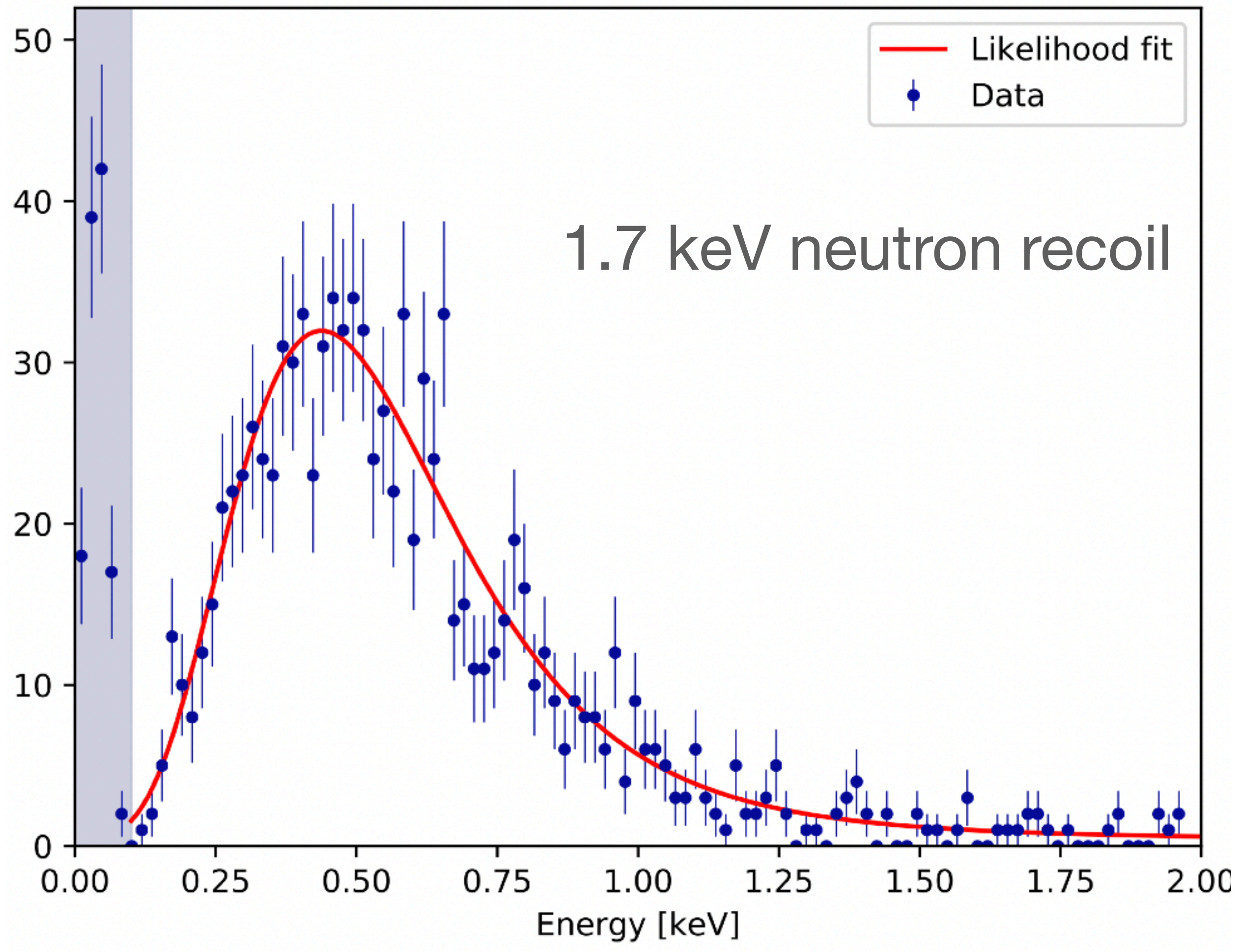

Paper on Ne+CH4 QF measurement at TUNL under journal review

https://arxiv.org/abs/2109.01055

Alpha-induced electrons

For a few seconds following an alpha decay:
-Rate increases
-Drift time decreases (measure with laser pulse)
Effects due to the electric field distortion induced by charges filling the detector volume.

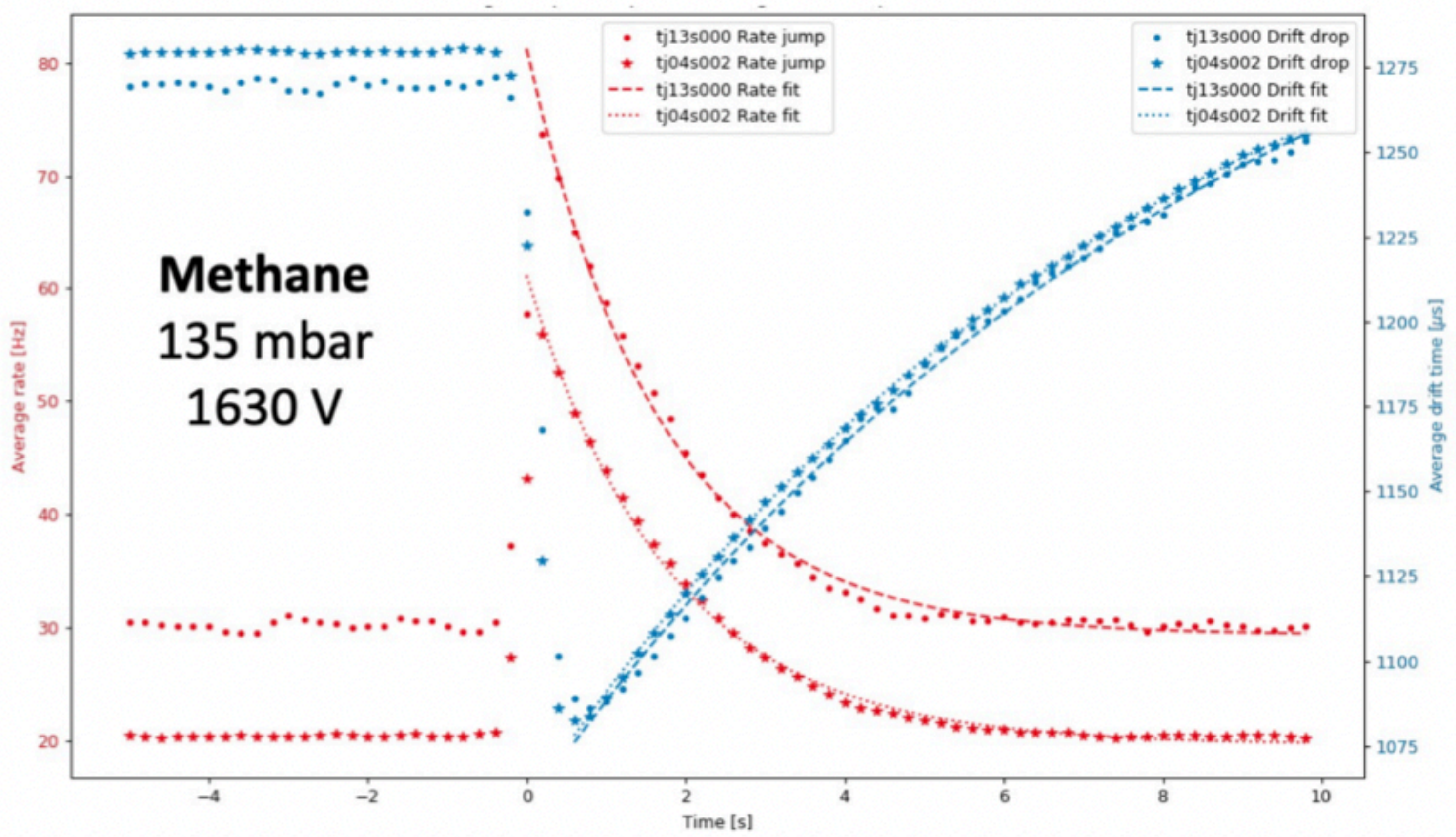

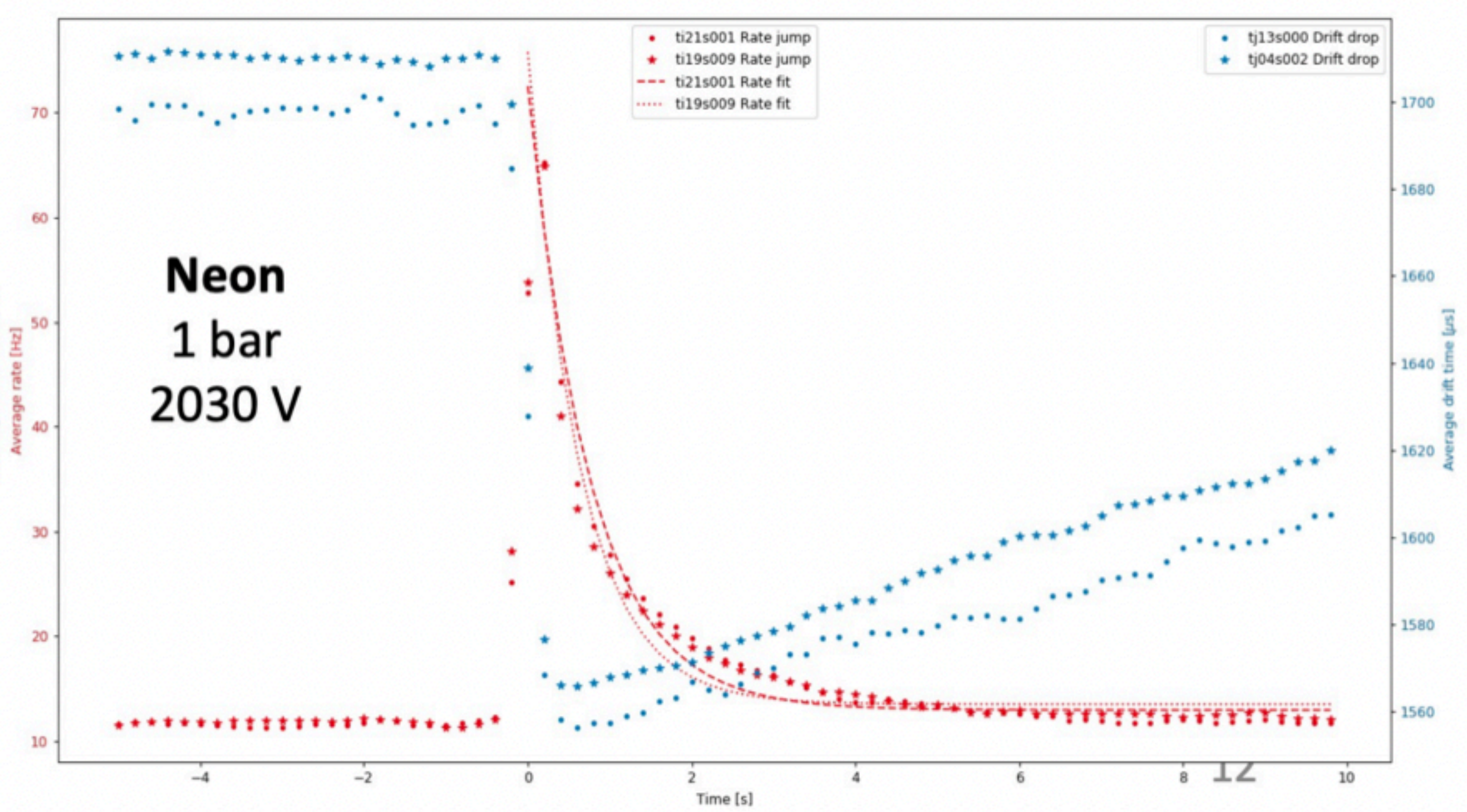

Cut on such high energy events leads to ~70% background events reduction with a 12% exposure reduction

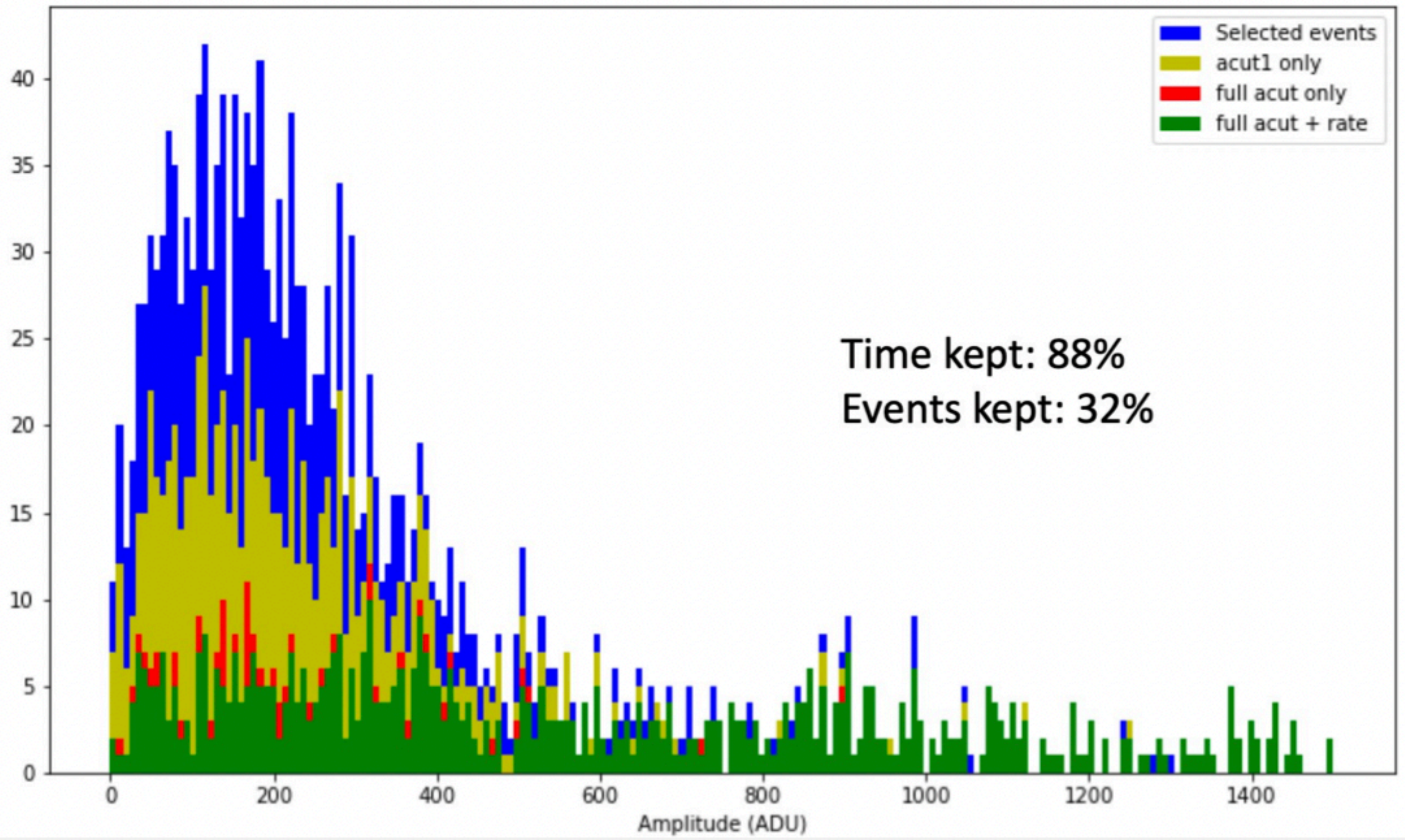

Jean-Marie Coquillat, M.S.c student, Queen's University

Other projects

Solar KK axions

Solar KK axion model predicts accumulation of heavy (~10 keV) axions in the Solar System. These axions decay into two photons of equal energy, absorbed at different locations in an SPC.

Can reject background at 99.99% in 2-22 keV range by keeping only events with two pulses of similar amplitude arriving shortly after each other.

With 42 day exposure of SEDINE detector, and an integrated sensitivity to solar KK axion decays of 16%, still improve over previous XMASS limit by factor ~6.

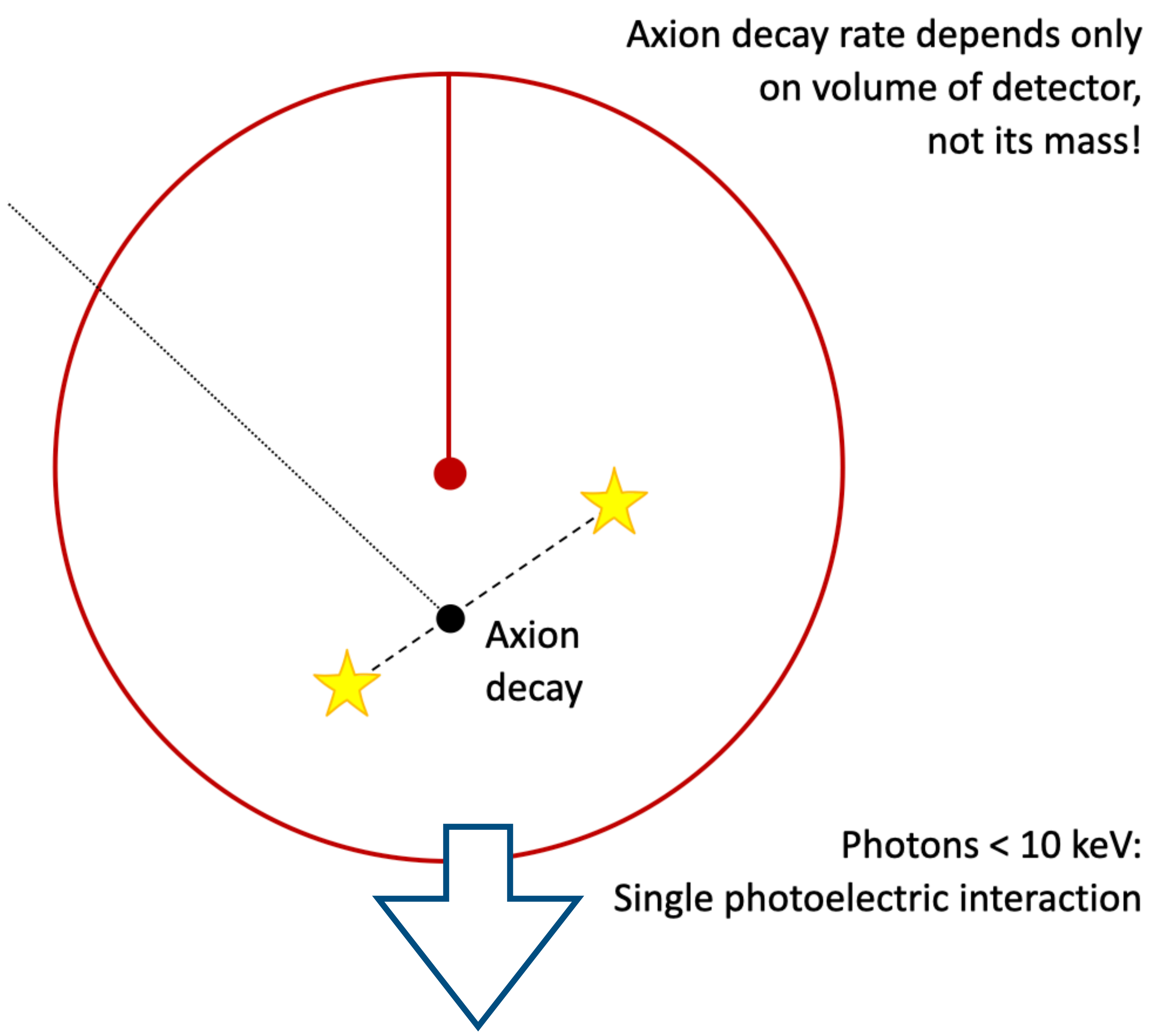

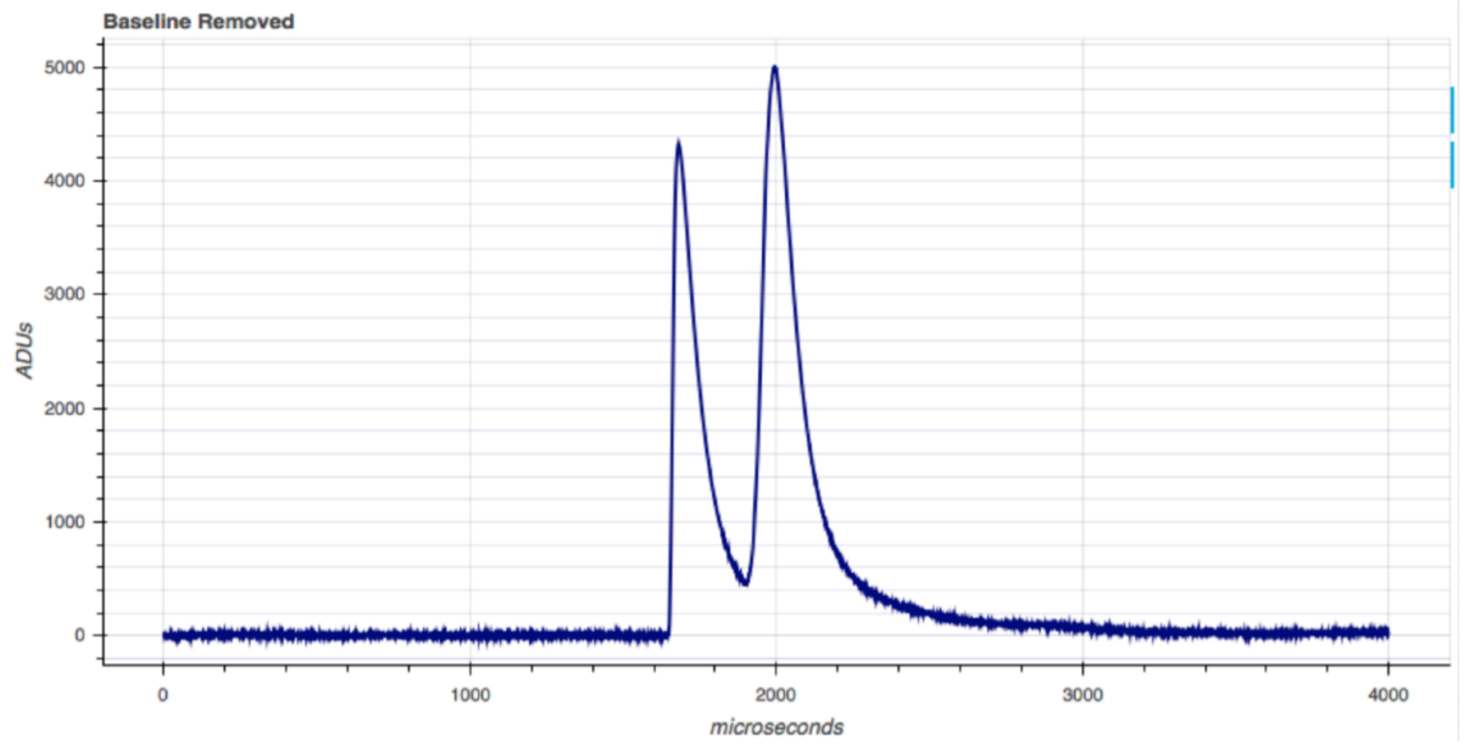

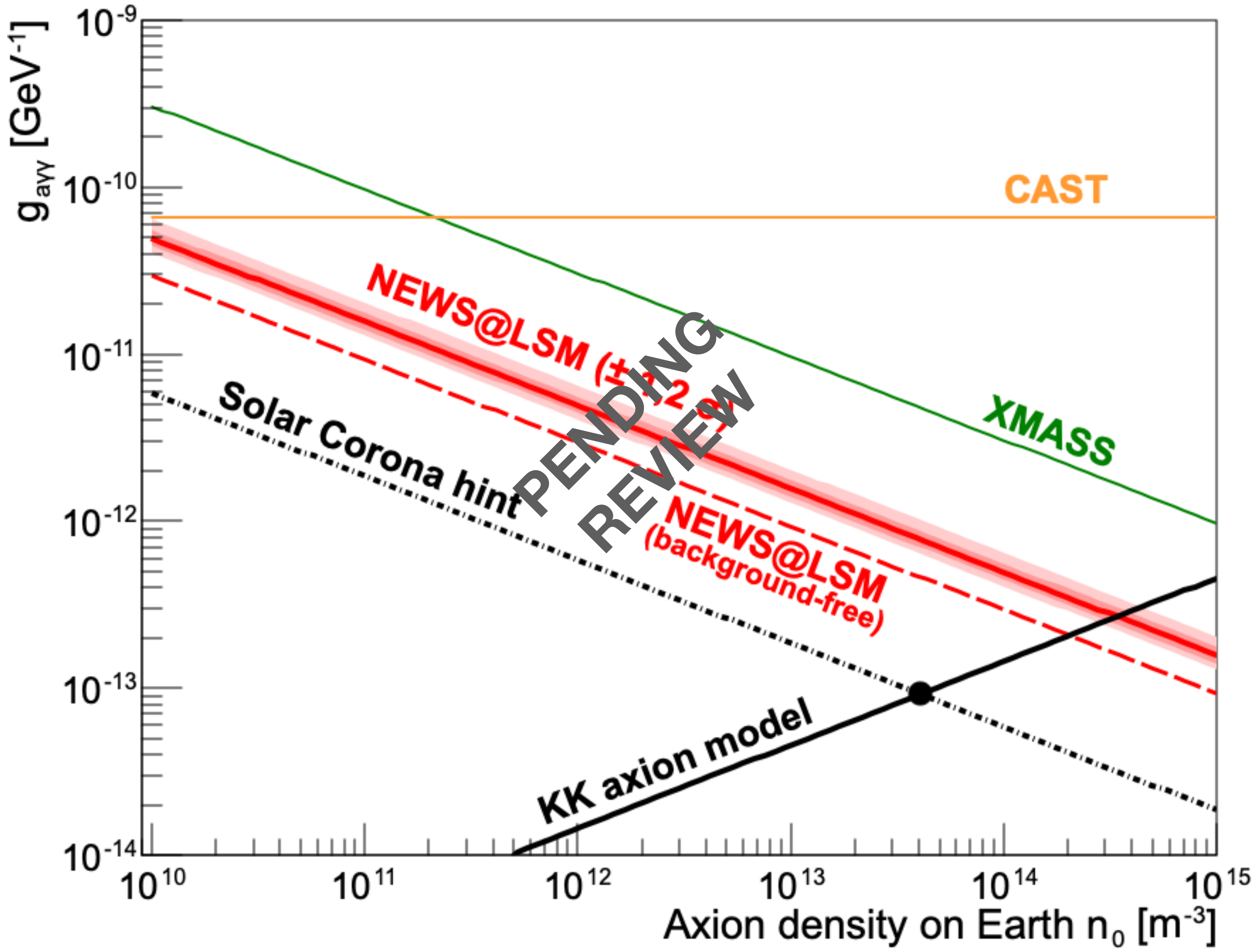

Solar KK axion paper under journal review

https://arxiv.org/abs/2109.03562

Sensor with E-field correction

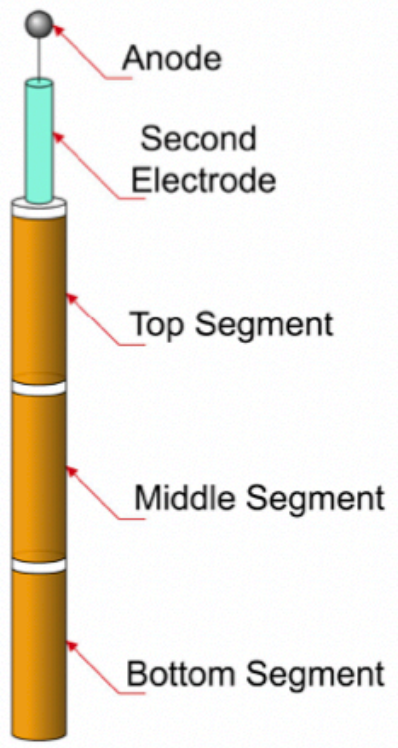

- **Grounded rod distorts electric field**
- **Voltage gradient along rod, as in ideal geometry, would restore ideal field.**
- **Voltage applied to each segment is the average ideal voltage over the segment.**

No correction

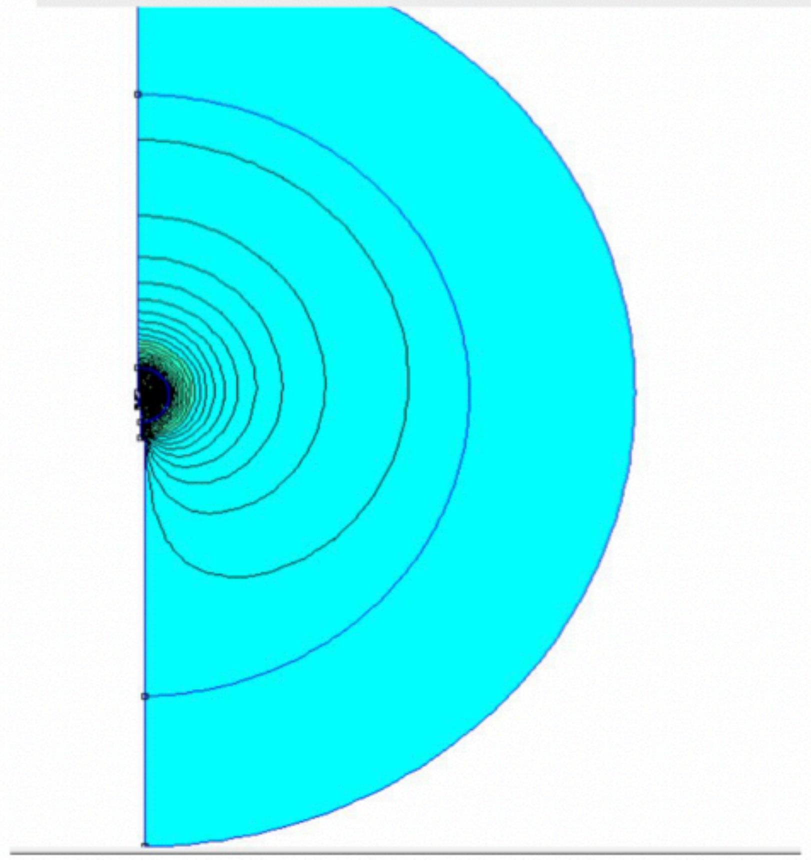

Voltage degrader

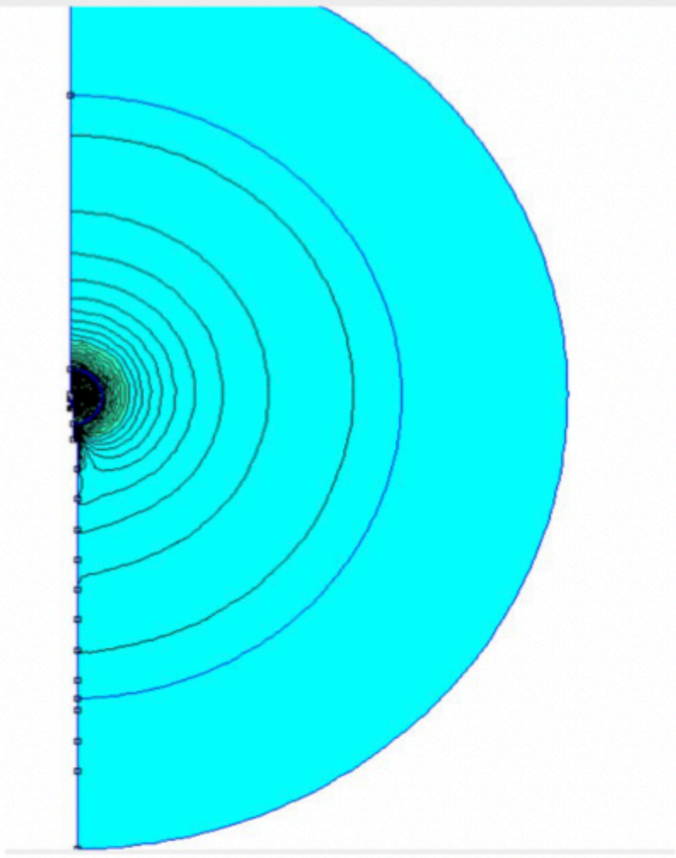

Resistive strip degrader

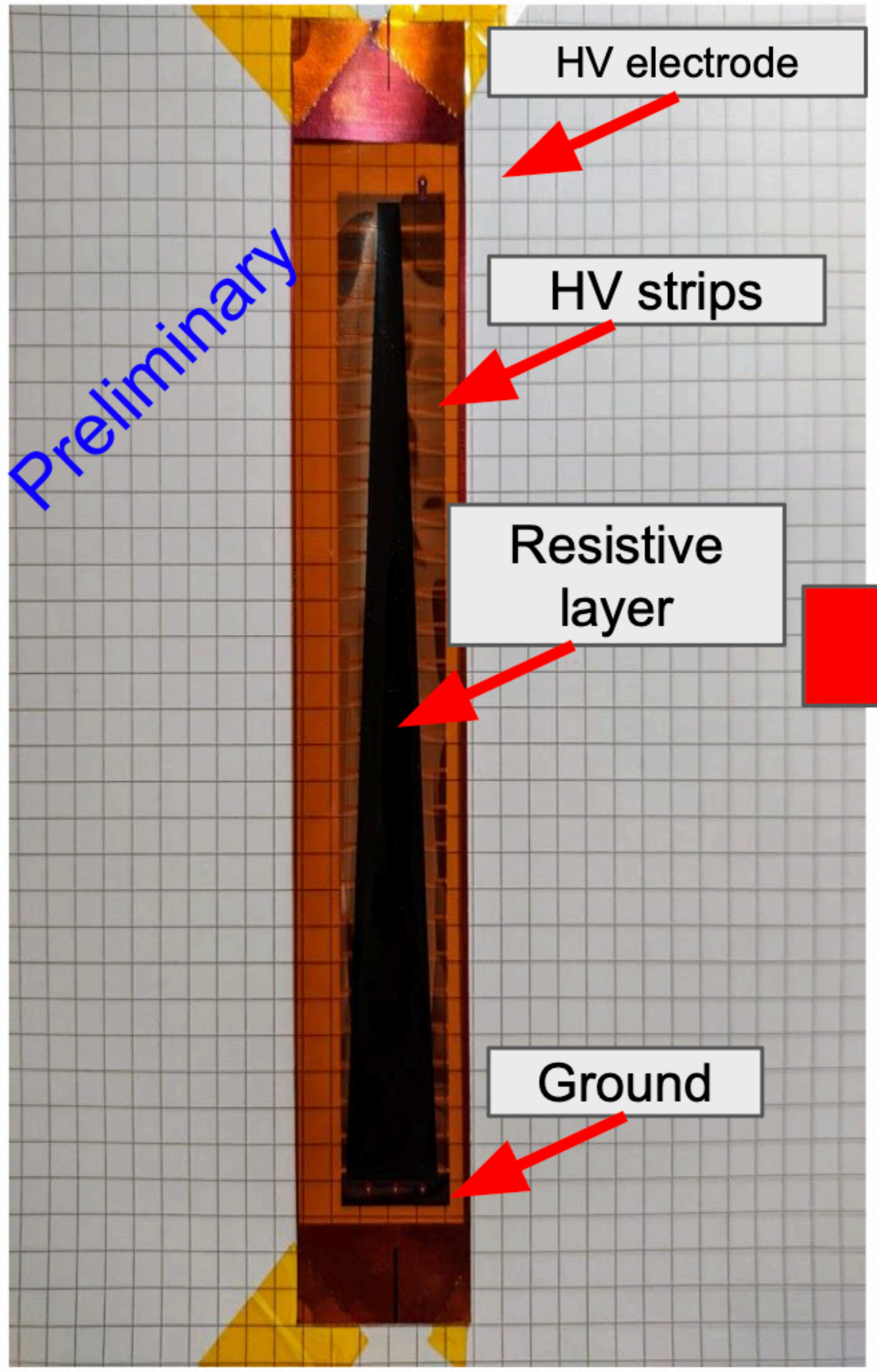

ACHINOS with Degrader

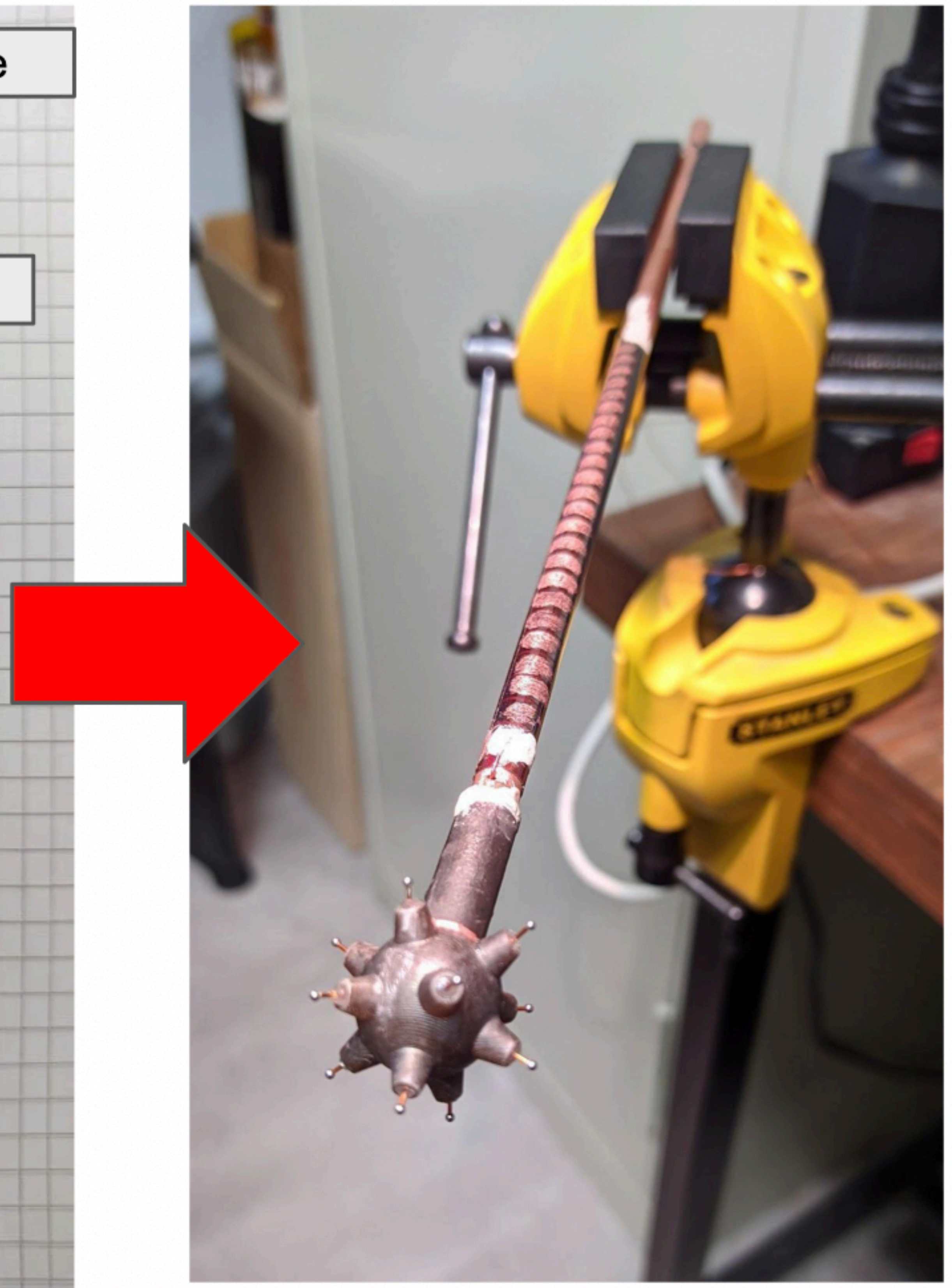

I. Katsioulas

Sensor development

ACHINOS : x60 configuration

Track reconstruction through individual anode readout

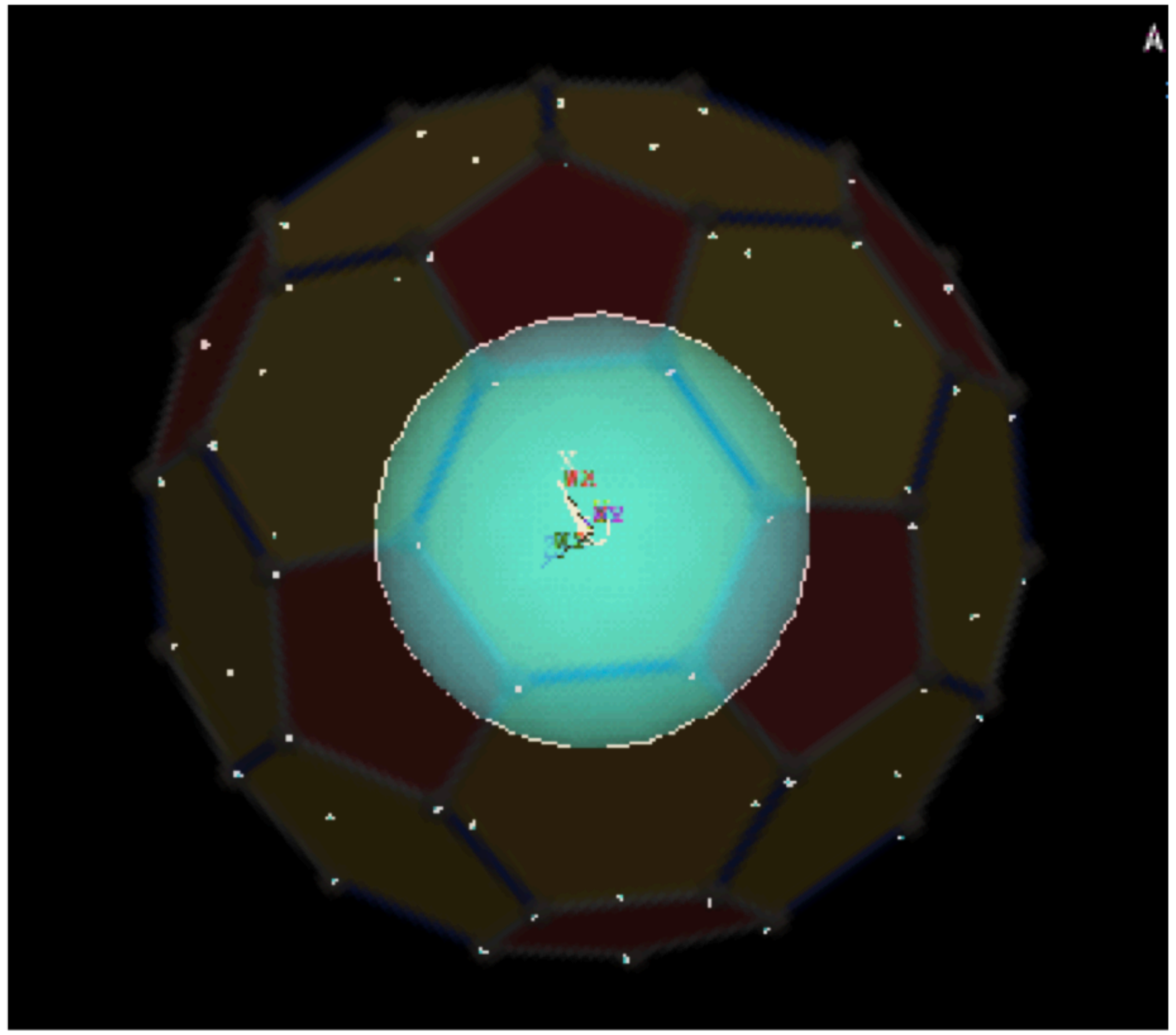

60-anodes (truncated icosahedron)

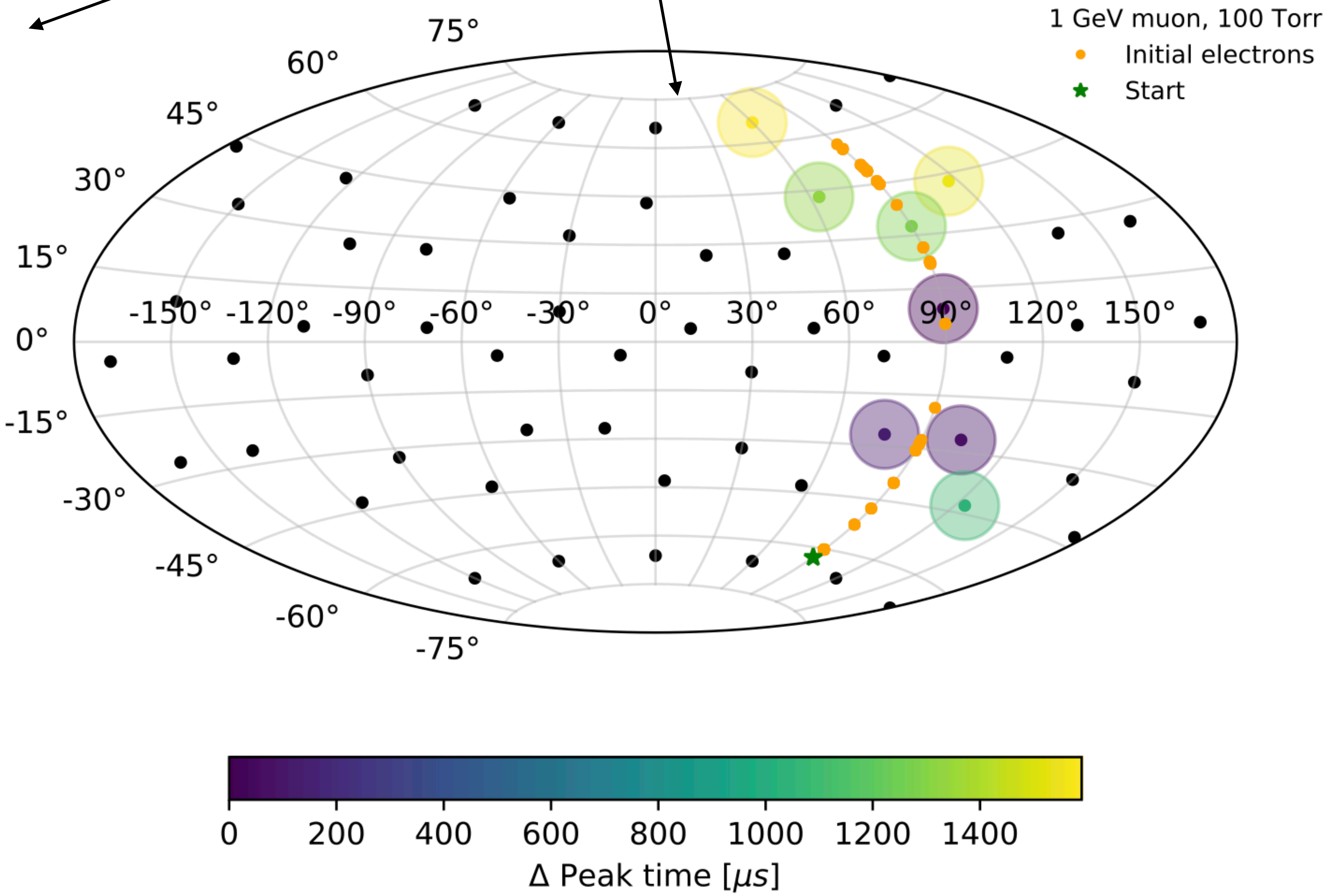

NEWS-G: Next Generation

- Next generation of detector will require even **lower background material**
- Two options:
  – **6N copper sphere**
  – **Electroformed intact sphere**
- 6N **less pure than electroformed** but **commercially available** and potentially **lower cost**
- 6N sphere planned to be ⌀ 60 cm, installed in NEWS-G@LSM shielding
- Electroformed copper would be at SNOLAB – demonstrated **growth ~ 1.3 cm/year**; 10 bar, ⌀ 60 cm sphere requires 4 mm walls ~ **4 months**

Sample	^{210}Pb contamination (mBq/kg)	^{210}Po contamination (mBq/kg)
OFC#1 (C1020) (MMC)	40±8	47±21
OFC#2 (C1020) (MMC)	20±6	33±14
OFC#3 (C1020) (MMC)	27±7	(1.6±0.3)×10^{2}
OFC#4 (C1020) (MMC)	23±8	(2.2±0.4)×10^{2}
OFC#5 (C1020) (SH copper products)	17±6	44±18
OFC#6 (C1020) (SH copper products)	27±8	24±17
OFC (class1) (SH copper products)	36±13	38±3
Coarse copper (MMC)	(57±1)×10^{3}	(16±2)×10^{3}
Bare copper (MMC)	8.4±4.0	(1.1±0.2)×10^{2}
OFC (MMC)	23±8	(1.3±0.3)×10^{2}
6N copper (MMC)	<4.1	<4.8
Electroformed copper (Asahi-Kinzoku)	<5.3	<18

Electroformed copper (PNNL) ~<100 nBq/kg ^{238}U & ^{232}Th